THE DEVELOPMENT AND VALIDATION OF A BIOFIDELIC SYNTHETIC EYE FOR THE FACIAL AND OCULAR COUNTERMEASURE SAFETY (FOCUS) HEADFORM

ERIC ALLEN KENNEDY

Dissertation submitted to the Faculty of the
Virginia Polytechnic Institute and State University
in partial fulfillment of the requirements for the degree of

Doctor of Philosophy
in
Biomedical Engineering

Stefan M. Duma, Ph.D., Chair
H. Clay Gabler, Ph.D.
Joel D. Stitzel, Ph.D.
Michael L. Madigan, Ph.D.
Ian P. Herring, D.V.M., M.S.
P. Gunnar Brolinson, D.O.

August 3, 2007

Blacksburg, Virginia

Keywords: FOCUS Headform, Eye, Injury, ATD Headform, Risk Function

THE DEVELOPMENT AND VALIDATION OF A BIOFIDELIC SYNTHETIC EYE FOR THE FACIAL AND OCULAR COUNTERMEASURE SAFETY (FOCUS) HEADFORM

Eric Allen Kennedy

ABSTRACT

There are over 1.9 million eye injuries per year in the United States with over 30,000 patients left blind in at least one eye as a result of trauma. Some of the most severe eye injuries can occur in automobile accidents and from sports related impacts. Eye injuries in the military environment are even more prevalent and are generally more severe than eye injuries to civilians. The rate of eye injuries has dramatically increased in warfare in recent years, rising from 2% of all casualties during World War I and World War II to over 13% of all combat injuries in Operation Desert Storm. While many of the conflict-related eye injuries are caused by shrapnel and other debris, nearly 25% of the injuries are also caused by blunt trauma from motor vehicle and helicopter crashes, falling, and direct hits from blunt objects.

In order to develop safety countermeasures effective at preventing these eye injuries, as well as evaluate the eye injury potential of different impacts, it is desirable to have the capability for distinguishing between injurious and non-injurious eye impacts. Current anthropometric test device (ATD) headforms lack instrumentation and facial features to allow detailed assessment of eye or discrete facial injuries. Therefore, the purpose of this dissertation is to present the development and validation of the Facial and Ocular CountermeasUre Safety (FOCUS) headform's synthetic eye and orbit and corresponding eye injury risk criteria.

ACKNOWLEDGEMENTS

Before I can feel the relief and celebration of finishing this dissertation I will have to figure out a way to adequately thank the many people who all were an integral part of making this all possible.

First, you cannot reach academic success without having a good teacher. For the past 5 years, working under Stefan Duma, I have had an enormity of opportunities to watch, learn, and participate – more than I ever could have hoped or ever dreamed of. On the occasions where I have achieved success, it is in no small part to the role he played in mentoring me along the way. I will never be able to say thanks enough, but I do hope to offer similarly effective advice to my own students in the future.

To the remainder of my committee: Joel Stitzel and Clay Gabler, whom I have interacted with almost every day, I can only say thanks for so often being an example for so much of which I hope to follow. Mike Madigan, thank you for the advice and conversations and for never failing to have a great answer to even the dumbest of questions. Gunnar Brolinson and Ian Herring, thanks to both of you for the medical perspective that you brought to our conversations and for always finding the time.

To my all of my friends from Maryland, Virginia Tech, elsewhere, but especially the Center for Injury Biomechanics. Sarah Manoogian, my office mate for most of my time at Virginia Tech and a wonderful friend that I will miss seeing every day. Doug Gabauer and Craig McNally for motivating from opposite perspectives on ways to improve a 5k time (and many other memories as well). Andrew Kemper for many "fun" (if that is the right word) testing "experiences" (I know that is the right word). And of course, literally everyone else who played an equally important role in providing me (and Schatzie – thank you Kate and Jared) a strong VT family.

I must thank of course my family – who I know are proud to know that I have finished and who offered so much support along the way: Mom and Dad, Grandmom and Granddad, Pop-Pop and Grandmal (who I know are just as proud looking down on me), Minda and Dan, Nancy and Tina, Mom and Dad McLaughlin, and my new brother and sister-in-law and favorite niece (Megan)!!! … which of course implies that a huge thank you is owed to a wonderful woman, who I know that I would not have made it down this road without…

To Carol, who toughed out four-hour drives to make this all work out (after she toughed out ten-hour drives to make this all work out). You have never failed to support me for anything that I have wanted, or needed to do, to get to this point. More amazingly, you have never expected nearly as much from me in return, and I hope that this accomplishment and our road in the future is some form of repayment for that. Thank you for always being there for me… and the dog.

And finally, to Schatzie the Shiloh Shepherd, who guarded the house by day and greeted me with a wagging tail (and tongue) as I got home at night. Day to day, no matter what any of these people think, it was probably you the most who helped me keep my sanity through all of this.

TABLE OF CONTENTS

LIST OF FIGURES

LIST OF TABLES

CHAPTER 1:
INTRODUCTION TO TRAUMATIC EYE INJURIES, CURRENT METHODS OF DETERMINING EYE INJURY POTENTIAL, AND GOALS OF RESEARCH

INTRODUCTION

This document is intended to describe the research for a biomechanical evaluation of the human eye for the purpose of predicting its injury potential due to blunt impact. For this ultimate goal, there are multiple research questions which need to be addressed. As such this document is organized into multiple chapters, which will serve to outline each research hypothesis and the methodology with which those hypotheses can be correctly answered.

EYE ANATOMY

The eye is the organ of the body that is responsible for visual perception. The human eye is comprised of a variety of tissues that each contribute to the overall function of the eye. The average human eye is approximately a spherical shape that is, generally 25 mm in diameter (Figure 1). A brief description of each of these structures follows.

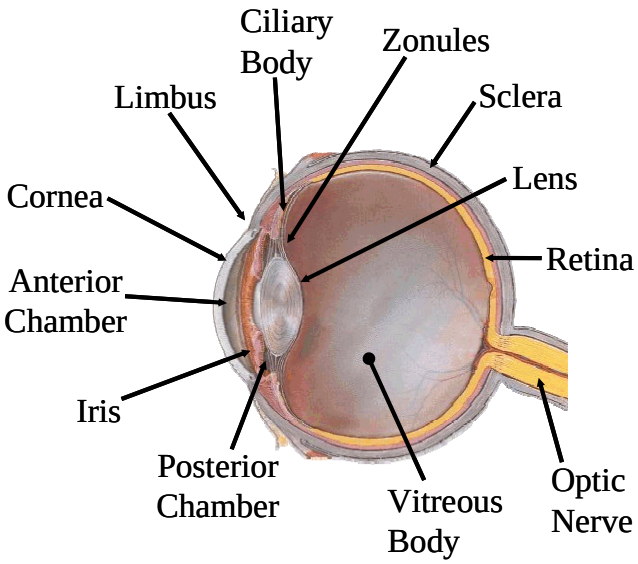

Figure 1: Schematic showing the various anatomical structures of the human eye.

The outer shell of the eye is comprised of the corneo-scleral shell, which is made up of two separate structures. The cornea is a transparent structure, made up of thin collagen fibrils. It is the anterior-most structure of the eye and allows light to enter the eye. It connects to the sclera of the eye at the limbus, which is a transition region of approximately 1.5 mm – 2.0 mm wide. The sclera is a non-transparent, tough, white, collagen fiber structure that makes up approximately 80% or more of the eye's outer surface (Bron 1997). Both the cornea and the sclera are avascular structures which affects their ability to heal after trauma.

The eye can be divided into two main segments, the anterior segment and the posterior segment. The anterior segment is comprised of the anterior and posterior chambers of the eye, which are filled with aqueous humor, as well as the lens, ciliary body, iris and the zonules. The lens is held in place by the zonules, which hold the lens in constant tension. When the ciliary body muscles tense, they release some of the tension in the zonules allowing the lens to bend and refocus. The iris is the pigment colored region of the eye that defines the color of each person's eyes, but more importantly, the iris contracts and relaxes to change the amount of light that is passed to the posterior segment of the eye (Bron 1997).

The posterior segment of the eye contains the vitreous body, the retina, the choroid and the optic nerve. The vitreous body is a thick fluid that helps to keep the retina pressed against the inner surface of the eye and attenuates shock transmitted to the eye. The retina is a thin layer on the perimeter outside of the vitreous that converts the focused light that is passed from the cornea and lens into electrical signals which are transmitted to the brain, via the optic nerve. The choroid is a thin layer that lies between the retina and the sclera and provides nutrients and oxygen to the retina (Bron 1997).

In addition to the internal structures of the eye, there are a total of six extraocular muscles that control the overall movement of the eye (Figure 2). There are four rectus muscles and two oblique muscles. The rectus muscles all originate at the posterior wall of the orbit and insert at four different regions on the eye, one superiorly, one inferiorly, one laterally, and one medially.

These are called the superior, inferior, lateral, and medial rectus, respectively. The four rectus muscles, due to their anterior-posterior lines of action, control eye movement to elevate or depress the eye as well as abduct or adduct the eye. The superior oblique muscle also originates from the posterior portion of the orbit, but it passes around a bony structure known as the trochlea, which serves as a pulley, prior to inserting in a medial-lateral direction across the superior portion of the eye. The superior oblique muscle serves to elevate the back of the eye and abduct the eye. The inferior oblique muscle originates on the medial wall of the orbit and inserts in a medial-lateral direction across the inferior portion of the eye. It serves to depress the back of the eye and adducts the eye (Bron 1997).

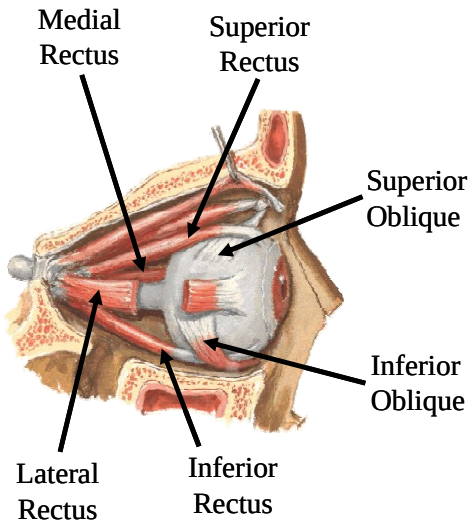

Figure 2: The six extraocular muscles of the eye are shown in this lateral-medial view of the right eye.

EYE INJURY TYPES

There are many different types of eye injuries that can occur as the result of trauma; however, for the purposes of this document, a total of five different injury classifications will be discussed. Corneal abrasion occurs when the outer layer of cells, the epithelial cells on the surface of the cornea, are scraped away due to application of external forces. Hyphema occurs when bleeding occurs and blood pools in the anterior and posterior chambers of the eye, generally as the result of blunt trauma to the eye which hemorrhages blood vessels in the iris or other anterior structures of the eye. Lens dislocation occurs when the lens of the eye is displaced from the zonules. Retinal damage frequently occurs in the form of retinal detachment, which is when the retina

separates from the choroid layer of the eye that supplies nutrients to the retina; however, retinal damage also can be in the form of retinal swelling, tearing, degeneration or other injuries that occur in the posterior segment of the eye. Globe rupture is the most immediately threatening and serious eye injury, that occurs when the cornea or sclera of the eye is punctured or ruptured, leading to the possibility of the loss of the intra-ocular contents of the eye.

For clarity, within this document, five different eye injury pathology groups have been established: corneal abrasion, hyphema, lens dislocation, retinal damage, and globe rupture. Obviously, this excludes specific details of particular types of eye injuries, but does allow for discrimination between different severities of various eye injuries, as well as distinction between the regions of the eye that have been injured during a particular traumatic event. For example, for simplification, pathologies with common anatomical and/or physiological characteristics were combined into a single group. For instance, hyphema includes hemorrhage whether originating from iris, ciliary body, or angle trauma, and retinal trauma, whether tears or detachment, was termed as retinal damage.

CIVILIAN EYE INJURIES

There are over 1.9 million eye injuries per year in the United States with over 30,000 patients left blind in at least one eye as a result of trauma (McGwin 2005, Lueder 2000, Parver 1986). The incidence of severe eye injuries is on the same order of magnitude as the number of passengers killed in vehicle crashes every year, with approximately 30,000 Americans left blind in one eye as a result of trauma (Parver 1986). Some of the most severe eye injuries can occur in automobile accidents, from sports related impacts, and from military accidents and casualties (Chisholm 1969, Berger 1978, Mader 1993, Duma 1996, Vinger 1997, Kuhn 2000, Duma 2002, Rodriguez 2003).

Blunt impact of the eye with an airbag or other objects can result in severe eye injury such as hyphema (bleeding in the anterior chamber of the eye), lens dislocation, or globe rupture (Chisholm 1969, Vichnin 1995, Duma 1996, Ghafouri 1997, Stein 1999, Lueder 2000, Power

2002, Hansen 2003, Stitzel 2005). Although not statistically significant (p=0.15), eye injuries sustained during automobile crashes occur at a higher rate (3.1%) when the occupant is exposed to a deploying airbag than when the occupant is not (2.0%) (Duma 2002). The airbag has been shown to be both directly responsible for eye injuries from blunt impact with the eye and indirectly responsible for eye injuries by propelling objects into the eye during the airbag deployment (Kuhn 1995, Duma 2002). The types of injuries sustained in automobile crashes are generally not penetrating injuries, but usually injuries to the anterior surface of the eye or contusion caused by blunt trauma. Corneal abrasion and hyphema are the most frequently occurring injuries in automobile crashes. Though no experimental studies have been reported that have specifically shown airbags to cause globe rupture, computational simulations have shown airbag interaction with the eye to lead to high corneo-scleral stress (Stitzel 2005). Additionally, several case studies in the literature specifically cite airbags as the primary cause of globe rupture, although this injury mechanism appears to be very rare (Kuhn 1994, Duma 1996, Pearlman 2001).

Eye injuries in sporting activities are also common, due to the close proximity of players and high energies involved. Globe rupture can occur from blunt trauma from many sports objects such as baseballs, golf balls, hockey sticks, squash balls and other objects (Chisholm 1969, Vinger 1996, Vinger 1999, Rodriguez 2003). Paintballs have also proven to have a devastating effect on the unprotected eye, often resulting in complete rupture of the globe and loss of intraocular contents, hyphema, retinal tearing, and traumatic cataracts are also very prevalent (Vinger 1997, Thach 1999, Fineman 2000, Listman 2004).

Some of the most severe eye injuries are caused by high speed projectiles from fireworks, sports equipment, firearms and BB guns, or contact with various parts of the car's interior in automobile crashes (Chisholm 1969, Berger 1978, Duma 1996, Vinger 1997, Kuhn 2000, Duma 2002a). The improvement of automobile safety systems has reduced the number of life threatening injuries sustained by crash victims (Libertiny 1995, Malliaris 1995). Whereas in most cases, these improved safety systems lower the overall incidence of injuries in crashes, certain types of injuries have become more prevalent with advanced restraint systems.

Eye injuries sustained during automobile crashes occur at a higher rate (3.1%) when the occupant is exposed to a deploying airbag than when the occupant is not (2.0%) (Duma 2002a). There are five general types of ocular trauma that have been shown to be associated with airbag deployment: contusions, abrasions, lacerations, detachments, and ruptures (Duma 1996, Aylward 1993, Bonnet 1991, Giovinazzo 1987).

In summary, eye injuries in the civilian sector can be debilitating and have an enormous societal cost. Besides superficial injuries to the eye and the orbit, the most frequently occurring injury is the presence of foreign bodies in the orbit or eye. The most potentially dangerous activities for eye injuries occur when high energy levels are available to cause injury, such as by sports equipment, fireworks, BB guns, and automobile crashes.

MILITARY EYE INJURIES

The eye is particularly at risk in high-energy blunt object impacts (Duma 1996, Vinger 1999, Duma 2000, Duma 2002a). Therefore, of particular interest is the epidemiology of eye injuries in the United States military both in peacetime and wartime environments. The number of debilitating eye trauma injuries in the US military per year is not widely reported, though it is expected that the numbers would be disproportionately greater than experienced in the civilian sector (Wong 2000).

Changes in operational procedures, tactical doctrine and technological advancements in the military environment mean that the types of eye injuries sustained in the present day military environment may differ from injuries seen historically in wartime activities. However, in order to understand and quantify those particular changes, this chapter will present a retrospective analysis of eye injuries in previous conflicts as well as the more recent military involvement in Operation Desert Shield and Operation Desert Storm.

The rate of eye injuries has dramatically increased in warfare since the American Civil War (Figure 3) (Heier 1993). Eye injuries in World War I and World War II accounted for

approximately 2.0% to 2.5% of all injuries. During the U.S. involvement in Vietnam, this percentage increased to 5% to 9%. In recent conflicts, such as Operation Desert Storm, the percentage of eye injuries has dramatically increased to over 13% of all combat injuries (Stone 1950, Heier 1993, Wong 2000). While many of the conflict-related eye injuries are caused by shrapnel and other debris, nearly 25% of the injuries are also caused by blunt trauma from motor vehicle and helicopter crashes, falling, and direct hits from blunt objects (Mader 1993, Biehl 1999).

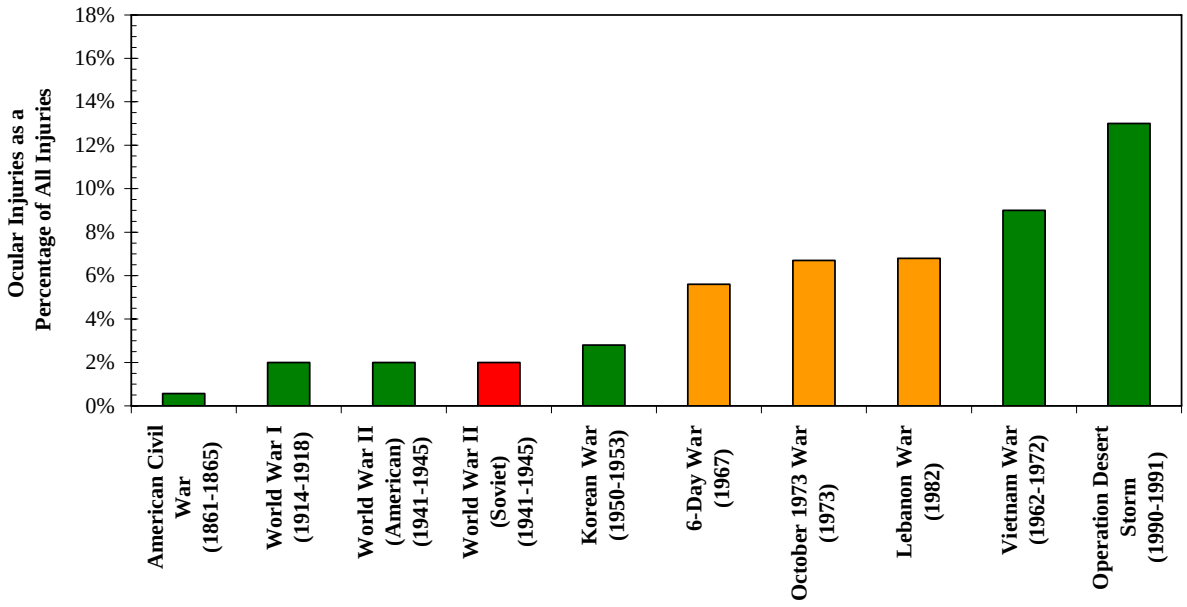

Figure 3: Ocular injuries shown as a percentage of total war injuries from 1861 to present. (Data in this figure are from Stone 1950, Heier 1993, Wong 2000)

Many have pointed out that this injury rate is largely disproportionate based upon the surface area of the eye compared to the total surface area of the human body. The ocular surface area is only 0.10% to 0.27% of the body surface area (Heier 1993, Biehl 1999). However, from World War I to the Six-Day War in 1967, ocular injuries have been reported at a rate 20 times to 50 times greater would be expected based on surface area alone (Treister 1969).

Three reasons that eye injuries are disproportionately injured in modern day military conflicts are the increased firepower and explosive thrust of weapons of war, the increased urbanization of the battlefield, and a lack of modernization of protective goggles and face shields to keep up with advances in weaponry (Biehl 1999). Another is the fact that the eye is particularly vulnerable to injury from particles that would only minimally affect or injure other parts of the body (Mader 1993). Therefore, it is possible that the eye is not being struck a disproportionate number of times on the battlefield, but it is more susceptible to injury than other body regions when it is hit, illustrating the importance of protective eyewear on the battlefield.

The explosive power of ordnance often leads to eye injuries as the pressure and fragmentation of the device and debris field is distributed over very large areas. The debris and shrapnel from these explosions often results in small projectiles which are very threatening to the unprotected eye, and pose a significant risk for penetration or laceration of the corneo-scleral shell. These penetrating wounds pose significant risk for losing an eye. In World War II and early in the Vietnam War, nearly 50% of all penetrating eye injuries ultimately resulted in the enucleation of the eye as a result of ophthalmologic treatment (Treister 1969). During the recent conflict in Bosnia, grenade and land mine explosions were found to cause approximately 85% of all eye injuries, with 60% of those injuries resulting in perforation or globe rupture (Smiljanic 1996).

In addition to the threat of permanent visual impairment, injuries to the orbital region are also potentially very deadly. During World War II, the mortality rate for soldiers with penetrating orbito-cranial wounds was twice as high as with other head injuries (Webster 1946). In World War II, approximately 13% of all skull fractures were to the orbital region; and of those injuries, over half resulted in eye injury, such as globe rupture and traumatic enucleation. One of the reasons for the high mortality rate is that the orbital roof of the skull is relatively weak and that objects can easily pass through the orbital plate into the frontal lobes of the brain; also, the optic canal and the superior orbital fissure provide access to the cranial cavity without encountering any bone (Biehl 1999). The causes for these types of wounds are similar to those of nearly all other wound types. Of orbital, cranial, and facial fractures as a result of war injuries, over 50% of the fractures were the result of explosive devices (Ivanovic 1996).

The most recent US conflict that documents ocular injuries is the first Persian Gulf War (Operation Desert Shield and Operation Desert Storm). Several studies have been published to analyze the wounds incurred by soldiers involved in the conflict. Of a study of the wounded that were evacuated to US Army Seventh Corps hospitals, approximately 17.3% suffered head wounds (Carey 1996). Of those head wounds, approximately one-third were wounded in the eye (Table 1).

Table 1: Distribution of head injuries treated at a US Army Corps hospital during Operation Desert Storm.
(adapted from Carey 1996)

Head Wound Location	Number of Injuries (%)
Eye	8 (33)
Face	7 (29)
Forehead	4 (17)
Subocciptal	1 (4)
Temporal	1 (4)
Unknown	3 (13)
Total	24 (100)

During Operation Desert Storm, approximately 1/3 of the wartime ocular injuries were corneo-scleral lacerations, as well as additional injury pathologies that included intraocular and corneo-scleral foreign bodies (Mader 1993). Though each injury is not reported by causation, the vast majority of the injuries reported in this study are classified as unknown blast injuries (78 patients), with the second leading cause of eye injury being classified as mines (19 patients). Overall, this indicated that over 78% of all ocular injuries treated in Operation Desert Storm were the result of blast fragmentation (Mader 1993).

BENEFITS OF EYE PROTECTION

According to the Office of the Assistant Secretary of Health, in the civilian sector, studies show that only about 1.5% of those suffering an eye injury were wearing protective goggles or eyewear at the time of their injury, with only 10% wearing any type of eyewear at all (1993). There are far fewer penetrating eye injuries in the civilian sector, and possibly due to the lower

energy levels and lower amount of debris, the long-term injury prognosis for civilian eye injuries is much better than for military service related eye injuries (Biehl 1999).

Protective equipment in warfare has been proven to be effective in reducing the number of battle casualties. During the initial phases of the Korean conflict, approximately 20% of all casualties suffered chest wounds. As protective flak jackets were issued to combat soldiers, the incidence of chest injuries decreased to 8% (Biehl 1999). Similarly, numerous studies have been performed to show the benefits and reduced risk of eye injuries as a result of wearing eye protection. It is commonly reported that over 90% of eye injuries would be preventable if the injured person had utilized protective eyewear (Biehl 1999, Buckingham 2005).

The protection of the eye in warfare has been long recognized, with publications describing the ability to prevent penetrating and impact injuries. During World War I, military ophthalmologists noted that of the many penetrating eye injuries they had treated, the majority were due to small particles (Cruise 1917). To mitigate this eye injury risk, various types of protective visors were devised, including some chain mail shields. Whether any of these shields were actually used in combat is unknown; however, such devices likely presented a minimal protective benefit at the high cost of decreased visual acuity.

In contrast to early attempts at eye protection, the effectiveness of protective eyewear has been proven in the modern military environment. Several studies have been performed that demonstrate the effectiveness of protective glass and plastic lens in protecting the eye from ballistic impact (Stewart 1961, Simmons 1984). Unfortunately, just as in the civilian sector, it is not the inability of the eyewear to effectively protect against injury, rather the lack of use of protective eyewear that leads to injury.

In a retrospective study performed on Israeli army personnel, it was observed that the Israeli troops were issued protective eyewear after the Arab-Israel conflict of 1973. Following the issue of such goggles, the only eye injuries sustained by Israeli soldiers during conflict were sustained

by soldiers who removed their glasses because the glasses were felt to limit their field of view. Soldiers who were using their protective eyewear sustained no eye injuries (Belkin 1984). A total of 15 eye injuries were suffered by US troops during Operation Just Cause in Panama. Of those 15 injuries, military ophthalmologists believe that 14 of those injuries would have been preventable if the troops had been wearing early model ballistic and laser protection goggles (Biehl 1999). Of the cases reviewed by Heier *et al.* (1993) from Operation Desert Storm, only three of 92 US Army personnel were wearing their protective goggles at the time of ocular injury. Fortunately, despite the lack of protective equipment, only a very small percentage (0.4%) of eye injuries reported were globe ruptures.

Analyzing unofficial ocular injury data collected at the Walter Reed Army Medical Center (WRAMC) from the current military actions in Iraq and Afghanistan, over 2/3 of US soldiers who suffer a serious eye injury are not wearing proper eye protection at the time of their injury. Most of the serious ocular injuries are intraocular foreign bodies (31% of all patients) and globe rupture (25% of all patients), along with orbital fractures (27% of all patients) and other orbital injuries (25% of all patients). Based on the injury data of only those patients who were wearing protective eyewear at the time of their injury, it appears that protective equipment lowers the risk of both corneo-scleral lacerations and intraocular foreign bodies. However, the use of protective equipment may actually increase the chance of orbital fracture, as well as less serious injuries such as corneal abrasion. As a testament to the improved quality of ophthalmologic care, a great percentage (63%) of documented out-going patients with severe eye injuries recover to a visual acuity of 20/50 or better.

Without question, the merits of the proper eye protection in reducing the number of ocular injuries have been proven. But the question remains how to discern between different types of eye protection and what types of protection are best in certa*in-situ*ations? Various groups such as NOCSAE and ANSI, for the civilian sector, as well as military biomechanics groups, seek to answer this question using experimental tests and surrogate human headforms. These physical tests are conducted with the intent that data will be generated to discern differences in the performance of various styles or designs of protective eyewear.

ATD HEADFORMS

Current anthropometric test device (ATD) headforms lack instrumentation and facial features to allow detailed assessment of eye or discrete facial injuries (Figure 4). The current state-of-the-art ATD headform used for most impact biomechanics testing is the Hybrid-III headform, which is typically instrumented with a tri-axial accelerometer mounted at the center of gravity of the head.

Figure 4: The Hybrid-III headform lacks detailed facial features.

The resultant linear acceleration of the head center of gravity over time has been used to calculate head injury measures. The injury criterion most commonly used for head injury assessment is Head Injury Criteria (HIC), which can be used to assess global injuries to the skull and the brain (Eppinger 1999). Although previous research has shown different injury tolerance values for different facial bones, the HIC cannot distinguish between impacts at different regions of the skull; therefore, HIC assumes equal probability of injury for the entire skull. Additionally,

because of the limited array of instrumentation, there is no way of detecting any type of impact to the eyes and assess eye injury risk.

Other ATD headforms are used for standards testing of protective goggles and other eye protective equipment. The American National Standards Institute (ANSI) headform was developed from the Hybrid-II ATD, the predecessor to the Hybrid-III. While both the ANSI and the Hybrid-II headforms include geometric representations of the eyes, nose, and mouth, the difference between the ANSI headform and the Hybrid-II headform is the detailed ear (Figure 5). The ear allows eye and face protection to be worn correctly on the headform during testing. Although this headform's main application is standards testing for eye and facial protective equipment, it is not capable of predicting eye or facial injuries, because it carries no instrumentation. Instead, protective devices are evaluated for pass-fail based on whether there is contact to the eyes or face, as well as inspection of the structural integrity of the protective equipment post-impact.

Figure 5: The ANSI headform has the correct anthropometric features for testing eye and face protection, but no instrumentation for measuring impact forces.

Additional ATD headforms, such as the National Operating Committee on Standards for Athletic Equipment (NOCSAE) headform or the THOR (Test device for Human Occupant Restraint)

exist for the purposes of evaluating injury risk to the head, with THOR even having four distinct facial regions with load cell instrumentation. However, neither of these headforms have the capability of measuring impacts to the eyes nor assessing eye injury risk.

FOCUS HEADFORM

The purpose of this dissertation is to present the development and validation of the synthetic eye and eye injury criteria developed for use in the FOCUS headform. In order to assess the capability of protective equipment in reducing eye and facial injuries, a new advanced headform is under development that can predict fracture of facial bones, as well as eye injury from impact loading. Because of its emphasis on eye and orbital injuries, the name of this new advanced headform will be the FOCUS Headform, which stands for Facial and Ocular CountermeasUre Safety Headform.

The FOCUS headform is being developed as a new headform for integration onto a linear slider table using a Hybrid-III ATD neck assembly or directly mounted to a Hybrid-III ATD. The external geometry of the FOCUS headform is designed to replicate the 50^{th} percentile male soldier across the three branches of the military (Army, Navy, and Air Force). This geometry is represented by a physical headform known as the USAARL headform (Figure 6).

Figure 6: The USAARL headform models the 50th percentile tri-services soldier facial anthropometry.

The geometry of the USAARL headform was imported into a computer aided design (CAD) program (Figure 7). This geometry served to define the exterior envelope of the FOCUS headform; the internal structures of this headform were then designed to accommodate the specific sensor requirements while maintaining the mass and inertial properties necessary for biofidelic response of the head to impact loading. Specific design and packaging work was performed by engineering personnel at Denton ATD, Inc. (Milan, OH).

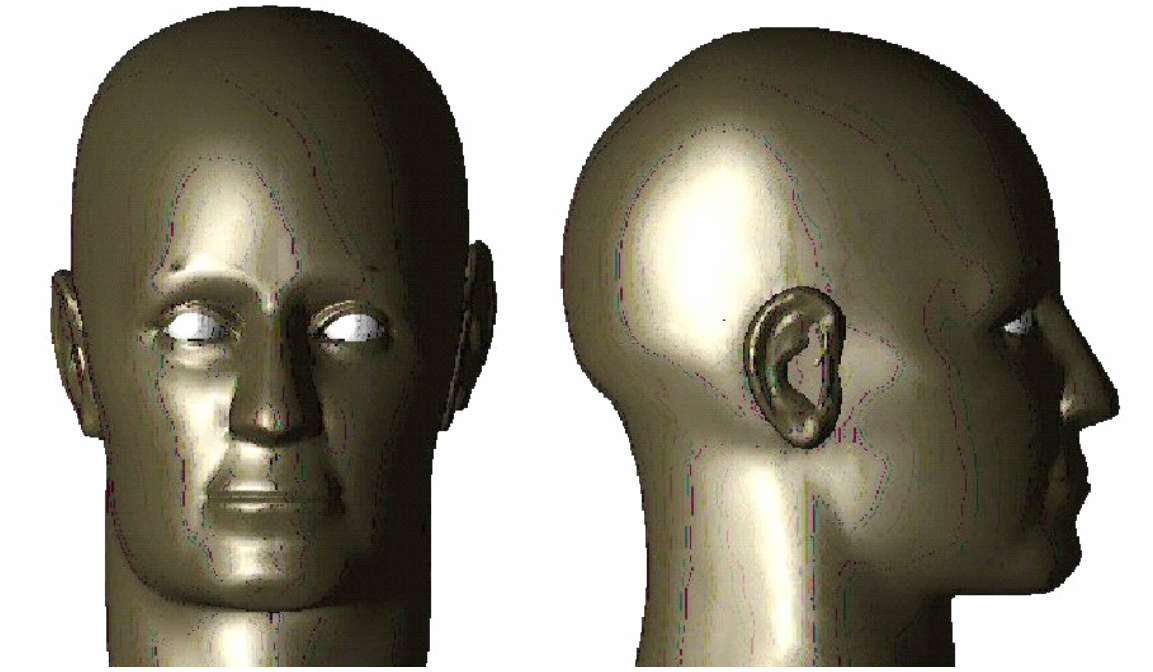

Figure 7: The FOCUS headform exterior geometry is modeled after the specified USAARL headform.

In order to assess the severity of blows to various regions of the face, the skull is segmented into various sensing areas consistent with the anthropometric regions of the human skull. Five facial bones are monitored for injury with the frontal, zygoma, and maxilla monitored separately on left and right sides, and the nasal and mandible monitored as individual regions with no distinction between left and right sides (Figure 8).

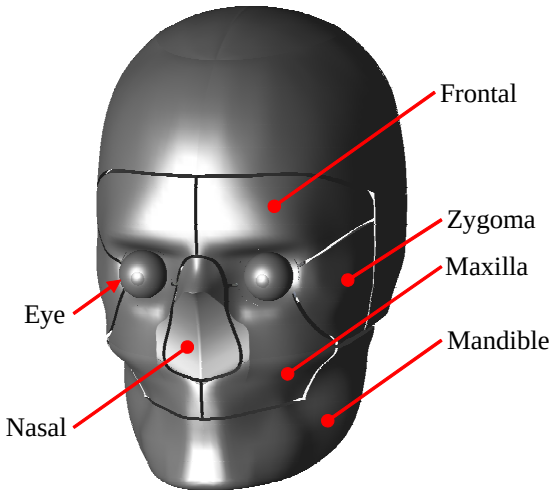

Figure 8: Segmentation of instrumented FOCUS headform.

Each facial bone segment is monitored by a three-axis load cell capable of detecting loads imparted onto this facial region from any direction. Injuries are predicted by correlating measured loads from the load cells to known failure limits from previously analyzed impact tests using human cadavers (Hodgson 1967, Melvin 1969, Schneider 1972, Nyquist 1986, Yoganandan 1993, Hopper 1994, Allsop 2001, Viano 2004).

In addition to the facial segmentation and measurements from facial load cells, the headform is capable of predicting eye injury risk. This is accomplished via a modular design capable of testing using a synthetic eye for blunt impacts or a frangible eye for penetrating impacts (Figure 9).

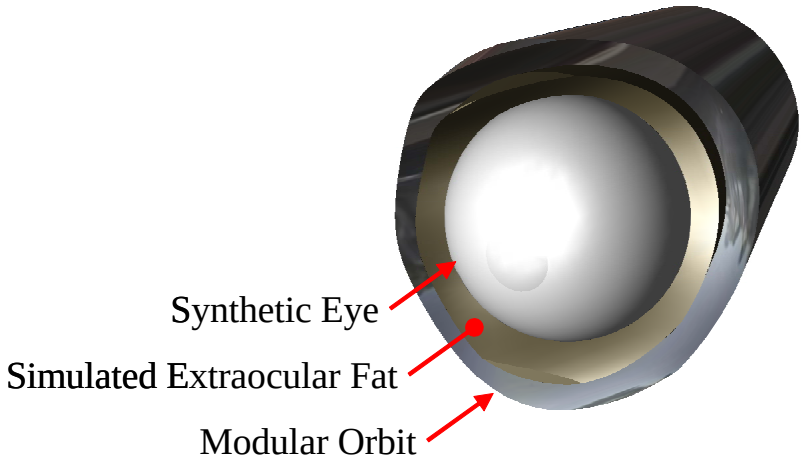

Figure 9: Synthetic eye in modular simulated orbit. The synthetic eye and simulated extraocular fat can be removed for use of frangible eyes as well.

The synthetic eye is simulated eye that matches as closely as possible the force-deflection characteristics of the human eye *in-situ*. Due to the modularity of the FOCUS headform design, the orbit of the headform is a removable mounting cup, which allows a frangible eye to be placed in the headform where penetrating injuries are expected. Frangible eyes allow the user to test for penetrating injuries using post-mortem human or porcine eyes, as well as potentially other surrogates.

A uni-axial load cell at the posterior of the modular orbit is used for injury assessment. The load cells measure impact loads transmitted to the eye and surrounding soft tissue. Injury assessment is performed by correlating the loads measured by the eye load cells to the injury risk functions developed from experimental eye impact tests and computational models of eye impacts.

Prior to the implementation of the FOCUS headform for assessment of facial and eye injury risk, the advanced ATD head will be tested, evaluated, and injury responses of each of the sensors validated. Each of the discretized facial load cells and the synthetic eyes will be subjected to impact testing with blunt objects and injury risk functions will be verified that known injurious events from cadaver test data are likewise measured to be injurious events by the advanced headform. As previously stated, the purpose of this dissertation is to present the development and validation of the synthetic eye and eye injury criteria developed for use in the FOCUS headform.

CONCLUSION

The relative severity of both eye and facial injuries is much greater for the military than in the civilian population; however, these injuries in both the civilian and military sectors can be severely debilitating and pose an enormous health cost. Due to a lack of instrumentation, the prediction of eye and facial injuries using anthropomorphic test devices is not currently possible. The current study presents a new technology currently being developed to determine the risk of eye and facial injuries from impacts. The final, validated FOCUS headform will allow for accurate assessment of the effectiveness of goggles, faceshields, and other protective devices for preventing serious eye and facial injuries. It is expected that once fully developed, this technology will be useful not only for the military to evaluate protective equipment prior to deployment, but also will be useful in the civilian population for evaluation of various facial impact scenarios, such as sports injuries and automotive accidents.

RESEARCH OBJECTIVES

This dissertation is expected to yield several new and significant contributions to the field of injury biomechanics. The research objectives from these studies are designed for the purpose of developing an ATD headform that is capable of measuring impacts to the eyes and assessing injury risk for a number of different types of eye injuries. This headform will be able to be used both to evaluate the risk of an object directly causing an eye injury, and also indirect injuries, such as evaluating protective equipment's ability to prevent an eye injury from occurring. Although not the focus of discussion within this document, the headform will also be able to measure and predict the risk of injuries due to impacts to the facial region of the skull.

At the conclusion of this research program, multiple research objectives have been realized:

1. The effects of post-mortem extraocular muscles on the force-deflection and injury response of the eye to blunt trauma will have been determined.
2. The projectile characteristics which are the most significant predictors of eye injury will have been determined and used to generate injury risk curves to predict the likelihood of eye injuries from specific impacts.
3. The amount of experimental data on globe rupture will have been increased through additional experimental tests, and injury risk functions for globe rupture from blunt projectile impacts will have been determined.
4. The relationship between projectile parameters and resultant tissue level response of the eye by use of a computational model of the eye will have been determined.
5. A biofidelic synthetic eye for use in the FOCUS headform will have been developed, tested and validated for measuring eye impact scenarios and predicting injury risk.

Ultimately, this research must be combined into the final product of an advanced ATD headform; the headform will be validated for blunt impacts to the eye and assessed for its capability to predict eye injury risk.

REFERENCES

Aylward WG, Cooling RJ, Leaver PK. (1993) Trauma-induced retinal detachment associated with giant retinal tears. Retina 13: 136.

Belkin M, Treister G, Doton S. (1984) Eye injuries and ocular protection in the Lebanon War, 1982. Israeli Journal of Medical Science 20: 333-338.

Berger RE. (1978) A model for evaluating the ocular contusion injury potential of propelled objects. Journal of Bioengineering 2: 345-358.

Biehl JW, Valdez J, Hemady RK, Steidl SM, Bourke DL. (1999) Penetrating eye injury in war. Military Medicine 164(11): 780-784.

Bonnet H, Fleury J. (1991) Management of retinal detachment after penetrating eye injury. Graefes Arch Clin Exp Ophthalmol 229: 539.

Bron, A.J., Tripathi, R.C., Tripathi, B.J. (1997) Wolff's anatomy of the eye and orbit, 8th edition. Chapman and Hall, London.

Buckingham R.S., Whitwell K.J., Lee R.B. (2005) Cost analysis of military eye injuries in fiscal years 1988-1998. Military Medicine 170: 196-200.

Carey M.E. (1996) Analysis of wounds incurred by U.S. Army seventh corps personnel treated in corps hospitals during operation desert storm, February 20 to March 10, 1991. Journal of Trauma 40(3S): 165S-169S.

Chisholm L. (1969) Ocular injury due to blunt trauma. Applied Therapeutics 11(11): 597-598.

Cruise R. (1917) Protection of the eye in warfare. British Journal of Ophthalmology 1: 489-492.

Duma SM, Kress TA, Porta DJ, Woods CD, Snider JN, Fuller PM, Simmons RJ (1996) Airbag-induced eye injuries: a report of 25 cases. The Journal of Trauma: Injury, Infection, and Critical Care 41(1): 114-119.

Duma SM, Jernigan M, Stitzel JD, Herring I, Crowley J, Brozoski F, Bass C (2002a) The effect of frontal air bags on eye injury patterns in automobile crashes. Archives of Ophthalmology 120(11): 1517-1522.

Duma SM, Jernigan MV (2002b) The effects of airbags on orbital fracture patterns in frontal automobile crashes. Ophthalmic Plastic and Reconstructive Surgery 19(2): 107-111.

Eppinger, R., Sun, E., Bandak, F., Haffner, M., Khaewpong, N., Maltese, M., Kuppa, S., Nguyen, T., Takhounts, E., Tannous, R., Zhang, A., Saul, R. (1999) Development of Improved Injury Criteria for the Assessment of Advanced Automotive Restraint Systems - II. NHTSA, USA.

Fineman, M.S., Fischer, D.H., Jeffers, J.B., Buerger, D.G., Repke, C. (2000) Changing trends in paint ball sport related ocular injuries. Archives of Ophthalmology 118(1): 60-64.

Ghafouri A, Burgess SK, Hrdlicka ZK, Zagelbaum BM (1997) Air bag - related ocular trauma. American Journal of Emergency Medicine 15(4): 389-392.

Giovinazzo VJ. (1987) The ocular sequelae of blunt trauma. Adv Ophthalmic Plast Reconstr Surg 6: 107.

Hansen GA, Stitzel JD, Duma SM (2003) Incidence of elderly eye injuries in automobile crashes: The effects of lens stiffness as a function of age. Association for the Advancement of Automotive Medicine, 47th Annual Proceedings, Lisbon Portugal.

Heier JS, Enzenauer RW, Wintermeyer SF, *et al.* (1993) Ocular injuries and diseases at a combat support hospital in support of Operations Desert Shield and Desert Storm. Archives of Ophthalmology 111: 795-798.

Ivanovic A, Jovic N, Vukelic-Markovic S (1996) Frontoethmoidal fractures as a result of war injuries. Journal of Trauma 40(3S): 177S-179S.

Kuhn F, Collins P, Morris R, Witherspoon CD (1994) Epidemiology of motor vehicle crash-related serious eye injuries. Accident Analysis and Prevention 26(3): 385-390.

Kuhn, F., Morris, R., Witherspoon, C.D. (1995) Eye injury and the airbag. Current Opinion in Ophthalmology 6(iii): 38-44.

Kuhn F, Morris R, Witherspoon CD, *et al.* (2000) Serious fireworks-related eye injuries. Ophthalmic Epidemiology 7: 139-148.

Libertiny GZ (1995) Air bag effectiveness: Trading major injuries for minor ones. SAE International Congress and Exposition.

Listman, D.A. (2004) Paintball injuries in children: more than meets the eye. Pediatrics 113(1): e15-e18.

Lueder GT (2000) Airbag associated ocular trauma in children. Journal of Ophthalmology 107(8): 1472-1475.

Mader THL, Aragones JV, Chandler AC, *et al.* (1993) Ocular and ocular adnexal injuries treated by United States military ophthalmologists during Operation Desert Shield and Desert Storm. Ophthalmology 100: 1462-1467.

Malliaris AC, Digges KH, DeBlois JH (1995) Evaluation of air bag field performance. SAE International Congress and Exposition.

McGwin G, Xie A, Owsley C (2005) Rate of eye injury in the United States. Archives of Ophthalmology 123: 970-976.

Office of the Assistant Secretary for Health USA: Health Reports. (1993) Public Health Report 108: 1-8.
Parver LM. (1986) Eye trauma: the neglected disorder. Archives of Ophthalmology 104: 1452-1453.
Pearlman JA, AuEong KG, Kuhn F, Pieramici DJ (2001) Airbags and eye injuries: epidemiology, spectrum of injury, and analysis of risk factors. Survey of Ophthalmology 46(3): 234-242.
Power ED, Stitzel JD, Duma SM, Herring IP, West RL (2002) Investigation of ocular injuries from high velocity objects in an automobile collision. SAE Technical Paper Series 2002-01-0027: 1-8.
Rodriguez, J.O., Lavina, A.M. (2003) Prevention and treatment of common eye injuries in sports. American Family Physician 67: 1481-1488.
Simmons ST, Krohel GB, Hay PB. (1984) Prevention of ocular gunshot injuries using polycarbonate lenses. Ophthalmology 91: 977-982.
Smiljanic NS, Vivi DO. (1996) Combat eye injury: laser photocoagulation phophylaxis of retinal detachment. Journal of Trauma 40: S157-S158.
Stein JD, Jaeger EA, Jeffers JB (1999) Air bags and ocular injuries. Tr. Am. Ophth. Soc.97: 59-82.
Stewart GM. (1961) Eye protection against small high-speed missiles. American Journal of Ophthalmology 51: 80-87.
Stitzel J.D., Hansen G.A., Herring, I.P., Duma S.M. (2005) Blunt trauma of the aging eye. Archives of Ophthalmology 123: 789-794.
Stone W. (1950) Ocular injuries in the armed forces. Journal of the American Medical Association 142: 151-152.
Thach, A.B., Ward, T.P., Hollifield, R.D., et. al. (1999) Ocular injuries from paintball pellets. Ophthalmology 105: 533-547.
Treister B. (1969) Ocular casualties in the Six Day war. American Journal of Ophthalmology 68: 669-673.
Vichnin MC, Jaeger EA, Gault JA, Jeffers JB (1995) Ocular injuries related to air bag inflation. Ophthalmic Surgery and Lasers 26: 542-548.
Vinger, P.F. (1996) Baseball eye protection: the effect of impact by major league and reduced injury factor baseball on currently available eye protectors. International Symposium on Safety in Baseball and Softball, American Society for Testing and Materials.
Vinger PF, Sparks JJ, Mussack KR, Dondero J, Jeffers JB. (1997) A program to prevent eye injuries in paintball. Sports Vision 3: 33-40.
Webster JE, Schneider RC, Lofstrom JE (1946) Observations upon management of orbitocranial wounds Journal of Neurosurgery 3: 329-336.
Wong TY, Smith GS, Lincoln AE, Tielsch JM. (2000) Ocular trauma in the United States Army: hospitalization records from 1985 through 1994. American Journal of Ophthalmology 129(5): 645-650.

CHAPTER 2:
THE EFFECTS OF THE EXTRAOCULAR MUSCLES ON EYE INJURY BIOMECHANICS

ABSTRACT

There are over 1.9 million eye injuries per year in the United States, with blunt impacts the cause of approximately one half of all civilian eye injuries. No previous experimental studies have investigated the effects of the extraocular muscles on the impact response of the eye. A total of ten dynamic impact tests were performed on five human cadaver heads to determine the effects that the extraocular muscles have on the force-deflection and injury response of the eye to blunt trauma. With the muscles left intact, the average peak force was found to be 268 N with a 75% cutoff displacement at 9.4 mm, compared to average peak force of 267 N with a 75% cutoff displacement of 9.9 mm with the muscles transected. From the data available from this study, the peak impact force and overall amount of translation during the impact are not affected by the extraocular muscles. Additionally, from the data presented in this study, the eyes with the extraocular muscles left intact do not rupture in a different injury pattern or at a lower threshold than the eyes with the extraocular muscles transected. Therefore, is believed that the effect of the extraocular muscles is not sufficient to drastically alter the response of the eye under dynamic impact.

INTRODUCTION

There are over 1.9 million eye injuries per year in the United States (McGwin 2005). Some of the most severe eye injuries can occur in automobile accidents, from sports related impacts, in the workplace and even at home (Figure 10) (Chisholm 1969, Berger 1978, Mader 1993, Duma 1996, Vinger 1997, Kuhn 2000, Duma 2002, Rodriguez 2003). Blunt impacts are the largest single cause of eye injuries at approximately one half of all civilian eye injuries (Figure 11) (McGwin 2005).

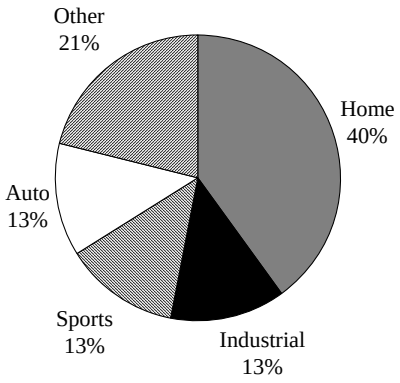

Figure 10: Location where eye injuries are suffered in the civilian sector
(Data in this figure are from McGwin 2005).

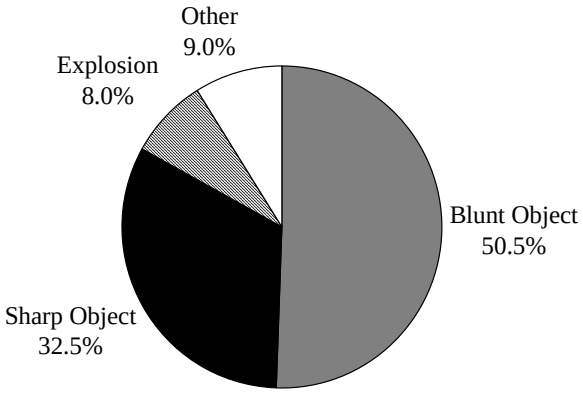

Figure 11: Type of insult which resulted in eye injury in the civilian sector
(Data in this figure are from McGwin 2005).

Previous studies have been performed to determine the injury tolerance of the human eye to globe rupture from blunt impact (Vinger 1999, Bass 2002, Stitzel 2002); however, none have investigated the effects of the extraocular muscles on the impact response of the eye. There are a total of six extraocular muscles of the human eye, four rectus muscles, and two oblique muscles, the superior oblique and the inferior oblique. These extraocular muscles control the movements of the eye. Under typical conditions, these muscles actively control the movements of the eye with less than 0.5 N of force (Clement 1987, Simonsz 1986, Miller 2002). It is currently unknown how the muscle attachments to the eye and the surrounding fatty tissue affect the *in-situ* response of the eye to impact loading, and therefore the potential for injury.

It is hypothesized that the presence of the extraocular muscles may lead to a stress concentration on the corneo-scleral shell and earlier failure *in-situ*, compared to *ex-vivo* experiments where the eye has been enucleated and potted in a simulated orbit for testing (Figure 12). This effect is expected to manifest itself in the force-deflection response of the human eye to blunt impact, with more force being required to force the eye a given distance into the orbit with the muscles intact versus the muscles transected. This is important for the determination of relevant eye impact tests that can be used for the development of eye injury criteria as well as determining

biofidelity requirements for a synthetic human eye. The purpose of the dynamic impact testing is to determine the effects that the extraocular muscles have on the force-deflection and injury response of the eye to blunt trauma.

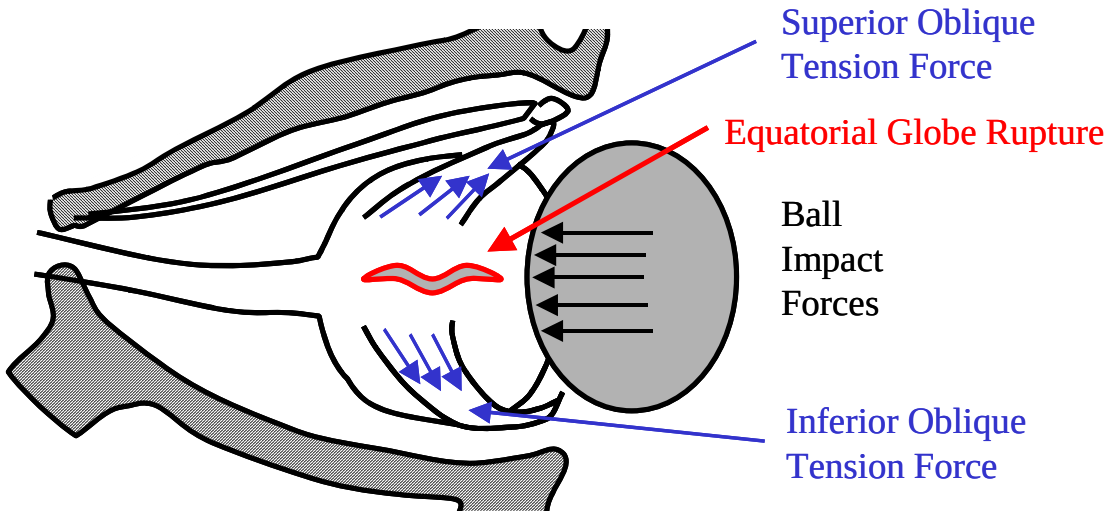

Figure 12: Illustration of research hypothesis that the superior oblique and inferior oblique muscles develop tension forces causing globe rupture or a change in the location of globe rupture as compared to with the muscles transected.

METHODOLOGY

A total of 10 tests were performed on five human cadaver heads. All tests were performed on fresh refrigerated cadavers which were never frozen, tests were performed after the specimens equalized to room temperature. All test procedures were reviewed and approved by the Virginia Tech Institutional Review Board. In order to make a comparison on the effects of the extraocular muscles, in each head the extraocular muscles were left intact on one eye and transected on the contra-lateral eye. The post-mortem human head was mounted in a rigid plastic container using expandable foam. The impact tests were performed using a spring-powered dynamic impactor, which was accelerated to a velocity of approximately 10 m/s before it impacted the eye (Figure 13). The impact tests were performed using a spring-powered, Delrin cylindrical indenter with a diameter of 19 mm and a flat face. The impactor had approximately 30 mm of free travel prior to impacting the eye and after contacting the eye, had approximately 25 mm of travel prior to striking the rubber stops.

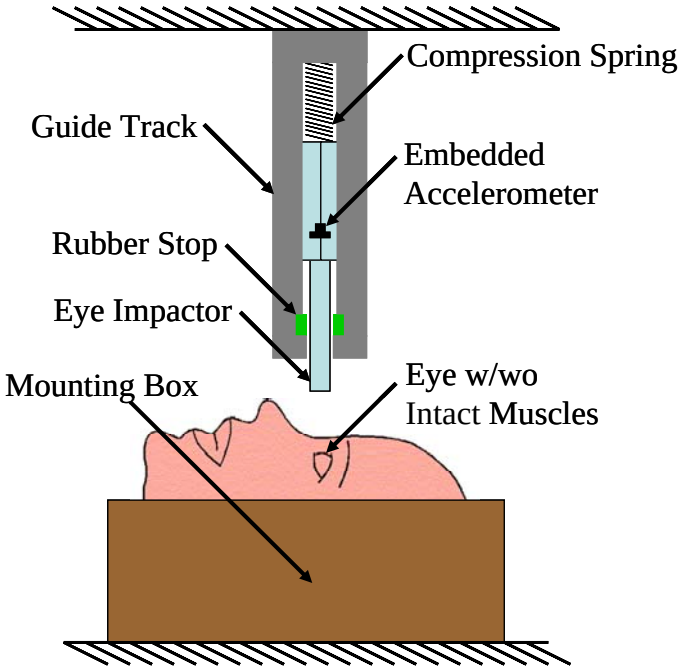

Figure 13: Test apparatus for dynamic extraocular muscle force-deflection impact tests.

An embedded accelerometer (Endevco 7264B-2000, Endevco Corp., San Juan Capistrano, CA) was used to collect data at a sampling rate of 100 kHz for the duration of the test on each eye. Acceleration data was filtered to CFC 1000, then double-integrated to determine impactor tip displacement and also multiplied by the impactor mass (104.05 g) to determine impactor force, this data was used to determine the force-deflection characteristics of the *in-situ* eyes.

For both test conditions, muscles intact and muscles transected, the characteristic average response was determined using a method similar to that described by Lessley *et al.* (2004). Additionally, force-deflection corridors were calculated using the average force-deflection response plus or minus the standard deviation of the force at each displacement step. The force-deflection response is the amount of force required to displace the eye a given distance into the orbit. The force-deflection corridor defines the region where the typical response may be expected, it is defined as the average response plus or minus a standard deviation.

Because it is hypothesized that the presence of the extraocular muscles, in particular, the two oblique muscles will develop tension to resist the force of the impacting projectile, it is possible that a stress concentration will develop around the equator of the eye from these tensile forces. Therefore, the injury outcome of each of the matched pairs of eyes was documented to assess whether or not different injury patterns are seen between the two test conditions.

RESULTS

Force-deflection results for eyes with muscles intact are shown in Figure 14, while tests with the muscles transected are shown in Figure 15. From both datasets (muscles intact and muscles transected) the characteristic average response is calculated (Figure 16 and Figure 17). With the muscles left intact, the average peak force was found to be 268 N with a 75% cutoff displacement at 9.4 mm, compared to average peak force of 267 N with a 75% cutoff displacement of 9.9 mm with the muscles transected. Combining the standard deviation of force to the characteristic average force-deflection, corridors are created for both muscles intact and muscles transected (Figure 18 and Figure 19). Responses of the two different response corridors as well as all tests versus the corridors are shown (Figure 20). Overall, the force-deflection corridors for the eyes with extraocular muscles intact and with muscles transected were very similar, with the corridor being slightly wider for the extraocular muscles intact scenario.

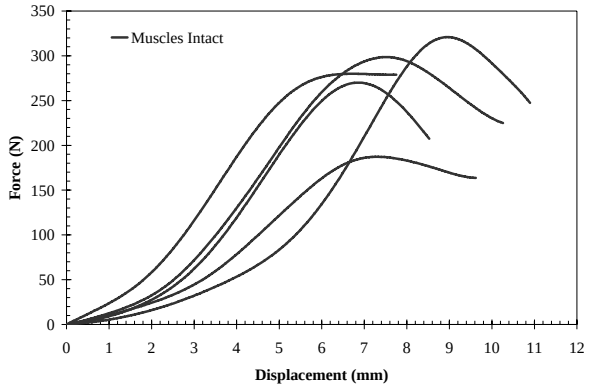

Figure 14: Force-deflection responses of the five *in-situ* eye impact tests with extraocular muscles left intact.

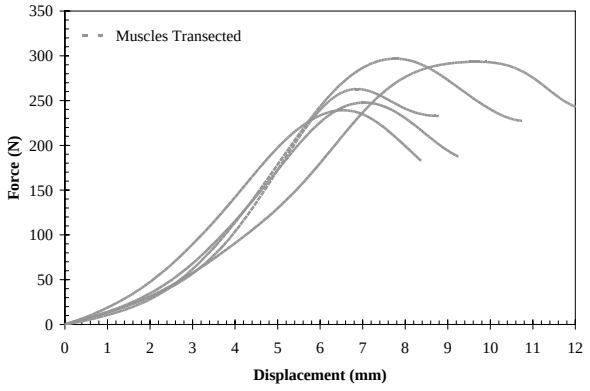

Figure 15: Force-deflection responses of the five *in-situ* eye impact tests with extraocular muscles transected.

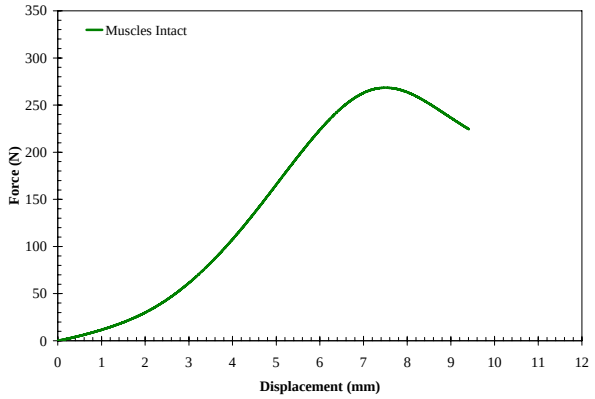

Figure 16: Characteristic average force-deflection response of the *in-situ* eye impact tests with extraocular muscles left intact.

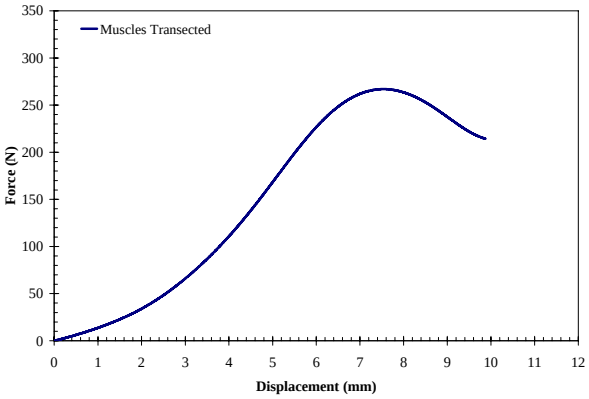

Figure 17: Characteristic average force-deflection response of the *in-situ* eye impact tests with extraocular muscles transected.

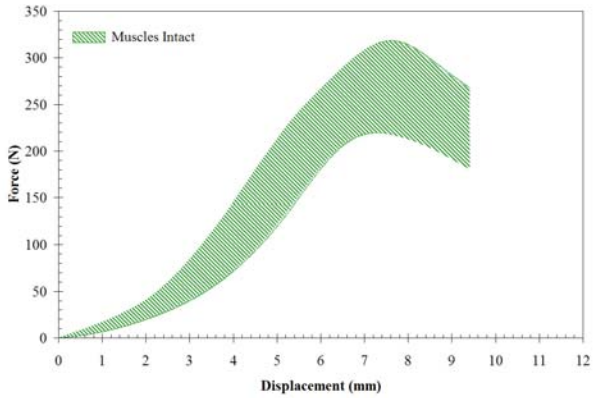

Figure 18: Force-deflection corridors generated from the five *in-situ* eye impact tests with extraocular muscles left intact.

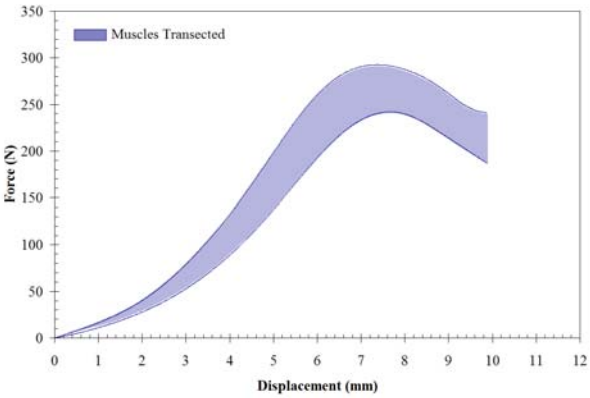

Figure 19: Force-deflection corridors generated from the five *in-situ* eye impact tests with extraocular muscles transected.

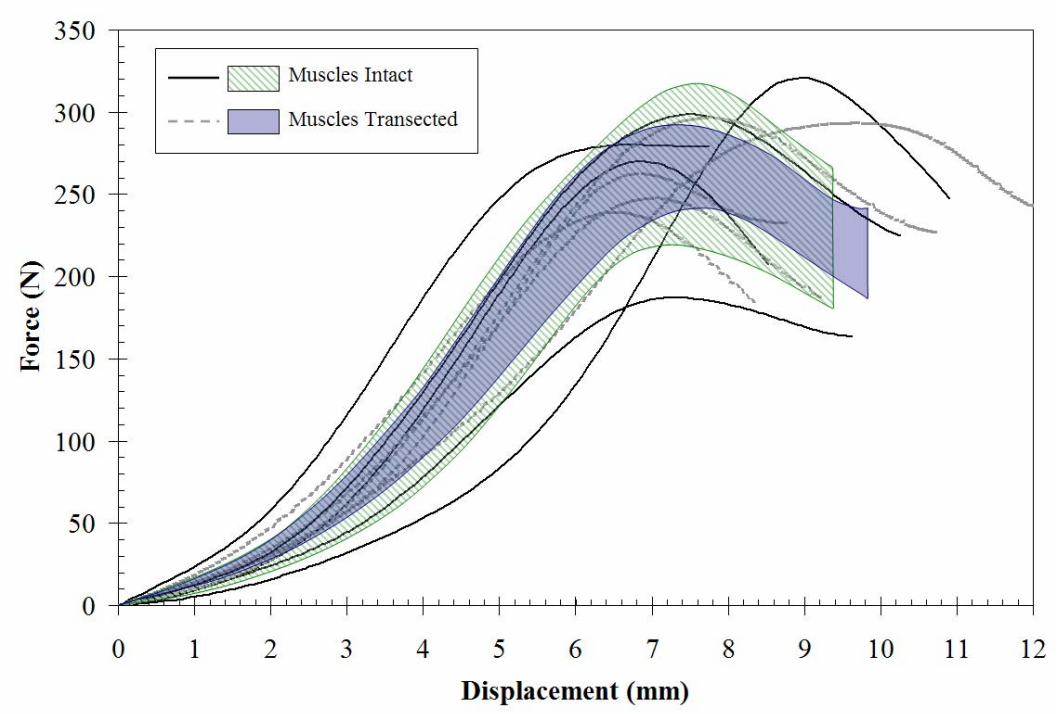

Figure 20: Force-displacement comparison between corridors developed for the two test conditions, with the extraocular muscles intact vs. the extraocular muscles transected. Individual test results are also plotted.

Of the ten dynamic impact tests conducted, there were only three cases of globe rupture observed. All three injuries were similar, and consistent with typically reported cases of globe rupture, spanning from the equator of the eye up to the limbus, at the corneo-scleral interface (Stitzel 2002). Of the three ruptures, two occurred in eyes in which the muscles were transected, while one occurred in the eye where the muscles were left intact. Also, of the three injuries, two occurred in the same test subject, potentially suggesting a weaker overall tolerance to injury in that particular subject. Overall, it was concluded that no appreciable differences were noted in injury outcome (globe rupture) between the eyes with muscles transected versus eyes with muscles left intact. The results indicate that the extraocular muscles do not create an appreciable stress concentration at the muscle insertions to the eye. Therefore, the extraocular muscles do not lead to premature failure of the eye at lower overall loading than enucleated eyes tested *ex-vivo,* for example, in simulated orbits.

DISCUSSION

The purpose of this study was to determine the effects of the extraocular muscles on the impact response of human eyes. From the data available from this study, the peak impact force and overall amount of translation during the impact are not affected by the extraocular muscles. Additionally, from the data presented in this study, the eyes with the extraocular muscles left intact do not rupture in a different injury pattern or at a lower threshold than the eyes with the extraocular muscles transected. Therefore, it is believed that the effect of the extraocular muscles is not sufficient to drastically alter the response of the eye under dynamic impact.

Based on results observed in previous *ex-vivo* studies (Stitzel 2002, Kennedy 2006), the displacement of the eye at rupture is approximately 6 mm to 8 mm. Because these eyes were tested *in-situ*, it was impossible to visually determine the exact timing of rupture from high speed video. Also, because of the presence of extraocular tissue around the eye, there was not a sudden drop in load to indicate when failure may have occurred. It is thought that perhaps, even in the case of rupture, the surrounding tissues of the orbit and the large diameter impactor would impede the sudden release of intraocular fluids and effectively shield the impactor from measuring a sharp drop-off in the impactor force.

Qualitatively, with the extraocular muscles left intact, a slightly stiffer force-deflection response and less translation occurs to the point of the peak force. However, there is much overlap between the two test scenarios, suggesting a region where the response is the same either with the muscles intact or transected. So, while the extraocular muscles increase the resistive force of the eye and lower the posterior translation during impact, it is not sufficient to drastically alter the response of the eye even if the extraocular muscle attachments are not accounted for. This finding is consistent with that of other researchers (Cirovic 2005) and shows that it is not necessary to account for the effects of extraocular muscles when doing *ex-vivo* eye impact experiments.

A limitation of the current study is that tests were only conducted at one impact energy level. All tests were conducted at approximately 10 m/s, with an impactor energy of up to 5 J. Due to the large surface area of the flat 19 mm diameter impactor tip, the normalized energy of this impactor is a maximum 16,000 J/m^2. This level of normalized energy poses less than a 10 % risk of globe rupture based on the results of other studies (Kennedy 2006). Not surprisingly, most of the tests in this study did not result in globe rupture, with only three out of ten total tests resulting in globe rupture – and two of those injuries from the same specimen, suggesting perhaps a weaker overall tolerance to injury. Based on the results of this study and by Cirovic *et al.* (2005), it is not expected that testing at alternative speeds would have elucidated a different response from the extraocular muscles; however, this is something that may be of interest in the future.

The finding that the extraocular muscles do not influence the injury outcome or the response of the human eye to blunt impact is also important because of the frequent use of porcine and other animal species' eyes as surrogates for human eye impact testing. These species do not have the same anatomical layout of extraocular muscles as that of human eyes and if the extraocular muscles were shown to have a significant effect on determining eye injury response, then the choice of these eyes as surrogates for human eyes would be inappropriate. An equally important factor in the choice of a surrogate species for human eyes is the histology of the corneo-scleral shell and other anatomical structures of the eye. For instance, previous studies have shown an increased tolerance to globe rupture of porcine eyes compared to human eyes (Kennedy 2004, Kennedy 2006) and overall increased thickness of the porcine sclera to the human sclera (Olsen 1998, Olsen 2002).

Additionally, it should be noted that the actual orbital dimensions vary from individual to individual. It is currently unknown how various geometrical changes within the orbit would affect the force-deflection response of the eye. This would potentially be an interesting topic for a computational modeling study.

CONCLUSION

This purpose of this study was to determine the influence that extraocular muscles have on eye impact response and injury outcome. This is extremely important because much of the eye impact testing reported in the literature utilize enucleated human eyes, potted in a gelatin solution to perform eye impact studies and interpret injury response. In these simulated orbits, the extraocular muscles are no longer intact, and therefore the injury response for these *in-vitro* tests may be different than for eyes that are tested *in-situ*. In order to analyze the effects that the extraocular muscles have on eye impact response, dynamic eye impact tests were conducted using a custom-designed eye impact device. Eyes were tested *in-situ* as matched pairs, with the extraocular muscles from one eye transected, and the extraocular muscles from the contra-lateral eye intact. Similar overall force-deflection and injury responses were observed between the eyes with the extraocular muscles left intact and the extraocular muscles transected. Therefore, it is concluded from this study that the extraocular muscles do not have an appreciable influence on the impact response of human eyes. The results of this study validate the use of gelatin-filled orbits and other testing methods which do not account for the effects of extraocular muscles, as acceptable means to conduct eye injury tests.

REFERENCES

Bass C., Davis M., Stitzel J., Duma S. (2002) Airbag interaction with night vision goggles. Report to the United States Army Aeromedical Research Laboratory, Fort Rucker, Alabama.

Berger, R.E. (1978) A model for evaluating the ocular contusion injury potential of propelled objects. Journal of Bioengineering 2: 345-358.

Chisholm, L. (1969) Ocular injury due to blunt trauma. Applied Therapeutics 11(11):597-598.

Clement R.A. (1987) Description of the length-tension curves of the extraocular muscles. Vision Research 27(3): 491-492.

Cirovic S., Bhola R.M., Hose D.R., Howard I.C., Lawford P.V., Parsons M.A. (2005) A computational study of the passive mechanics of eye restraint during head impact trauma. Computer Methods in Biomechanics and Biomedical Engineering 8(1): 1-6.

Duma S.M., Kress T.A., Porta D.J., *et al.* (1996) Air Bag Induced Eye Injuries: A Report of 25 Cases. J of Trauma. 41(1):114-119.

Duma, S.M., Jernigan, M., Stitzel, J.D., Herring, I., Crowley, J., Brozoski, F., Bass, C. (2002) The effect of frontal air bags on eye injury patterns in automobile crashes. Archives of Ophthalmology 120(11): 1517-1522.

Kennedy EA, Ng TP, McNally C, Stitzel JD, Duma SM (2006) Risk functions for human and porcine eye rupture based on projectile characteristics of blunt objects. Stapp Car Crash Journal 50.

Kennedy, E.A., Voorhies, K.D., Herring, I.P., Rath, A.L., Duma, S.M. (2004) Prediction of severe eye injuries in automobile accidents: static and dynamic rupture pressure of the eye. The Proceedings of the 48th Association for the Advancement of Automotive Medicine Conference, Key Biscayne, Florida.

Kuhn F., Morris R., Witherspoon C.D., *et al.* (2000) Serious fireworks-related eye injuries. Ophthalmic Epidemiol. 7:139-148.

Lessley D, Crandall JR, Shaw CG, Kent RW, Funk JR (2004) A normalization technique for developing corridors from individual subject responses. SAE 2004-01-0288.

Mader, T.H.L., Aragones, J.V., Chandler, A.C., *et al.* (1993) Ocular and ocular adnexal injuries treated by United States military ophthalmologists during Operation Desert Shield and Desert Storm. Ophthalmology 100: 1462-1467.

McGwin, G., Xie, A., Owsley, C. (2005) Rate of eye injury in the United States. Archives of Ophthalmology 123: 970-976.

Miller, J.M., Bockisch, C.J., Pavolvski, D.S. (2002) Missing lateral rectus force and absence of medial rectus co-contraction in ocular convergence. Journal of Neurophysiology 87: 2421-2433.

Olsen, T.W., Aaberg, S.Y., Geroski, D.H., Edelhauser, H.F. (1998) Human sclera: thickness and surface area. American Journal of Ophthalmology 125(2): 237-241.

Olsen, T.W., Sanderson, S., Feng, X., Hubbard, W.C. (2002) Porcine sclera: thickness and surface area. Investigative Ophthalmology and Visual Science 43(8): 2529-2532.

Rodriguez, J.O., Lavina, A.M. (2003) Prevention and treatment of common eye injuries in sports. American Family Physician 67: 1481-1488.

Simonsz H.J., Kolling, G.H., Kaufman, H., van Dijk, B. (1986) Intraoperative length and tension curves of human eye muscles including stiffness in passive horizontal eye movement in awake volunteers. Archives of Ophthalmology 104(10): 1485-1500.

Stitzel J.D., Duma S.M., Cormier J.M., Herring I.P. (2002) A nonlinear finite element model of the eye with experimental validation for the prediction of globe rupture. Stapp Car Crash Journal 46.

Vinger P.F., Duma S.M., Crandall J.R. (1999) Baseball hardness as a risk factor for eye injuries. Archives of Ophthalmology 117: 354-358.

Vinger, P.F., Sparks, J.J., Mussack, K.R., Dondero, J., Jeffers, J.B. (1997) A program to prevent eye injuries in paintball. Sports Vision 3:33-40.

CHAPTER 3:
DETERMINATION OF SIGNIFICANT PARAMETERS FOR EYE INJURY RISK FROM PROJECTILE CHARACTERISTICS

ABSTRACT

Eye injuries affect a large proportion of the population and are expensive to treat. This chapter presents a parametric analysis of experimental data to determine the most significant factors for predicting ocular injuries or tissue lesions. Using logistic regression, statistical values were generated to determine significant projectile characteristics for predicting ocular injury in published studies. Projectiles included BBs, metal rods, and foam particles with velocities ranging from 2 m/s to 122 m/s. A normalized energy (energy per projected area) value was found as the best predictor for ocular injury. Using this predictor, a 50% injury risk of corneal abrasion, lens dislocation, hyphema, retinal damage, and globe rupture was found to be 1,503 J/m^2, 19,194 J/m^2, 20,188 J/m^2, 30,351 J/m^2, and 23,771 J/m^2, respectively. Normalized energy was the most significant predictor of injury type and tissue lesion. This finding can be used to minimize the risk of ocular injury for consumer products as well as understand injury potential of objects in sports, automotive accidents, and other impact environments.

INTRODUCTION

In the civilian sector alone, there are over 1.9 million eye injuries in the United States each year. This results in personal misery and the loss of billions of dollars in direct and indirect costs, making the societal cost of eye trauma enormous (Parver 1986, Schein 1988, Lueder 2000, McGwin 2005). Some of the most severe eye injuries are caused by high speed projectiles from fireworks, sports equipment, firearms and BB guns, or contact with various parts of the car's interior in automobile crashes (Berger 1978, Duma 1996, Vinger 1997, Kuhn 2000, Duma 2002). Sporting equipment most often involved in eye injuries includes baseballs, squash balls, and hockey sticks. Fingers and elbows of the players are also common sources (Vinger 1997, Chisholm 1969, Vinger 1999). A relatively new phenomenon which is responsible for numerous eye injuries is Airsoft guns (Fleischhauer 1999, Endo 2000, Endo 2001).

In the military sector, the rate of eye injuries suffered in conflict has risen steadily throughout the decades from less than 1% of all battle casualties in the American Civil war to more than 13% of all casualties in Operation Desert Storm (Heier 1993). A review of ocular injuries treated at the Walter Reed Army Medical Center reveals that over 66% of US soldiers who suffer a serious eye injury are not wearing proper eye protection at the time of their injury (Kennedy 2006). Most of the serious ocular injuries are intraocular foreign bodies (31% of all patients) and globe rupture (25% of all patients) which, are likely caused by shrapnel and debris striking the eye.

Currently, eye injury assessment tools for automobile, consumer product, sports, and military are not based on biomechanically determined injury limits. For automobile safety, anthropometric test devices (ATDs) such as the Hybrid-III dummy have no capability for measuring eye injury risk. The THOR dummy, utilizes four facial load cells to predict facial injury, but has no eye injury assessment capability. Conversely, the National Operating Committee on Standards for Athletic Equipment (NOCSAE) headform and the American National Standards Institute (ANSI) Alderson headform have detailed facial geometry including the eyes, nose, and mouth, but no instrumentation to determine eye or other head injury.

Due to the lack of appropriate measurement capabilities of these headforms, being able to predict eye injury occurrence based on missile characteristics would help both prevention and treatment. While numerous studies have examined the eye's response to projectile loading, none have attempted to combine all previously published experimental data to develop risk functions for the most common eye injuries (Berger 1978, Vinger 1999, Weidenthal 1964, Weidenthal 1966, Delori 1969, McKnight 1988, Green 1990, Galler 1995, Duma 2000, Scott 2000, Stitzel 2002). These risk functions could then be utilized to predict the occurrence of eye injury from various projectile impacts, or to evaluate the effectiveness of eye protective equipment in reducing the risk of eye injury.

Therefore, the purpose of this study, based on a metaanalysis of data from previous eye impact experiments, is to determine which projectile characteristics are the most significant predictors of

eye injury and to generate injury risk curves for significant predictors. These curves allow for the calculation of the probability of eye injury based on the energy and geometry of various projectiles.

METHODOLOGY

A literature review was conducted on ocular contusion experiments. Data from all relevant publications were sorted according to projectile characteristics such as type, mass, and diameter, as well as tissue lesion. Since eyes that have undergone radial keratotomy (RK) are known to sustain open globe injury at lower energy levels than eyes without RK, only un-operated eyes were included in this study (McKnight 1988, Galler 1995, Peacock 1997).

All types of tissue lesions potentially resulting from projectile impact were included in the dataset and the occurrence or lack of each pathology was noted. Five eye injury groups were established: corneal abrasion, hyphema, lens dislocation, retinal damage, and globe rupture. For simplification, certain pathologies with common anatomical and/or physiological characteristics were combined into a single group. For instance, hyphema includes hemorrhage whether originating from iris, ciliary body, or angle trauma, and retinal trauma, whether tears or detachment, was termed as retinal damage.

Eye specimens evaluated for this study include human, porcine, monkey, and cat. Some studies have employed anesthetized living animal models for impact experiments. Since no studies have concluded that *in-vivo* eyes suffer injury at different energy levels than fresh *in-vitro* eyes, *in-vivo*, *in-situ*, and *in-vitro* studies were analyzed together. Projectiles used to impact the eye include BBs, foam, metal rods, baseballs, and squash balls. Impact velocities ranged from 2 m/s to 122 m/s.

A logistic regression analysis was performed on the experimental data to determine significant predictors for eye injury based on p-values and Goodman-Kruskal Gamma values (a correlation

coefficient with values near 0.0 indicating no association between two subjects and values of 1.0 representing high association between predictor and injury).

Predictors used in the statistical analysis include normalized energy and kinetic energy. The normalized energy value of energy per projected area of the projectile (Equation 1). The projected area is the contact surface area for a flat impacting object or the cross-sectional area of a sphere.

$$Normalized\ Energy\ \left(\frac{J}{m^2}\right) = \frac{Kinetic\ Energy}{Projected\ Area} = \frac{1/2 mv^2}{\pi r^2} (\ for\ a\ sphere\ ) \qquad \text{Eq. (1)}$$

RESULTS

A total of eight studies have already been identified in the literature that involve projectile impact experiments on eyes. These eight studies contained 104 individual tests with some noting a variety of observed injuries. Eye injuries noted for some experiments include corneal abrasion, retinal detachment, and globe rupture (Table 2).

Table 2: Summary of previous ocular experiments.

Injury Studied	Projectile	Cases	Studies
Corneal Abrasion	Foam, Metal Rod	24	Duma (2000), Scott (2000)
Hyphema	Foam, Metal Rod, BB	39	Weidenthal (1964), McKnight (1988), Scott (2000)
Lens Dislocation	Foam, Metal Rod, BB	44	Weidenthal (1964), Weidenthal (1966), Duma (2000), Scott (2000)
Retinal Damage	Foam, Metal Rod, BB	26	Weidenthal (1966), Duma (2000), Scott (2000)
Globe Rupture	Foam, Metal Rod, BB, Baseball, Squash Ball, Golf Ball	71	Weidenthal (1964), Delori (1969), Green (1990), Umlas (1995), Duma (2000), Scott (2000), Stitzel (2002)

The statistical analysis revealed that normalized energy was the most effective injury predictor, yielding the most statistically significant p-values and Goodman-Kruskal Gamma values (Table 3 and Table 4). Both mass and velocity were considered poor predictors, with relatively higher p-values and lower Goodman-Kruskal Gamma values in comparison with other measures.

Table 3: Summary of p-values for various eye injuries and predictors.

	Normalized energy (J/m^2)	Diameter (m)	Kinetic energy (J)	Mass (g)	Velocity (m/s)
Corneal abrasion	0.001	0.964	0.001	0.001	0.520
Hyphema	0.001	0.001	0.244	0.005	0.001
Lens dislocation	0.001	0.001	0.678	0.001	0.200
Retinal damage	0.001	0.001	0.001	0.141	0.540
Globe rupture	0.001	0.003	0.019	0.499	0.003

Table 4: Summary of Goodman-Kruskal Gamma values for various eye injuries and predictors.

	Normalized energy (J/m^2)	Diameter (m)	Kinetic energy (J)	Mass (g)	Velocity (m/s)
Corneal abrasion	0.97	0.01	0.97	0.71	0.31
Hyphema	0.94	1.00	0.20	0.82	0.82
Lens dislocation	0.98	1.00	0.26	0.12	0.38
Retinal damage	1.00	1.00	0.92	0.01	0.27
Globe rupture	0.80	0.24	0.51	0.26	0.45

A general form of the injury risk function (Equation 2) can be used with specific injury parameters (Table 5) to predict the probability of injury given a projectile's normalized energy or kinetic energy. The variable "x" refers to a predictor and its corresponding value used for a specific study. The variables "a" and "b" are constants specific to a particular predictor and eye injury. For all predictors of eye injury, a logit analysis was performed to calculate the confidence intervals at 50% risk.

$$\text{Probability of Injury}\,(\%) = \frac{1}{1+e^{a-bx}} \qquad \text{Eq. (2)}$$

Table 5: Injury risk curve coefficients for significant predictors and injury groups.

	Predictor (x)	A	B
Corneal abrasion	Normalized energy (J/m^2)	5.03	0.0034
	Kinetic energy (J)	5.07	27.5371
Hyphema	Normalized energy (J/m^2)	10.60	0.0005
Lens dislocation	Normalized energy (J/m^2)	7.38	0.0004
Retinal damage	Normalized energy (J/m^2)	71.47	0.0023
	Kinetic energy (J)	5.50	5.0481
Globe rupture	Normalized energy (J/m^2)	4.65	0.0002
	Kinetic energy (J)	3.04	0.7688

Among all of the predictors tested, normalized energy yielded the best injury risk curve with the lowest p-values and highest Goodman-Kruskal Gamma values, where all injuries showed normalized energy to be a significant predictor ($p<0.05$ for all cases). The formulation of normalized energy to predict corneal abrasion, lens dislocation, hyphema, retinal damage, and globe rupture are presented (Figure 23). Using normalized energy, a 50% injury risk of corneal abrasion, lens dislocation, hyphema, retinal damage, and globe rupture was found to be 1,503 J/m^2, 19,194 J/m^2, 20,188 J/m^2, 30,351 J/m^2, and 23,771 J/m^2, respectively.

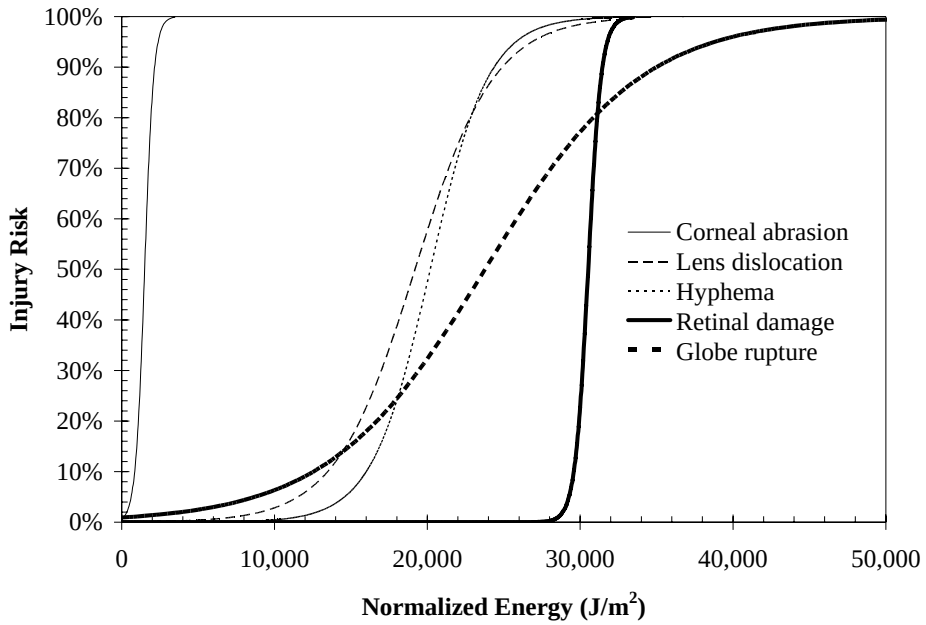

Figure 21: Injury risk curves for corneal abrasion, lens dislocation, hyphema, retinal damage, and globe rupture as a function of normalized energy ($p<0.05$ for all cases).

Occasionally it is more useful and statistically significant to exclude projectile area when evaluating injury risk functions. Kinetic energy alone was not as significant a predictor for ocular injury as normalized energy, yielding less significant p-values and lower Goodman-Kruskal Gamma values. Kinetic energy was found to be a significant predictor for corneal abrasion, retinal damage, and globe rupture ($p<0.05$ for all cases); therefore, injury risk curves for these injuries were also generated (Figure 22). A 50% risk of corneal abrasion occurred at 0.184 J, as opposed to 1.090 J for retinal damage and 3.949 J for globe rupture.

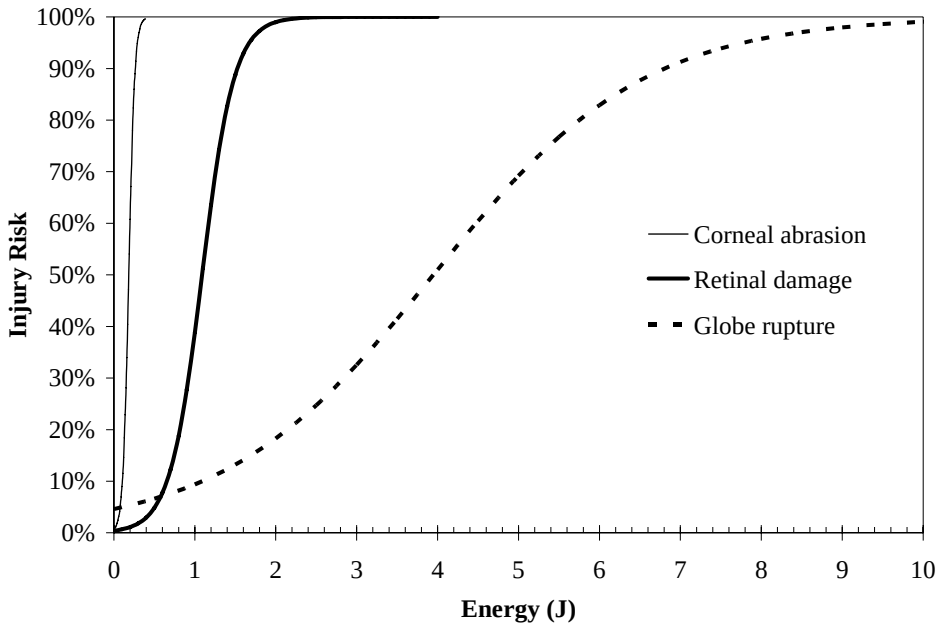

Figure 22: Injury risk curves for corneal abrasion, retinal damage, and globe rupture as a function of kinetic energy ($p<0.05$ for all cases).

For all significant predictors of eye injury, a logit analysis was performed to calculate the confidence intervals at 50% risk (Table 6). In the case of normalized energy for predicting hyphema or retinal damage, insufficient data exists from which to develop confidence intervals, which will be discussed in more detail later in this paper.

Table 6: Confidence intervals for 50% risk of injury.

	Predictor	50% Risk	Lower Bound	Upper Bound
Corneal abrasion	Normalized energy (J/m^2)	1,503	775	2,214
	Kinetic energy (J)	0.184	0.096	0.266
Hyphema	Normalized energy (J/m^2)	20,188	--*	--*
Lens dislocation	Normalized energy (J/m^2)	19,194	1,367	24,242
Retinal damage	Normalized energy (J/m^2)	30,531	--*	--*
	Kinetic energy (J)	1.090	0.810	1.514
Globe rupture	Normalized energy (J/m^2)	23,771	20,194	30,714
	Kinetic energy (J)	3.949	2.865	10.545

* Insufficient data for estimating upper and lower confidence limits.

DISCUSSION

This study was the first to derive injury risk functions based on a pooling and reevaluation of data from previously published eye impact experiments. Many researchers have presented data from eye impact tests and noted injury outcome. While the specific measurements from each test setup may vary, the measurements that are common to nearly every study are the characteristics of the projectile used to impact the eye. Therefore, data pooling such as this yields a larger database able to cover a broader range of projectile characteristics and observed injuries.

Previous experiments attempted to determine thresholds at which specific tissue pathologies in the eye occur. Several studies used projectile characteristics such as velocity and energy to predict the occurrence of various eye injuries. Duma *et al.* (2000) studied corneal abrasion in porcine eyes loaded with foam particles ejected from seamless module covers in automobile airbags. It was determined from the study that the combination of mass and velocity as kinetic energy served as the most significant predictor of corneal abrasion. In the study from Scott *et al.* (2000), the internal structures of enucleated porcine eyes were studied after being impacted by projectiles of various velocities and mass. In conjunction with the Duma study, Scott found that

injury occurrence was directly associated with the kinetic energy of the projectile, while momentum was shown to be a poor predictor. These findings were confirmed in the current study.

Previous experimental studies have determined various factors for predicting eye injuries including tissue level failure stresses (Duma 2000, Scott 2000, Stitzel 2002). While tissue level failure stress provides a clear understanding of the injury mechanism, it is not always feasible to investigate risk in this manner. For the purpose of developing injury risk functions that are applicable, for instance in an instrumented eye of an advanced headform, it is desirable to have a simple injury model that shows high correlation to impact and a high sensitivity to various severity impacts. Therefore, an injury prediction tool based on the energy applied to the eye from the projectile should be an effective means for physically measuring and quantifying eye injury risk.

The overall goal of the research program described in this dissertation is to develop an advanced headform with an instrumented eye for the purposes of evaluating the injury potential of blunt eye impacts. Since the injury risk functions for this study are input based, they could be useful in development of a biofidelic sensor and injury thresholds for a synthetic eye sensor. Projectile tests can be conducted on an instrumented synthetic eye and the sensor outputs calibrated to the predicted injury risk based on the input parameters. This approach to injury threshold determination for ATDs may ultimately yield more accurate injury risk prediction due to the fact that a direct mapping from input energy and known injury risk are correlated to sensor output. A development such as a synthetic eye in an advanced ATD headform would allow experimental testing and evaluation of possible eye injury hazards, even in scenarios such as automobile crash testing where it may be extremely difficult to isolate and determine projectile characteristics that may assault the eye.

The study also has limitations. These originate in certain assumptions that are necessary to achieve a sufficiently large dataset from previously published studies. The analysis described for

this study assumes that there are no species variations between human and animal eyes; it is also assumed that there is no difference between testing *in-vivo* versus *in-vitro*. These assumptions were made based on a lack of experimental data showing that these assumptions cannot be made. Where possible, the results presented in this study will represent the authors' attempts to minimize the effects of such assumptions. Unfortunately, species-specific analysis is not possible for all injury types due to the relative lack of data available for all injury types. With more experimental data it may be possible to elucidate the effects of these assumptions and validate the injury risk curves for use in predicting injury. In the meantime, especially due to the difficulties in testing for those types of injury pathologies, it is strongly felt that the present findings of this study will serve as a reasonable and accurate basis for eye injury prediction for the injury assessment using an advanced, instrumented headform and other experimental models.

CONCLUSION

Many researchers have performed numerous eye impact experiments for the purposes of elucidating injury mechanisms and determining injury thresholds of the eye. This study leverages previously reported data for the purposes of developing injury risk functions for various types of eye injuries, ranging from relatively minor injuries, such as corneal abrasion, to more severe injuries, such as globe rupture. Being able to predict eye injury occurrence based on missile characteristics would help both prevention and treatment. The findings from this study will provide a promising model for evaluating eye injury potential from various eye impacts. The results can be used as an aid to conduct innovative research in impact biomechanics for the military, automotive, aviation, and recreational industries. Specifically, these injury criteria can be used in conjunction with an advanced headform capable of predicting the occurrence of eye and facial injuries for various projectile impacts, or to evaluate the effectiveness of eye protective equipment in reducing the risk of eye injury. The injury risk functions developed in this study will serve as the foundation for the development and validation of injury risk calculations for the advanced eye and facial injury headform.

REFERENCES

Berger R.E.. (1978) A model for evaluating the ocular contusion injury potential of propelled objects. J of Bioengineering. 2:345-358.

Chisholm L.. (1969) Ocular injury due to blunt trauma. Applied Therapeutics. 11(11):597-598.

Delori F., Pomerantzeff O., Cox M.S. (1969) Deformation of the globe under high speed impact: its relation to contusion injuries. Invest Ophthalmol. 8:290-301.

Duma S.M., Jernigan M.V., Stitzel J.D., *et al.* (2002) The effect of frontal air bags on eye injury patterns in automobile crashes. Arch Ophthalmol. 120:1517-1522.

Duma S.M., Crandall J.R.. (2000) Eye injuries from airbags with seamless module covers. J Trauma. 48(4):786-9.

Duma S.M., Kress T.A., Porta D.J., *et al.* (1996) Air Bag Induced Eye Injuries: A Report of 25 Cases. J of Trauma. 41(1):114-119.

Endo S., Ishida N., Yamaguchi T. (2000) The BB gun is equivalent to the airsoft gun in the japanese literature. Archives of Ophthalmology 118: 732.

Endo S., Ishida N., Yamaguchi T. (2001) Tear in the trabecular meshwork caused by an airsoft gun. American Journal of Ophthalmology 131: 656-657.

Fleischhauer J.C., Goldblum D., Frueh B.E., Koerner F. (1999) Ocular injuries caused by airsoft guns. Archives of Ophthalmology 117: 1437-1439.

Galler E.L., Umlas J.W., Vinger P.F., Wu H.K. (1995) Ocular integrity after quantitated trauma following photorefractive keratectomy and automated lamellar keratectomy. Invest Ophthalmol Vis Sci. 36(4):S580.

Green R.P., Jr., Peters D.R., Shore J.W., Fanton J.W., Davis H. (1990) Force necessary to fracture the orbital floor. Ophthal Plast Reconstr Surg. 6(3):211-217.

Heier JS, Enzenauer RW, Wintermeyer SF, *et al.* (1993) Ocular injuries and diseases at a combat support hospital in support of Operations Desert Shield and Desert Storm. Archives of Ophthalmology 111: 795-798.

Kennedy E.A., Manoogian S.J., Duma S.M. (2006) Epidemiology of eye and facial injuries: comparison of civilian and military injury trends. Prepared for United States Army Aeromedical Research Laboratory, CIB Report 2006-020.

Kuhn F., Morris R., Witherspoon C.D., *et al.* (2000) Serious fireworks-related eye injuries. Ophthalmic Epidemiol. 7:139-148.

Lueder G.T. (2000) Airbag associated ocular trauma in children. Journal of Ophthalmology. 107(8):1472-1475.

McKnight S.J., Fitz J., Giangiacomo J. (1988) Corneal rupture following keratotomy in cats subjected to BB gun injury. Ophthalmic Surgery. 19(3):165-167.

Parver L.M. (1986) Eye trauma: the neglected disorder. Arch Ophthalmol. 104:1452-1453.

Peacock L.W., Slade S.G., Martiz J., Chuang A., Yee R.W. (1997) Ocular Integrity After Refractive Procedures. Ophthalmology. 104(7):1079-1083.

Schein O.D., Hibberd P.L., Shingleton B.J., *et al.* (1988) The spectrum and burden of ocular injury. Ophthalmology. 95(3):300-305.

Scott W.R., Lloyd W.C., Benedict J.V., Meredith R. (2000) Ocular injuries due to projectile impacts. Association for the Advancement of Automotive Medicine. 205-217.

Stitzel J.D., Duma S.M., Cormier J.M., Herring I.P. (2002) A nonlinear finite element model of the eye with experimental validation for the prediction of globe rupture. Stapp Car Crash Journal. 46:81-102.

Vinger P.F., Duma S.M., Crandall J. (1999) Baseball hardness as a risk factor in eye injuries. Arch Ophthalmol. 117:354-358.

Vinger P.F., Sparks J.J., Mussack K.R., Dondero J., Jeffers J.B. (1997) A program to prevent eye injuries in paintball. Sports Vision. 3:33-40.

Weidenthal D.T., Schepens C.L. (1966) Peripheral fundus changes associated with ocular contusion. Am J Ophthalmol. 62:465-477.

Weidenthal D.T. (1964) Experimental ocular contusion. Arch Ophthalmol. 71:111-115.

CHAPTER 4:
RISK FUNCTIONS FOR HUMAN GLOBE RUPTURE BASED ON PROJECTILE CHARACTERISTICS OF BLUNT OBJECTS

ABSTRACT

Eye ruptures are among the most devastating eye injuries and can occur in automobile crashes, sporting impacts, and military events, where blunt projectile impacts to the eye can be encountered. The purpose of this study was to develop injury risk functions for globe rupture of both human and porcine eyes from blunt projectile impacts. This study was completed in two parts by combining published eye experiments with new test data. In the first part, data from 57 eye impact tests that were reported in the literature were analyzed. Projectile characteristics such as mass, cross-sectional area, and velocity, as well as injury outcome were noted for all tests. Data were sorted by species type and areas were identified where a paucity of data existed, based on the kinetic and normalized energy of assaulting objects. For the second part, a total of 126 projectile tests were performed on human and porcine eyes. Projectiles used for these tests included blunt aluminum projectiles, BBs, foam pellets, Airsoft pellets, and paintballs. Data for each projectile were recorded prior to testing and high-speed video was used to determine projectile velocity prior to striking the eye. In part three the data were pooled for a total of 183 eye impact tests, 83 human and 100 porcine, and were analyzed to develop the injury risk criteria. Binary logistic regression was used to develop injury risk functions based on kinetic and normalized energy. Probit analysis was used to estimate confidence intervals for the injury risk functions. Porcine eyes were found to be significantly stronger than human eyes in resisting globe rupture ($p=0.01$). For porcine eyes a 50% risk of globe rupture was found to be 71,145 J/m^2, with a confidence interval of 63,245 J/m^2 to 80,390 J/m^2. Human eyes were found to have a 50% risk of globe rupture at a lower, 35,519 J/m^2, with confidence intervals of 32,018 J/m^2 to 40,641 J/m^2. The results presented in this paper are useful in estimating the risk of globe rupture when projectile parameters are known, or can be used to validate computational eye models.

INTRODUCTION

Injury Background

There are over 1.9 million eye injuries per year in the United States (McGwin 2005). The incidence of severe eye injuries is on the same order of magnitude of the number of passengers killed in vehicle crashes every year, with approximately 30,000 Americans left blind in one eye as a result of trauma (Parver 1986). Some of the most severe eye injuries can occur in automobile accidents, from sports related impacts, and from military accidents and causalities (Chisholm 1969, Berger 1978, Mader 1993, Duma 1996, Vinger 1997, Kuhn 2000, Duma 2002, Rodriguez 2003).

Blunt impact of the eye with an airbag or other objects can result in severe eye injury such as hyphema (bleeding in the anterior chamber of the eye), lens dislocation, or globe rupture (Chisholm 1969, Vichnin 1995, Duma 1996, Ghafouri 1997, Stein 1999, Lueder 2000, Power 2002, Hansen 2003, Stitzel 2005). Although not statistically significant ($p=0.15$), eye injuries sustained during automobile crashes occur at a higher rate (3.1%) when the occupant is exposed to a deploying airbag than when the occupant is not (2.0%) (Duma 2002). The airbag has been shown to be both directly responsible for eye injuries from blunt impact with the eye and indirectly responsible for eye injuries by propelling objects into the eye during the airbag deployment (Kuhn 1995, Duma 2002). Though no experimental studies have been reported that have specifically shown airbags to cause globe rupture, computational simulations have shown airbag interaction with the eye to lead to high corneo-scleral stress (Stitzel 2005). Additionally, several case studies in the literature specifically cite airbags as the primary cause of globe rupture, although this injury mechanism appears to be very rare (Kuhn 1994, Duma 1996, Pearlman 2001).

Eye injuries in sporting activities are also common, due to the close proximity of players and high energies involved. Globe rupture can occur from blunt trauma from many sports objects such as baseballs, golf balls, hockey sticks, squash balls and other objects (Chisholm 1969, Vinger 1996, Vinger 1999, Rodriguez 2003). Paintballs have also proven to have a devastating effect on the unprotected eye, often resulting in complete rupture of the globe and loss of

intraocular contents, hyphema, retinal tearing, and traumatic cataracts are also very prevalent (Vinger 1997, Thach 1999, Fineman 2000, Listman 2004).

Eye injuries in the military environment are even more prevalent and are generally more severe than eye injuries to civilians. The rate of eye injuries has dramatically increased in warfare since the American Civil War (Figure 23) (Heier 1993). Eye injuries in World War I and World War II accounted for approximately 2.0% to 2.5% of all injuries, during the U.S. involvement in Vietnam, this percentage increased to 5% to 9%; in recent conflicts, such as Operation Desert Storm, the percentage of eye injuries has dramatically increased to over 13% of all combat injuries (Stone 1950, Heier 1993, Wong 2000). While many of the conflict-related eye injuries are caused by shrapnel and other debris, nearly 25% of the injuries are also caused by blunt trauma from motor vehicle and helicopter crashes, falling, and direct hits from blunt objects (Mader 1993, Biehl 1999).

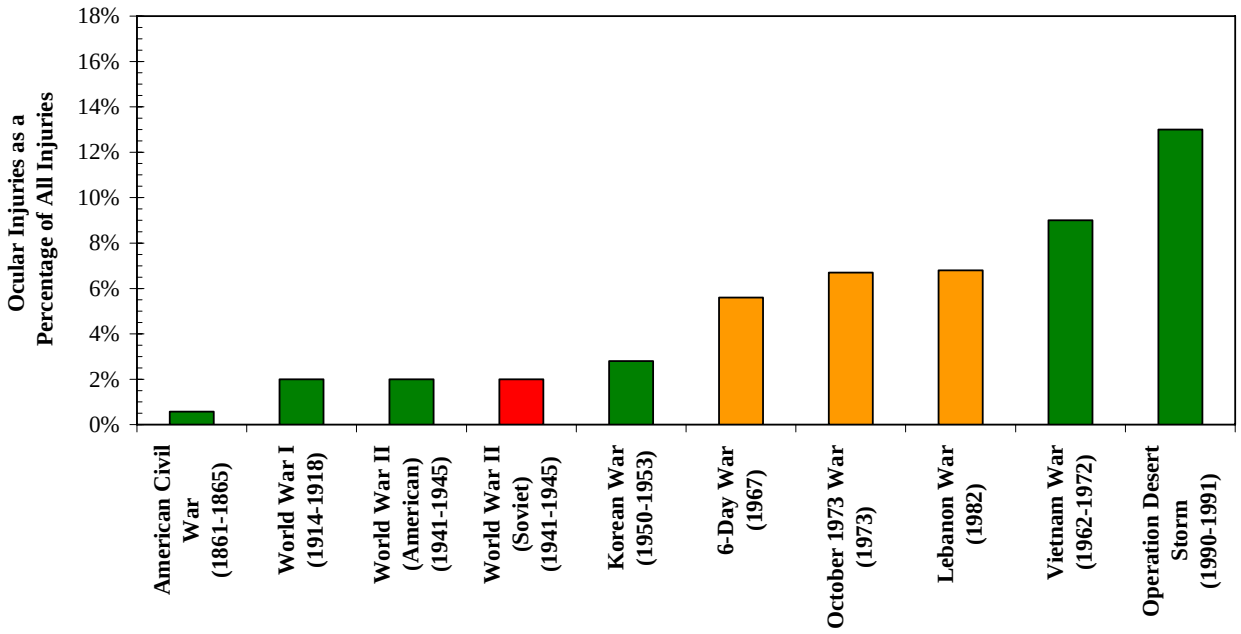

Figure 23: Ocular injuries shown as a percentage of total war injuries from 1861 to present. (Data in this figure are from Stone 1950, Heier 1993, Wong 2000)

Previous Research

Previous researchers have performed eye impact tests to determine the injury tolerance of eyes to a variety of blunt objects (Weidenthal 1964, Weidenthal 1966, Delori 1969, McKnight 1988, Green 1990, Duma 2000, Scott 2000, Stitzel 2002).

A study performed by Weidenthal and Schepens (1966) conducted BB impact experiments on over 235 porcine eyes. Similarly, over 75 BB impacts with porcine eyes and one set of human eyes were conducted by Delori *et al.* (1969). Unfortunately, insufficient data is presented to account for the specific injury pathologies and the frequency at which these injuries occurred.

Two experimental studies were performed to examine less severe eye injuries. Duma *et al.* (2000) performed a series of foam particle tests on 21 porcine eyes and developed an injury risk function based on kinetic energy to predict the risk of corneal abrasion. Globe rupture was not observed in any tests. Scott *et al.* (2000) used 21 enucleated porcine eyes for eye impact tests using three different blunt metal rods. An injury risk function was developed to predict the likelihood of various severity injuries, such as lens damage, lens dislocation, and retinal damage. It was observed that lens dislocations occurred at a kinetic energy of approximately 0.75 J and retinal damage at approximately 1.20 J. Globe rupture was not observed in any of the tests.

Stitzel *et al.* (2002) performed a series of 22 eye impact tests on enucleated human eyes using foam projectiles, BBs, and baseballs. The results of these tests were used to validate a failure stress level for a computational eye model. In the experimental tests, globe rupture was observed to occur from both BB impacts and baseball impacts. Globe rupture from BBs was observed at a kinetic energy level of 1.36 J and greater, while impacts at 0.67 J or less resulted in no injury. A baseball impact of 66 J resulted in no injury; however, other baseball impacts from 87 J and greater all resulted in globe rupture. Baseball tests resulted in interaction of the baseball to the edge of the simulated orbits used for testing; therefore, it is impossible to estimate the amount of energy that was directly transferred to the eye.

Others have performed impact experiments on various species of animals for the purposes of determining injury mechanisms for eye injuries, as well as the effect of corrective surgery in reducing the strength of the eye. These surrogate animals are used for testing because they are more readily available than post-mortem human eyes, and in the case of some researchers, *in-vivo* tests were performed on anesthetized animals.

Weidenthal (1964) conducted blunt trauma impact experiments using live rhesus monkeys to determine the force required to separate the ciliary body from the sclera and to cause globe rupture. McKnight *et al.* (1988) used cat eyes to investigate the effects of radial keratotomy (RK) in reducing the corneal strength of the eye. Green *et al.* (1990) conducted projectile tests on anesthetized monkeys to determine the fracture tolerance of the orbital floor, while also noting eye injury pathology. Galler *et al.* (1995) also used porcine eyes to evaluate the effects of photorefractive keratectomy (PRK) and automated lamellar keratectomy (ALK) surgery in reducing corneo-scleral integrity. Peacock *et al.* (1997) impacted surgically altered human eyes from ALK, RK, PRK, and Laser-assisted *in-situ* Keratomileusis (LASIK) to observe differences in the injury tolerance resulting from these surgical techniques.

Each of the previously reported studies are limited by one or more of the following factors: the number of tests performed, the range of projectile size, mass, or impact velocities used, and the detail in which resulting injury pathologies are reported. As such, due to the limitations of the available dataset no previous studies have been able to develop comprehensive injury criteria for human or porcine eyes for globe rupture. Therefore, the purpose of the current study is to pool the available data on globe rupture, increase the amount of available data through additional experimental tests, and develop injury risk functions for globe rupture from blunt projectile impacts. These risk functions can then be used for evaluation of current products and objects where it is desired to determine eye injury potential; also, these can be used in the design of new products so that their injury potential can be quantified prior even to fabrication. Given that porcine eyes are frequently used as surrogates for human eyes in impact studies, an additional goal of this study is to compare the relative strength of human eyes and porcine eyes to globe rupture.

METHODS

The current study is comprised of three parts. In Part I, existing data from blunt ocular impact studies were collected from the literature. The existing data were pooled and evaluated to determine areas where a paucity of data existed. Next, regions were identified where additional data were necessary. For Part II, experimental impact tests were performed using a variety of objects to develop a complete database for globe rupture using both human and porcine eyes. In Part III, the data from both parts were combined and then the total database was analyzed to develop injury risk functions for both human and porcine eyes from blunt projectile impact.

Part I: Published Experiments

An analysis of previous experiments was conducted in which data were sorted according to projectile characteristics such as type, mass, diameter, and velocities, as well as injury outcome. Since the purpose of this study was to elucidate any differences between human and porcine eyes, specimens were limited to only human or porcine eyes. Parameters such as velocity, kinetic energy, and normalized energy were calculated for each test and used to determine where additional experimental test data were necessary. The normalized energy is defined as the energy per projected area of the projectile (Equation 1). The projected area is the contact surface area for a flat impacting object or the cross-sectional area of a sphere.

$$Normalized\ Energy\ \left(\frac{J}{m^2}\right) = \frac{Kinetic\ Energy}{Projected\ Area} = \frac{1/2 mv^2}{\pi r^2} (\ for\ a\ sphere\ ) \qquad \text{Eq. (1)}$$

Only unoperated eyes were included in this study because eyes that have undergone radial keratotomy (RK) are known to sustain open globe injury at lower energy levels than eyes without RK (McKnight 1988, Galler 1995, Peacock 1997, Vinger 2005). For each test, the occurrence or lack of occurrence of globe rupture was noted.

Part II: Experimental Test Methods

A total of 126 additional impact tests were conducted in order to supplement the amount of available data for both human and porcine globe rupture. All tests were conducted by striking the cornea directly with objects of varying size and velocity. Each combination of object size,

mass and velocity was carefully selected to add experimental data where a paucity of data previously existed.

Prior to testing, human and porcine eyes were harvested within 24 hours of death. Hydration of the eyes was maintained by storage in a saline-filled specimen jar and refrigerated fresh prior to testing. For testing, the eyes were removed from refrigeration and kept hydrated as they returned to room temperature just prior to the actual testing. All test procedures were reviewed and approved by the Virginia Tech Institutional Review Board.

For each test, the human or porcine eye was mounted in a simulated polycarbonate orbit (Figure 24). The eye was encapsulated in the orbit by a 10% gelatin solution which has been used previously to represent the extraocular tissue surrounding the eye in the orbit (Vinger 1999, Stitzel 2002). The gelatin was filled inside the simulated orbit to the posterior limbus. The dimensions of the orbit of 53 mm in the anterior-posterior direction, 41 mm in the superior-inferior direction, and 48 mm in the medial-lateral direction, and were selected to represent the approximate size of a human orbit (Stitzel 2002). The porcine eyes were potted in the same simulated orbits as the human eyes. The simulated orbit was mounted inside an enclosed plexiglass gallery where projectile testing could be safely conducted.

Four mechanisms were used to propel the projectiles used in this testing. Projectiles included Airsoft pellets fired from Airsoft pellet guns (Cybergun S.A., Beretta Softair - Beretta 92FS Spring, France and HFC, M80.45 Series Model "Combat Commander" Gas Gun, Taiwan), paintballs fired from a paintball gun (Kingman, Spyder TL-X, Baldwin Park, CA), foam projectiles and BBs from a BB rifle (Daisy Outdoor Products, Model 880, Rogers, AR), and aluminum and plastic projectiles from a custom designed pneumatic cannon. All eyes were struck directly at the center of the cornea.

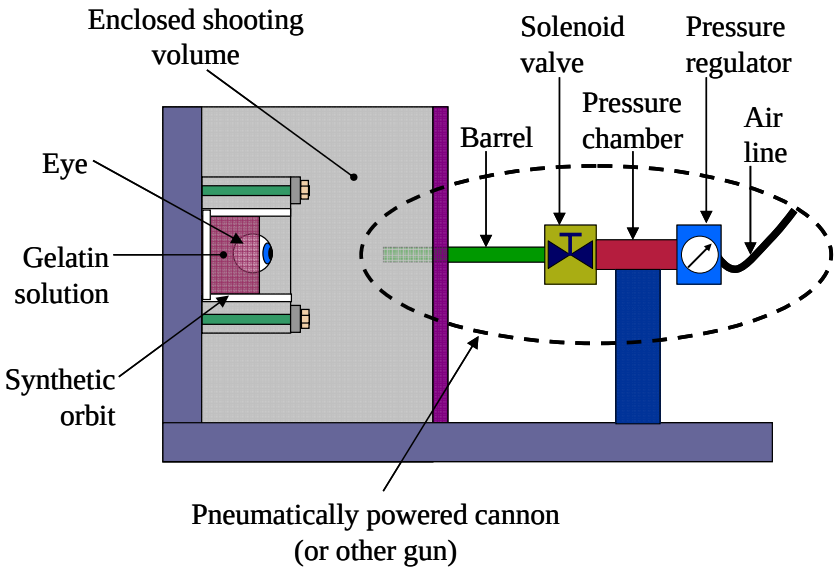

Figure 24: Experimental testing was performed in an enclosed shooting gallery from a distance of 175mm, and the eyes were contained in a synthetic orbit by a 10% gelatin solution.

High-speed video (Phantom 4, Vision Research, Inc., Wayne, NJ) at 7400 frames/second was used to visualize the response of the eye as it was impacted by oncoming projectiles, as well as to calculate the velocity of the projectile when it was approximately 10 mm to 30 mm from striking the eye. Binary injury response data were collected for each test specimen based on visual and photographic documentation of globe rupture or corneal-scleral laceration (or no injury) for each test scenario. Kinetic energy (J) and normalized energy (J/m^2) were then calculated to elucidate the relationship of these quantities to injury response.

Part III: Data Analysis Methods

Results from Part I and Part II were combined into a database which was then used for all subsequent data analysis. Predictors used in the statistical analysis include the projectile diameter, projectile mass, projectile velocity, the kinetic energy of the projectile, and the normalized energy of the projectile. For each individual test, kinetic energy was calculated based on reported projectile mass and velocity. The normalized energy was analyzed as it has previously been shown to be a more significant injury predictor than kinetic energy alone (Duma 2005).

Logistic regression analyses were performed on the experimental data to determine significant predictors for eye injury based on p-values and Goodman-Kruskal Gamma values. P-values of 0.05 or less were interpreted to be statistically significant. For Goodman-Kruskal Gamma values, a correlation coefficient with values near 0.0 indicates no association between two subjects and a value of 1.0 represents a high association between predictor and injury (Collett 1991, Allison 1999).

A general form of the logistic regression injury risk function (Equation 2) can be used with specific injury parameters to predict the probability of globe rupture given a projectile's normalized energy or kinetic energy. The variable "x" refers to the level of input (such as kinetic energy or normalized energy) of the projectile onto the eye. The variables "a" and "b" are constants determined from the logistic regression and are unique to the specific predictor used (kinetic energy or normalized energy).

$$\text{Probability of Injury}(\%) = \frac{1}{1+e^{a-bx}} \qquad \text{Eq. (2)}$$

Additionally, a probit analysis was used in conjunction with the logistic regression analysis in order to estimate confidence intervals for the injury risk model (Collett 1991, Allison 1999). Confidence intervals from 5% to 95% were calculated assuming a logistic distribution.

In order to confirm the applicability of logistic regression analysis for the development of parametric injury risk functions, risk functions were also developed using the Consistent-Threshold (CT) technique, the modified median rank method, and the certainty method. These techniques have been previously suggested for analysis of biological data, in particular for doubly censored data (Mertz 1996, Eppinger 1999, DiDomenico 2003, Kent 2004). Results of the comparisons between the various risk functions are presented in the discussion section.

RESULTS

Part I: Results from Published Experiments

A total of 57 impact tests were collected and analyzed from published studies. Of these, 35 tests were conducted on porcine eyes (Table 7) (Duma 2000, Scott 2000). Objects used for the eye impact tests were foam particles and a steel rod.

Another 22 tests were analyzed that utilized human eyes (Table 8) (Delori 1969, Stitzel 2002). These tests utilized objects such as foam, a baseball, and BBs. In these tests, there were approximately 17 non-injury tests and 5 injury tests.

Table 7: Test results reported in the literature from previous eye impact tests on porcine eyes.

Test	Author (Year)	Object	Projectile Diameter (mm)	Projectile Mass (g)	Projectile Velocity (m/s)	Kinetic Energy (J)	Normalized Energy (J/m^2)	Globe Rupture (Yes / No)
PL-1	Duma (2000)	Foam	12.50	0.30	4.80	0.00	28	No
PL-2	Duma (2000)	Foam	12.50	0.30	5.60	0.00	38	No
PL-3	Duma (2000)	Foam	12.50	0.30	7.00	0.01	59	No
PL-4	Duma (2000)	Foam	12.50	0.21	18.30	0.03	280	No
PL-5	Duma (2000)	Foam	12.50	0.16	25.50	0.05	411	No
PL-6	Duma (2000)	Foam	12.50	0.16	39.30	0.12	975	No
PL-7	Duma (2000)	Foam	12.50	0.16	41.60	0.13	1093	No
PL-8	Duma (2000)	Foam	12.50	0.16	46.00	0.16	1336	No
PL-9	Duma (2000)	Foam	12.50	0.57	26.80	0.21	1671	No
PL-10	Duma (2000)	Foam	12.50	0.55	29.90	0.25	2007	No
PL-11	Duma (2000)	Foam	12.50	0.58	29.90	0.26	2124	No
PL-12	Duma (2000)	Foam	12.50	0.16	57.70	0.27	2225	No
PL-13	Duma (2000)	Foam	12.50	0.55	31.70	0.28	2244	No
PL-14	Duma (2000)	Foam	12.50	0.21	57.70	0.35	2876	No
PL-15	Duma (2000)	Foam	12.50	0.17	87.60	0.63	5159	No
PL-16	Duma (2000)	Foam	12.50	0.55	72.40	1.44	11768	No
PL-17	Scott (2000)	Steel Rod	9.53	45.50	4.00	0.36	5103	No
PL-18	Scott (2000)	Steel Rod	9.53	45.50	4.30	0.42	5897	No
PL-19	Scott (2000)	Steel Rod	9.53	45.50	5.20	0.62	8624	No
PL-20	Scott (2000)	Steel Rod	6.35	3.50	18.90	0.63	19739	No
PL-21	Scott (2000)	Steel Rod	6.35	3.50	19.20	0.65	20371	No
PL-22	Scott (2000)	Steel Rod	6.35	2.60	23.80	0.74	23252	No

Table 7 (cont.): Test results reported in the literature from previous eye impact tests on porcine eyes.

Test	Author (Year)	Object	Projectile Diameter (mm)	Projectile Mass (g)	Projectile Velocity (m/s)	Kinetic Energy (J)	Normalized Energy (J/m^2)	Globe Rupture (Yes / No)
PL-23	Scott (2000)	Steel Rod	6.35	2.60	23.80	0.74	23252	No
PL-24	Scott (2000)	Steel Rod	6.35	3.50	20.70	0.75	23678	No
PL-25	Scott (2000)	Steel Rod	6.35	2.60	27.10	0.95	30147	No
PL-26	Scott (2000)	Steel Rod	6.35	3.50	26.20	1.20	37932	No
PL-27	Scott (2000)	Steel Rod	6.35	2.60	30.50	1.21	38186	No
PL-28	Scott (2000)	Steel Rod	6.35	2.60	32.30	1.36	42826	No
PL-29	Scott (2000)	Steel Rod	6.35	2.60	33.20	1.43	45246	No
PL-30	Scott (2000)	Steel Rod	6.35	2.60	36.00	1.68	53200	No
PL-31	Scott (2000)	Steel Rod	6.35	2.60	38.10	1.89	59588	No
PL-32	Scott (2000)	Steel Rod	6.35	3.50	33.00	1.91	60177	No
PL-33	Scott (2000)	Steel Rod	6.35	3.50	18.60	0.61	19117	No
PL-34	Scott (2000)	Steel Rod	6.35	45.50	5.20	0.62	19425	No
PL-35	Scott (2000)	Steel Rod	6.35	3.50	20.70	0.75	23678	No

Table 8: Test results reported in the literature from previous eye impact tests on human eyes.

Test	Author (Year)	Object	Projectile Diameter (mm)	Projectile Mass (g)	Projectile Velocity (m/s)	Kinetic Energy (J)	Normalized Energy (J/m^2)	Globe Rupture (Yes / No)
HL-1	Delori (1969)	BB	4.50	0.35	71.93	0.91	56930	Yes
HL-2	Stitzel (2002)	Foam	6.35	0.08	4.30	0.00	22	No
HL-3	Stitzel (2002)	Foam	6.35	0.08	5.40	0.00	35	No
HL-4	Stitzel (2002)	Foam	6.35	0.08	6.00	0.00	44	No
HL-5	Stitzel (2002)	Foam	6.35	0.08	10.60	0.00	137	No
HL-6	Stitzel (2002)	Foam	6.35	0.08	14.20	0.01	245	No
HL-7	Stitzel (2002)	Foam	6.35	0.08	14.30	0.01	249	No
HL-8	Stitzel (2002)	Foam	6.35	0.08	18.90	0.01	434	No
HL-9	Stitzel (2002)	Foam	6.35	0.08	23.00	0.02	643	No
HL-10	Stitzel (2002)	Foam	6.35	0.08	26.70	0.03	867	No
HL-11	Stitzel (2002)	Foam	6.35	0.08	26.80	0.03	873	No
HL-12	Stitzel (2002)	Foam	6.35	0.08	28.60	0.03	994	No
HL-13	Stitzel (2002)	Foam	6.35	0.08	31.00	0.04	1168	No
HL-14	Stitzel (2002)	Baseball	76.10	146.50	30.10	66.37	14591	No
HL-15	Stitzel (2002)	BB	4.50	0.38	53.00	0.53	33116	No
HL-16	Stitzel (2002)	BB	4.50	0.38	53.80	0.54	34123	No
HL-17	Stitzel (2002)	BB	4.50	0.38	55.80	0.58	36707	No
HL-18	Stitzel (2002)	BB	4.50	0.38	59.70	0.67	42018	No
HL-19	Stitzel (2002)	BB	4.50	0.38	85.20	1.36	85579	Yes
HL-20	Stitzel (2002)	BB	4.50	0.38	90.40	1.53	96344	Yes
HL-21	Stitzel (2002)	BB	4.50	0.38	91.70	1.58	99135	Yes
HL-22	Stitzel (2002)	BB	4.50	0.38	122.40	2.81	176624	Yes

Part II: Experimental Results

A total of 126 experimental eye impact tests were performed. Of these, 65 tests were conducted on porcine eyes (Table 9). Objects used for the eye impact tests were Airsoft pellets, BBs, paintballs, foam particles, plastic rods, and aluminum rods. A total of 42 non-injury tests were conducted, along with 23 tests that resulted in globe rupture.

In addition, 61 tests were performed with human eyes (Table 10). These tests utilized Airsoft pellets, BBs, paintballs, foam particles, plastic rods, and aluminum rods. A total of 39 non-injury tests were performed, and globe rupture was noted for 22 tests.

A comparison of high-speed video of two separate impact tests is shown (Figure 25). Both tests were conducted with an 11 mm aluminum rod traveling at approximately 40 m/s ± 3 m/s. The test on the left was a porcine eye which did not rupture, compared to the human eye on the right, which experienced globe rupture.

Table 9: Test results from experimental eye impact tests on porcine eyes.

Test	Author (Year)	Object	Projectile Diameter (mm)	Projectile Mass (g)	Projectile Velocity (m/s)	Kinetic Energy (J)	Normalized Energy (J/m^2)	Globe Rupture (Yes / No)
PE-1	Present Study	Airsoft Pellet	6.00	0.12	97.78	0.56	19746	No
PE-2	Present Study	Airsoft Pellet	6.00	0.12	101.75	0.60	21384	No
PE-3	Present Study	Airsoft Pellet	6.00	0.11	94.65	0.51	18110	No
PE-4	Present Study	Airsoft Pellet	6.00	0.12	115.63	0.77	27330	No
PE-5	Present Study	Paintball	17.30	3.21	71.69	8.24	35061	No
PE-6	Present Study	Paintball	17.30	3.17	99.03	15.53	66070	No
PE-7	Present Study	Paintball	17.30	3.21	106.10	18.06	76837	Yes
PE-8	Present Study	Paintball	17.30	3.17	108.94	18.81	80003	Yes
PE-9	Present Study	Airsoft Pellet	6.00	0.20	74.65	0.57	20125	No
PE-10	Present Study	Airsoft Pellet	6.00	0.20	77.08	0.60	21351	No
PE-11	Present Study	Airsoft Pellet	6.00	0.20	72.46	0.54	18940	No
PE-12	Present Study	Airsoft Pellet	6.00	0.20	87.36	0.78	27559	No
PE-13	Present Study	Paintball	17.30	3.21	67.06	7.21	30685	No
PE-14	Present Study	Paintball	17.30	3.19	100.21	16.00	68086	Yes
PE-15	Present Study	Paintball	17.30	3.19	101.94	16.59	70586	No
PE-16	Present Study	Paintball	17.30	3.19	103.29	17.03	72463	Yes
PE-17	Present Study	Paintball	17.30	3.20	111.00	19.72	83900	Yes
PE-18	Present Study	Airsoft Pellet	6.00	0.12	92.50	0.49	17491	No
PE-19	Present Study	Airsoft Pellet	6.00	0.12	115.63	0.77	27306	No
PE-20	Present Study	Paintball	17.30	3.19	68.01	7.38	31411	No
PE-21	Present Study	Paintball	17.30	3.06	95.58	13.98	59476	No

Table 9 (cont.): Test results from experimental eye impact tests on porcine eyes.

Test	Author (Year)	Object	Projectile Diameter (mm)	Projectile Mass (g)	Projectile Velocity (m/s)	Kinetic Energy (J)	Normalized Energy (J/m^2)	Globe Rupture (Yes / No)
PE-22	Present Study	Paintball	17.30	3.20	109.46	19.15	81466	Yes
PE-23	Present Study	Paintball	17.30	3.16	108.94	18.74	79733	Yes
PE-24	Present Study	Airsoft Pellet	6.00	0.21	67.22	0.47	16483	No
PE-25	Present Study	Airsoft Pellet	6.00	0.20	84.02	0.71	25068	No
PE-26	Present Study	Paintball	17.30	3.14	66.81	7.00	29775	No
PE-27	Present Study	Paintball	17.30	3.21	100.55	16.24	69091	No
PE-28	Present Study	Paintball	17.30	3.19	114.08	20.75	88266	Yes
PE-29	Present Study	Paintball	17.30	3.17	106.38	17.96	76394	Yes
PE-30	Present Study	Paintball	17.30	3.20	109.69	19.25	81876	Yes
PE-31	Present Study	Paintball	17.30	3.21	106.38	18.17	77318	Yes
PE-32	Present Study	Paintball	17.30	3.19	101.75	16.50	70202	Yes
PE-33	Present Study	Airsoft Pellet	6.00	0.20	83.32	0.70	24873	No
PE-34	Present Study	Paintball	17.30	3.22	100.70	16.32	69420	Yes
PE-35	Present Study	Delrin Impactor	19.90	112.55	8.66	4.22	13583	No
PE-36	Present Study	Delrin Impactor	19.90	112.55	8.82	4.38	14079	No
PE-37	Present Study	Delrin Impactor	19.90	112.55	8.45	4.02	12914	No
PE-38	Present Study	Delrin Impactor	19.90	112.55	8.85	4.40	14163	No
PE-39	Present Study	Plastic Rod	7.62	0.35	5.68	0.01	122	No
PE-40	Present Study	Plastic Rod	7.62	0.35	15.46	0.04	904	No
PE-41	Present Study	Plastic Rod	7.62	0.35	10.82	0.02	443	No
PE-42	Present Study	Foam	4.50	0.04	25.93	0.01	826	No
PE-43	Present Study	Foam	4.50	0.04	21.97	0.01	593	No
PE-44	Present Study	Foam	4.50	0.04	29.27	0.02	1052	No
PE-45	Present Study	Plastic Rod	7.62	0.35	13.44	0.03	683	No
PE-46	Present Study	Plastic Rod	7.62	0.35	19.63	0.07	1457	No
PE-47	Present Study	Foam	4.50	0.04	16.46	0.01	333	No
PE-48	Present Study	Foam	4.50	0.04	32.82	0.02	1323	No
PE-49	Present Study	Aluminum Rod	11.16	5.19	33.78	2.96	30250	No
PE-50	Present Study	Aluminum Rod	11.16	5.19	37.78	3.70	37840	No
PE-51	Present Study	Aluminum Rod	9.25	3.57	28.13	1.41	21051	No
PE-52	Present Study	Aluminum Rod	9.25	3.57	34.91	2.18	32421	No
PE-53	Present Study	BB	4.37	0.34	96.02	1.58	105151	No
PE-54	Present Study	BB	4.37	0.34	165.62	4.64	309787	Yes
PE-55	Present Study	BB	4.37	0.34	142.13	3.39	225981	Yes
PE-56	Present Study	Foam	4.50	0.04	149.63	0.41	26020	No
PE-57	Present Study	BB	4.37	0.34	139.96	3.33	222202	Yes
PE-58	Present Study	BB	4.37	0.34	139.96	3.34	222986	Yes
PE-59	Present Study	BB	4.37	0.34	99.74	1.70	113213	Yes
PE-60	Present Study	BB	4.37	0.34	98.13	1.64	109398	Yes
PE-61	Present Study	BB	4.37	0.34	95.93	1.54	102911	Yes
PE-62	Present Study	BB	4.37	0.34	99.28	1.69	112772	Yes
PE-63	Present Study	BB	4.37	0.34	98.20	1.64	109723	Yes
PE-64	Present Study	BB	4.37	0.34	97.59	1.63	108904	No
PE-65	Present Study	BB	4.37	0.34	131.74	2.96	197388	Yes

Table 10: Test results from experimental eye impact tests on human eyes.

Test	Author (Year)	Object	Projectile Diameter (mm)	Projectile Mass (g)	Projectile Velocity (m/s)	Kinetic Energy (J)	Normalized Energy (J/m^2)	Globe Rupture (Yes / No)
HE-1	Present Study	Airsoft Pellet	6.00	0.12	88.32	0.45	15987	No
HE-2	Present Study	Airsoft Pellet	6.00	0.12	91.62	0.50	17531	No
HE-3	Present Study	Airsoft Pellet	6.00	0.12	92.12	0.49	17364	No
HE-4	Present Study	Airsoft Pellet	6.00	0.12	117.80	0.80	28439	No
HE-5	Present Study	Paintball	17.30	3.20	71.73	8.24	35070	Yes
HE-6	Present Study	Paintball	17.30	3.20	71.28	8.14	34613	Yes
HE-7	Present Study	Airsoft Pellet	6.00	0.21	73.03	0.56	19694	No
HE-8	Present Study	Airsoft Pellet	6.00	0.20	76.29	0.57	20330	No
HE-9	Present Study	Airsoft Pellet	6.00	0.20	78.30	0.62	22032	No
HE-10	Present Study	Airsoft Pellet	6.00	0.20	85.33	0.74	26292	No
HE-11	Present Study	Paintball	17.30	3.13	65.50	6.72	28604	Yes
HE-12	Present Study	Paintball	17.30	3.21	71.10	8.10	34461	No
HE-13	Present Study	Paintball	17.30	3.19	97.88	15.29	65030	Yes
HE-14	Present Study	Airsoft Pellet	6.00	0.11	93.63	0.50	17798	No
HE-15	Present Study	Airsoft Pellet	6.00	0.12	109.74	0.71	24939	No
HE-16	Present Study	Paintball	17.30	3.19	68.02	7.37	31370	No
HE-17	Present Study	Paintball	17.30	3.21	73.28	8.61	36645	Yes
HE-18	Present Study	Airsoft Pellet	6.00	0.21	75.00	0.58	20591	No
HE-19	Present Study	Airsoft Pellet	6.00	0.21	87.35	0.79	27849	No
HE-20	Present Study	Paintball	17.30	3.22	71.10	8.13	34572	Yes
HE-21	Present Study	Paintball	17.30	3.19	70.77	8.00	34032	No
HE-22	Present Study	Paintball	17.30	3.20	107.17	18.36	78120	Yes
HE-23	Present Study	Paintball	17.30	3.21	75.29	9.09	38684	Yes
HE-24	Present Study	Paintball	17.30	3.22	72.00	8.34	35478	Yes
HE-25	Present Study	Paintball	17.30	3.20	108.00	18.69	79493	Yes
HE-26	Present Study	Paintball	17.30	3.21	112.50	20.33	86503	Yes
HE-27	Present Study	Cork	30.00	9.48	8.86	0.37	527	No
HE-28	Present Study	Airsoft Pellet	6.00	0.21	81.19	0.68	23981	No
HE-29	Present Study	Airsoft Pellet	17.30	3.20	109.44	19.15	81471	Yes
HE-30	Present Study	Delrin Impactor	19.90	112.55	8.72	4.28	13761	No
HE-31	Present Study	Delrin Impactor	19.90	112.55	8.62	4.18	13435	No
HE-32	Present Study	Delrin Impactor	19.90	112.55	8.53	4.10	13167	No
HE-33	Present Study	Plastic Rod	7.62	0.35	23.50	0.10	2089	No
HE-34	Present Study	Plastic Rod	7.62	0.35	23.96	0.10	2171	No
HE-35	Present Study	Plastic Rod	9.75	0.69	20.16	0.14	1867	No
HE-36	Present Study	Plastic Rod	9.75	0.69	19.26	0.13	1704	No
HE-37	Present Study	Plastic Rod	7.62	0.35	23.75	0.10	2134	No
HE-38	Present Study	Plastic Rod	7.62	0.35	24.46	0.10	2264	No
HE-39	Present Study	Plastic Rod	9.75	0.69	19.23	0.13	1699	No
HE-40	Present Study	Plastic Rod	9.75	0.69	17.83	0.11	1460	No
HE-41	Present Study	Foam	4.50	0.04	45.73	0.04	2569	No
HE-42	Present Study	Foam	4.50	0.04	38.06	0.03	1780	No
HE-43	Present Study	Foam	4.50	0.04	44.66	0.04	2450	No
HE-44	Present Study	Foam	4.50	0.04	41.16	0.03	2081	No
HE-45	Present Study	Foam	4.50	0.04	47.23	0.04	2740	No
HE-46	Present Study	Foam	4.50	0.04	43.65	0.04	2341	No
HE-47	Present Study	BB	4.37	0.34	10.98	0.02	1370	No
HE-48	Present Study	BB	4.37	0.34	11.47	0.02	1496	No
HE-49	Present Study	BB	4.37	0.34	11.37	0.02	1469	No
HE-50	Present Study	BB	4.37	0.34	11.19	0.02	1425	No
HE-51	Present Study	BB	4.37	0.34	10.18	0.02	1179	No
HE-52	Present Study	Aluminum Rod	9.25	3.57	44.10	3.47	51752	Yes
HE-53	Present Study	Aluminum Rod	9.25	3.57	50.40	4.54	67585	Yes

Table 10 (cont.): Test results from experimental eye impact tests on human eyes.

Test	Author (Year)	Object	Projectile Diameter (mm)	Projectile Mass (g)	Projectile Velocity (m/s)	Kinetic Energy (J)	Normalized Energy (J/m^2)	Globe Rupture (Yes / No)
HE-54	Present Study	Aluminum Rod	9.25	3.57	56.05	5.61	83594	Yes
HE-55	Present Study	Aluminum Rod	9.25	3.57	59.20	6.26	93255	Yes
HE-56	Present Study	Aluminum Rod	9.25	3.57	43.58	3.39	50531	Yes
HE-57	Present Study	Aluminum Rod	9.25	3.57	42.13	3.17	47227	Yes
HE-58	Present Study	Aluminum Rod	11.16	5.19	43.71	4.96	50646	Yes
HE-59	Present Study	Aluminum Rod	11.16	5.19	44.10	5.05	51557	Yes
HE-60	Present Study	Aluminum Rod	11.16	5.19	53.21	7.35	75075	Yes
HE-61	Present Study	Aluminum Rod	11.16	5.19	44.69	5.18	52958	Yes

Time	Porcine Eye	Human Eye
0 ms		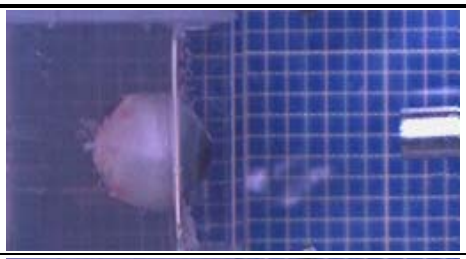
1 ms		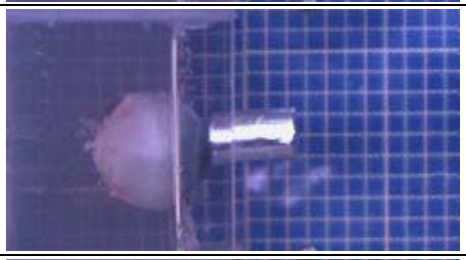
2 ms	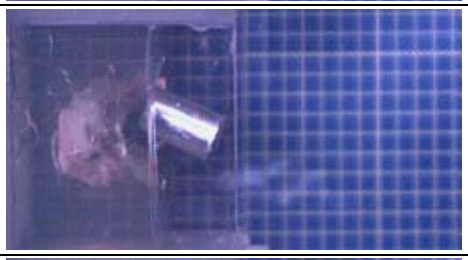	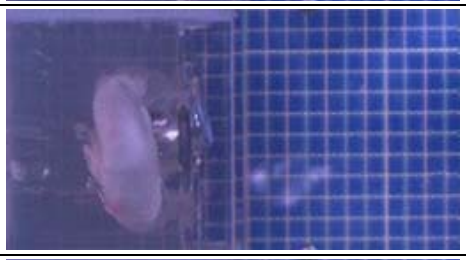
Final	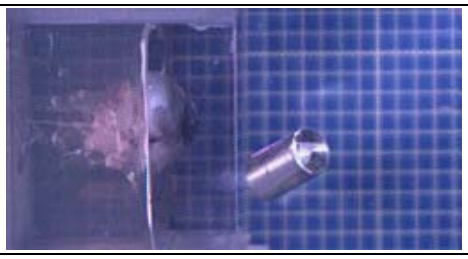	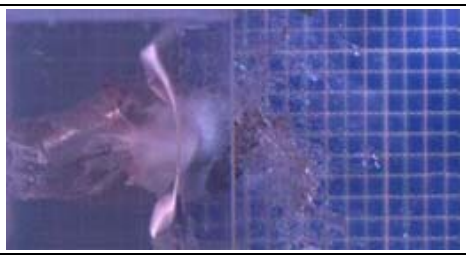

Figure 25: Comparison of similar tests using porcine and human eyes using high speed video; the porcine eye did not rupture, while the human eye sustained a ruptured globe.

Part III: Results of Data Analysis

Projectile characteristics of diameter, mass, velocity, kinetic energy, and normalized energy were evaluated by computing their significance and Goodman-Kruskal Gamma values. Logistic regression revealed that both kinetic energy and normalized energy were significant injury predictors for globe rupture, both porcine and human eyes ($p = 0.001$ for each) (Table 11). Similarly, the statistical analysis also showed that normalized energy presented the most statistically significant Goodman-Kruskal Gamma values for predicting globe rupture, with a value of 0.98 for normalized energy and human eyes, versus 0.87 for kinetic energy and

human eyes (Table 12). Similar results were found for Goodman-Kruskal Gamma values for porcine eyes and normalized energy (0.96) and for kinetic energy (0.83). Other injury risk parameters of diameter, mass, and projectile velocity were not found to be as significant and did not yield as high of Goodman-Kruskal Gamma values.

Table 11: P-values for different projectile characteristics for predicting globe rupture.

	Projectile Diameter (mm)	**Projectile Mass (g)**	**Projectile Velocity (m/s)**	**Kinetic energy (J)**	**Normalized energy (J/m^2)**
Porcine Eyes	0.095	0.078	< 0.001	< 0.001	< 0.001
Human Eyes	0.146	0.263	< 0.001	0.001	< 0.001

Table 12: Goodman-Kruskal Gamma values for different projectile characteristics for predicting globe rupture.

	Projectile Diameter (mm)	**Projectile Mass (g)**	**Projectile Velocity (m/s)**	**Kinetic energy (J)**	**Normalized energy (J/m^2)**
Porcine Eyes	0.06	-0.23	0.90	0.83	0.96
Human Eyes	0.47	-0.75	0.55	0.87	0.98

The coefficients for the injury risk function were estimated for each dataset, human and porcine eyes (Table 13). These coefficients can be coupled with the equation given in Equation 2, to represent the risk of globe rupture based on measured parameters from projectiles striking the eye.

Table 13: Injury risk function coefficients for globe rupture of both porcine and human eyes, using both kinetic and normalized energy. Standard errors for these parameters given in parenthesis.

	Kinetic energy (J)		**Normalized energy (J/m^2)**	
	Parameter "a"	**Parameter "b"**	**Parameter "a"**	**Parameter "b"**
Porcine Eyes	2.4416 (0.3987)	0.22071 (0.04436)	6.732 (1.675)	0.00009463 (0.00002380)
Human Eyes	1.2490 (0.3098)	0.14294 (0.05482)	9.123 (3.192)	0.00025684 (0.00009257)

The risk functions for kinetic energy for both porcine and human eyes are calculated. A 50% risk of globe rupture for porcine eyes was found to be 11.1 J (Figure 26), as opposed to 8.7 J for human eyes (Figure 27).

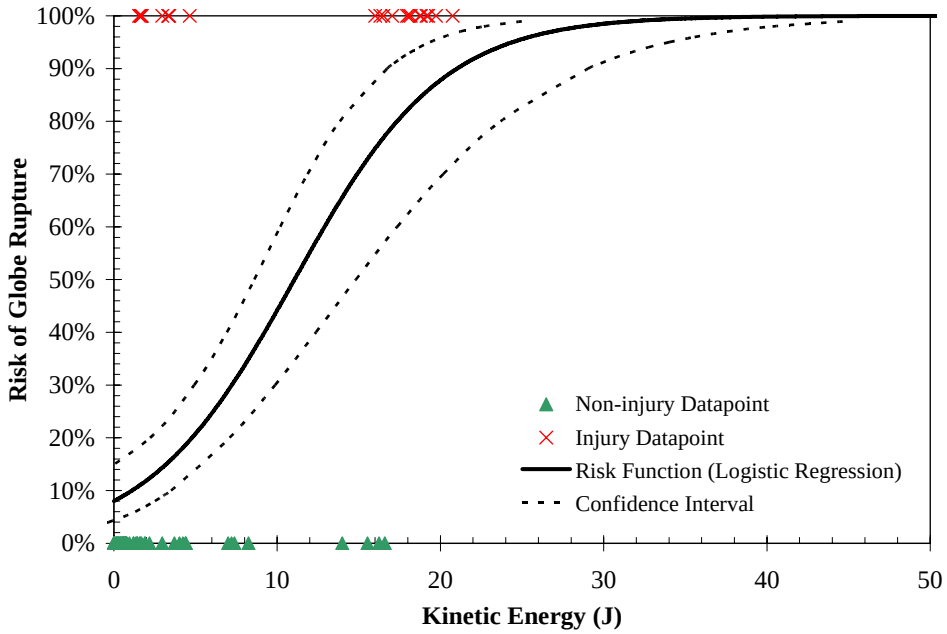

Figure 26: Injury risk curves for globe rupture of porcine eyes calculated from kinetic energy.

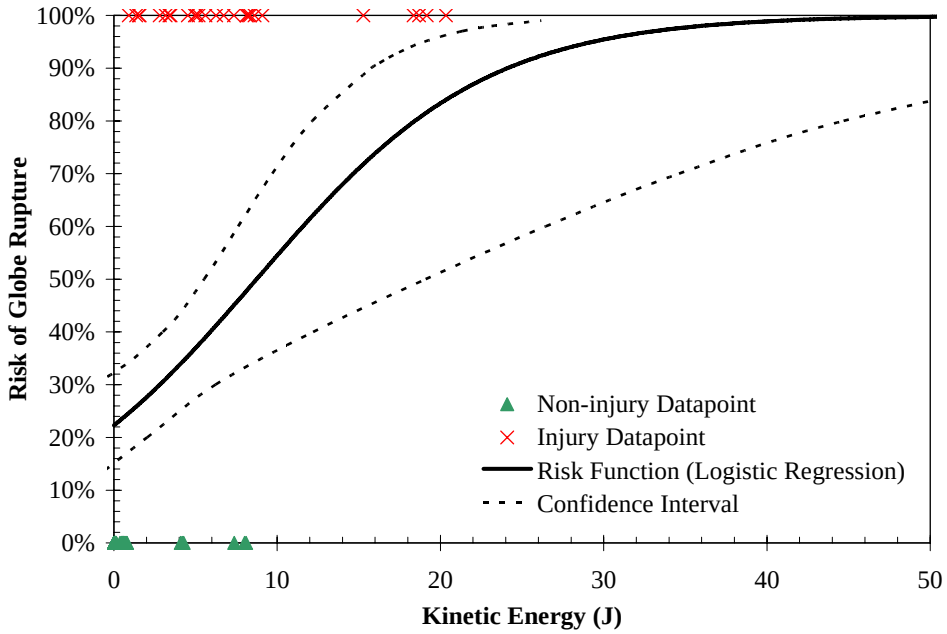

Figure 27: Injury risk curves for globe rupture of human eyes calculated from kinetic energy.

The risk functions for normalized energy for both porcine and human eyes are calculated. A 50% risk of globe rupture for porcine eyes was found to be 71,145 J/m^2 (Figure 28), as opposed to 35,519 J/m^2 for human eyes (Figure 29).

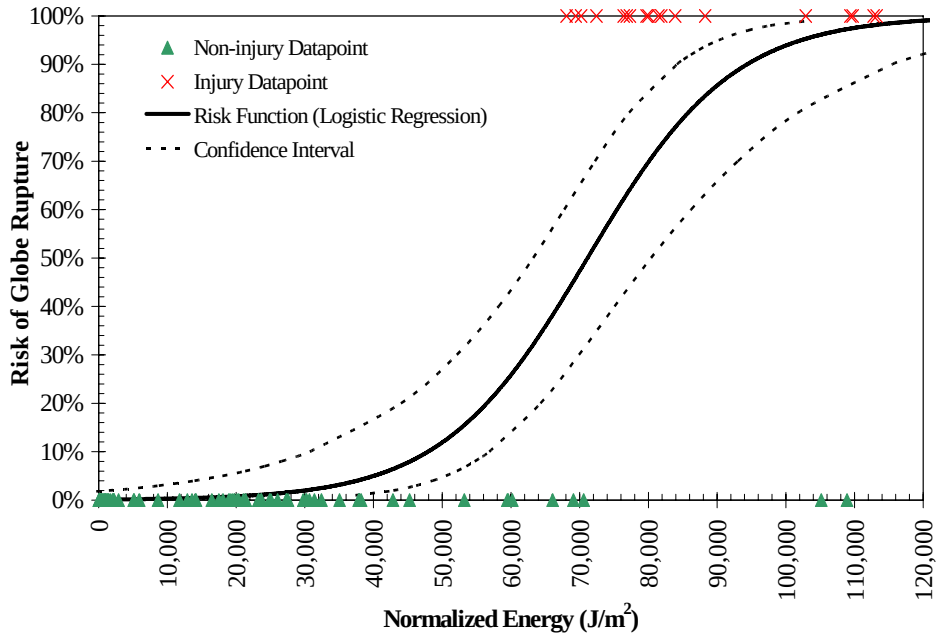

Figure 28: Injury risk curves for globe rupture of porcine eyes for normalized energy.

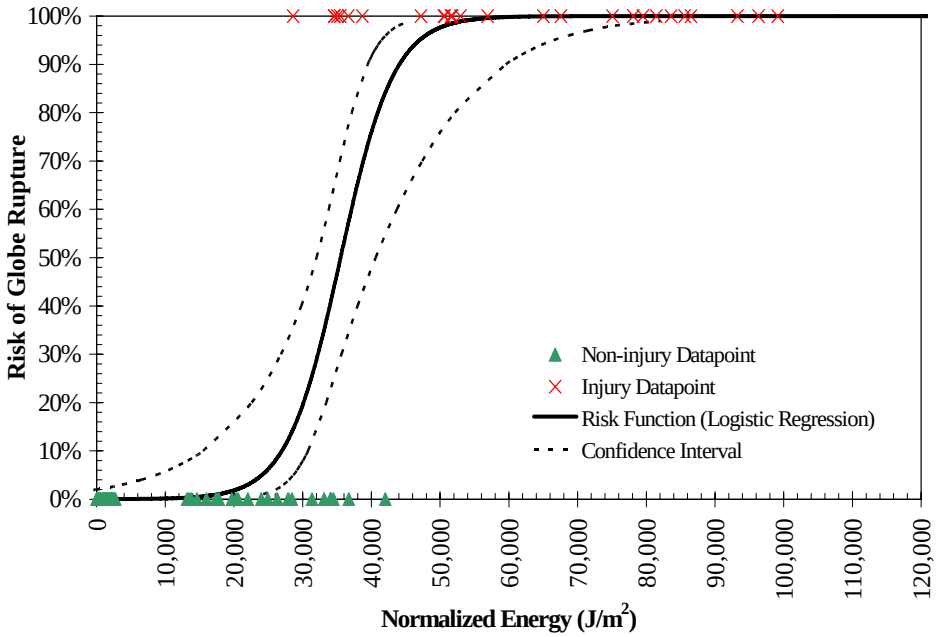

Figure 29: Injury risk curves for globe rupture of human eyes for normalized energy.

For all predictors of eye injury, a logit analysis was performed to calculate the confidence intervals at 50% risk (Table 14). Enough data were present for each of the four different risk functions to fully estimate confidence intervals for each risk function.

Table 14: Confidence intervals for 50% risk of injury.

	Kinetic energy (J)			Normalized energy (J/m2)		
	50% Risk	**Lower Bound**	**Upper Bound**	**50% Risk**	**Lower Bound**	**Upper Bound**
Porcine Eyes	11.1	8.6	14.8	71145	63245	80390
Human Eyes	8.7	5.5	19.1	35519	32018	40641

DISCUSSION

Binary Linear Regression vs. Other Injury Risk Functions

Other injury risk functions, such as the CT method, the modified median rank, and the certainty method, have been suggested because they offer a methodology to develop an injury risk function based strictly on the experimentally determined biomechanical data (Mertz 1996, Eppinger 1999, DiDomenico 2003, Kent 2004). In order to investigate the applicability of the logistic distribution and binary logistic regression, the injury risk function for human eyes is compared for these parametric and non-parametric methods (Figure 30). Comparing the injury risk functions, it can be observed that all methods predict a similar 50% risk of globe rupture, with the CT technique predicting a 50% risk at 34,572 J/m^2, the modified median rank at 35,310 J/m^2, and the certainty method at 35,000 J/m^2, compared to 35,519 J/m^2 from the logistic regression. Moreover, the certainty method risk curve lies within the 90% confidence interval of the logistic regression curve. The CT and the modified mean rank curves are almost completely within the boundaries.

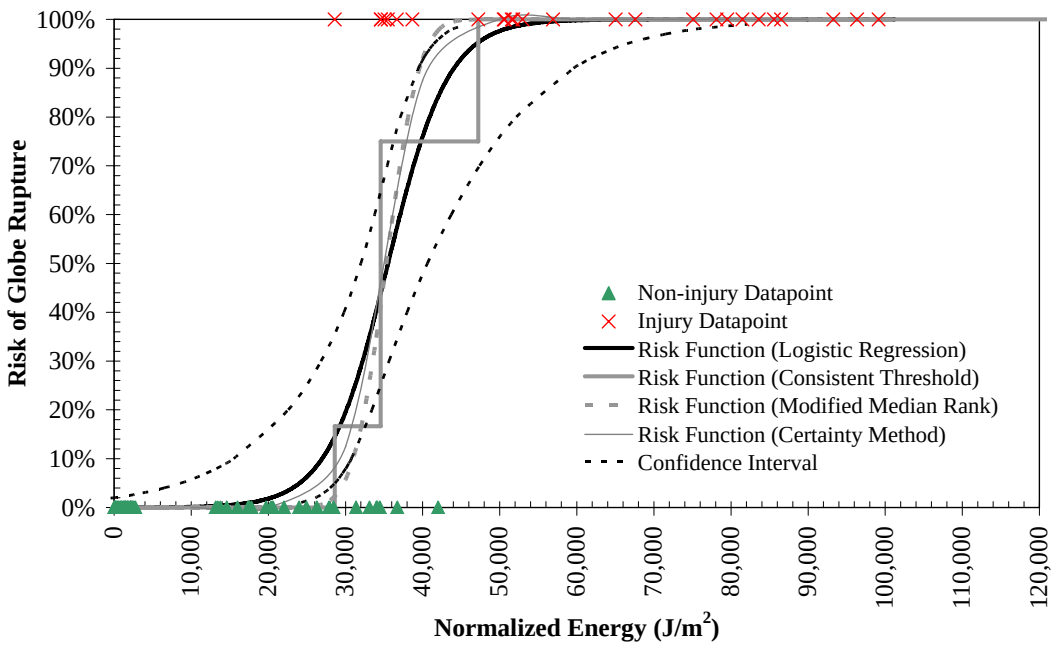

Figure 30: Comparison of binary logistic regression injury risk vs. consistent threshold, modified median rank, and certainty method injury risk for the prediction of globe rupture for human eyes based on normalized energy.

Based on the overall similarity of these injury risk functions, it is felt that the best way of determining injury risk based on the data at hand is by the binary logistic regression injury risk function. Despite the amount of data used to generate the risk functions in this study, there is still a limited amount of data that is being used to represent a much larger population. The CT injury risk model shows a 0% risk of injury for all levels of input below the first injury point and a 100% risk of injury for all levels of input above the last non-injury datapoint (Kent 2004). It would be unlikely that both the first injury datapoint and the last non-injury datapoint determined in this study represented the exact extreme tolerances for the overall human population. The binary logistic regression, the modified median rank, and the certainty method reflect this limitation of the experimental data while closely matching the specific injury risk depicted from our exact experimental dataset.

The median rank method and certainty method have also been used to generate injury risk functions from biological data (Mertz 1996, Eppinger 1999). Both of these methods compare very favorably overall to the binary logistic regression risk function. However, the logistic regression analysis shows a strong goodness of fit with $p < 0.001$ and a Goodman-Kruskal

Gamma value of 0.98. Due to its widespread acceptance and suitability for generating injury risk functions for biological data (Eppinger 1999, Kent 2004), the binary logistic regression is the recommended technique for generating the globe rupture injury risk function. While both the median rank and certainty methods are useful to validate the applicability of the logistic distribution and binary logistic regression analysis for this dataset, they are not the recommended final form of the injury risk function.

Kinetic Energy vs. Normalized Energy

Two types of parameters were used to generate injury risk functions for the prediction of globe rupture. The projectile's kinetic energy, accounts for both the mass and velocity of the assaulting object. Traditionally for eye injury prediction, the kinetic energy of the projectile is used to describe either a threshold for injury response, or has been used to generate injury risk functions to estimate the actual injury potential of an object (Duma 2000, Scott 2000). Kinetic energy has been proven to be related to eye injury response and much better than mass or velocity alone, since both a heavy but relatively slower moving particle and a lightweight, but relatively faster moving particle may, in fact, have the same injury potential. However, the measure of kinetic energy omits to reflect the actual physical size of the projectile, a parameter that is also highly correlated to injury response.

Normalized energy has been defined in this paper as the kinetic energy of a projectile divided by the projected area of the projectile. It could be said that the relationship of kinetic energy to normalized energy is analogous to the relationship of the force to its counterpart of stress. While stress reflects the amount of force acting over a given area, normalized energy reflects the amount of energy that is being presented to a given area of the eye. The projected area reflects the size of the projectile as it contacts the eye. Therefore, considering two objects with the same overall kinetic energy, the smaller projectile will, in turn, develop a higher normalized energy than the larger projectile. It has been experimentally shown in this study that this higher normalized energy directly correlates to a higher risk of globe rupture, and that normalized energy is a better predictor of injury than kinetic energy alone.

Normalized Energy vs. Material Stress

Due to the increase in use of computational models to study injury and predict when failure occurs, a comparison between the injury risk functions based on normalized energy and material stress predicted from computational models is warranted. Using results from previously conducted computational simulations (Stitzel 2002), the risk of globe rupture based on the normalized energy of the simulated projectile can be calculated and compared to overall peak stress levels generated in the computational model (Table 15).

Table 15: Comparison of peak stress level from computational simulation to predicted injury risk from parametric injury risk function.

Simulation Number	Object	Velocity (m/s)	Normalized Energy (J/m^2)	Peak Stress (MPa)	Failure Stress (MPa)	Predicted Injury Risk
S1	BB	56.0	36971	22.81	23.00	59%
S2	BB	92.0	99784	32.76	23.00	100%
SF1	Foam	10.0	122	3.18	23.00	< 1%
SF2	Foam	30.0	1094	7.83	23.00	< 1%
SB1	Baseball	34.4	19057 *	22.15	23.00	1% *
SB2	Baseball	41.2	27336 *	24.62	23.00	11% *

* Because the baseball is larger in diameter than the eye, the amount of normalized energy presented to the eye is underpredicted, resulting in a low estimation of injury risk

Two BB impact simulations were previously reported by Stitzel *et al.* (2002). For a 56 m/s impact velocity, the model predicted a peak stress of 22.81 MPa, just under the estimated failure stress of 23 MPa. The same impact parameters results in a 59% predicted risk of globe rupture from the normalized energy risk function. For the higher velocity impact of 92 m/s, the computer model predicts globe rupture by exceeding the failure stress limit and the normalized energy injury risk function predicts a 100% risk of globe rupture.

Foam impacts to the eye were also simulated using the computer model, and both scenarios were far under the failure stress limit of 23 MPa, at 3.18 MPa and 7.83 MPa for 10 m/s and 30 m/s foam impacts, respectively. When comparing to the normalized energy injury risk functions, both impacts are predicted to have a less than 1% risk of globe rupture.

Finally, two baseball impact simulations were compared to the normalized energy injury risk functions. Unfortunately this scenario shows that for objects larger than the diameter of the eye, using the normalized energy injury risk functions can be misleading. Because some of the energy is transmitted into the surrounding orbit in the computer simulation, not all of the energy from the model is actually transmitted to the eye. Additionally, the calculation for normalized energy assumes even distribution of energy across the entire projected area of the impacting object, when only a smaller local region of the baseball is actually interacting with the eye. This

results in underestimating the actual normalized energy being transferred to the eye. With this in mind, the predicted risk of injury of simulated 34.4 m/s and 41.2 m/s impacts is shown to be 1% and 11%, respectively. However, normalizing the energy only over the projected area of the eye (assumed 25 mm in diameter) the predicted injury risk for both scenarios is predicted to be 100%.

Given the increased use of computational models to study injuries and the paucity of data for dynamic material properties of the human eye, comparisons between the experimentally determined injury risk functions and the results of computational simulations should be made. A future area of research should be to further correlate all of the impact scenarios reported in this paper to the predicted injury risk from computational simulations. At present, using only limited comparisons, high injury risk (> 59%) is predicted as the material stresses from the finite element simulations approach their assumed material failure stresses.

Outlier Data Points

It should be noted that there are two high level non-injurious datapoints for the porcine eye injury risk functions using normalized energy (Figure 28). These two datapoints were both the result of non-injurious BB impact tests on porcine eyes that appear to be unusually strong compared to the rest of the test specimens. Given the analysis of 183 individual eye impact tests, it is expected that some unusually strong or weak eyes would be tested. While these two particular outliers skew the shape of the normalized energy, porcine globe rupture risk curve, they also do not appreciably affect the 50% risk value that was calculated to be 71,145 J/m^2, as opposed to 68,815 J/m^2, if these datapoints were omitted from the logistic regression analysis (Figure 31). If estimation of injury risk at other normalized energy levels is desired, then it may be warranted that further analysis of risk using an analysis that omits these two datapoints may be additionally conducted.

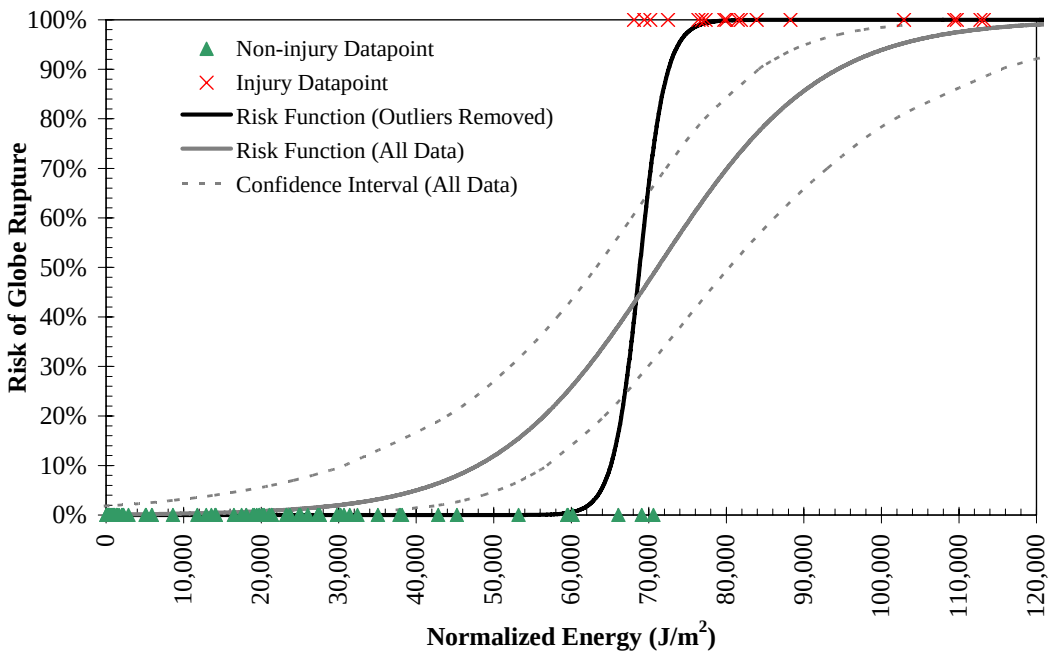

Figure 31: Comparison of injury risk functions for globe rupture of porcine eyes using normalized energy. The injury risk functions are generated using two methods: 1) using all data points and 2) excluding the two non-injury outlier datapoints. The confidence intervals shown are generated using all datapoints.

Human vs. Porcine Eye Strength

Given their relative geometric and anatomical similarities, porcine eyes have frequently been used as surrogates for human eyes for eye injury impact testing (Weidenthal 1966, Vinger 1997, Duma 2000, Scott 2000). The results of this study indicate that porcine eyes are appreciably stronger than human eyes. Using normalized energy, a 50% risk of globe rupture for porcine eyes was determined to be 71,145 J/m^2, as opposed to 35,519 J/m^2, for human eyes. This is almost exactly a 100% relative increase in strength in corneo-scleral strength for porcine eyes compared to human eyes.

In a previous study to determine the rupture pressures of eyes due to an increase in internal pressure, statistically significant differences were observed between human and porcine eyes under both static and dynamic loading conditions (Kennedy 2004). In this study, human and porcine eyes were subjected to increased internal pressure at both dynamic and quasi-static loading rates via pressurization through the optic nerve. Under static conditions porcine eyes

were nearly 3 times stronger than human eyes, rupturing at 1.00 ± 0.18 MPa compared to 0.36 ± 0.20 MPa for human eyes. Dynamic loading again showed porcine eyes to be stronger at rupture pressures of 1.64 ± 0.32 MPa, compared to the rupture pressure of human eyes of 0.91 ± 0.29 MPa.

While no known studies have been reported that compare the material properties of human and porcine corneo-scleral tissue, studies have reported an increase in thickness of porcine scleral thickness relative to human sclera (Olsen 1998, Olsen 2002). These histological studies show that the nominal thickness of porcine sclera can be up to approximately two times greater than the thickness of human sclera. This increase in relative thickness could explain the increased tolerance for globe rupture for porcine eyes versus the human eye; however, to fully understand this issue an area of future research is the characterization of material properties of both human and porcine sclera at dynamic rates.

Coupled with the results of previous studies, the results of this research show that caution must be exercised when evaluating the outcome of experimental tests conducted using porcine eyes. Most experimental eye impact tests on post-mortem eyes are conducted for the purposes of determining if globe rupture or corneal-scleral penetration will occur. This study shows that porcine eyes are nearly twice as resistant to these types of injuries as human eyes. Therefore, a lack of pathology of globe rupture on a porcine eye will not necessarily indicate that a human eye will have negative pathology as well. In this case, the use of the injury risk functions provided in this paper will allow for a more accurate assessment of the potential for injury.

Post-mortem Tissue Degradation

It should be noted that all eyes used for experimental testing as part of this study were enucleated within 24 hours of death, stored in a saline soaked gauze wrap, and refrigerated until just prior to testing. For testing, the eyes were removed from refrigeration and kept hydrated as they returned to room temperature just prior to the actual testing. All eyes were tested within 180 days of death, with most eyes tested within 1 month of death. Other studies have been shown that using

similar storage protocol, the number of days after death prior to testing is not correlated with the overall integrity of the corneo-scleral shell with an R^2 value of 0.14 (Kennedy 2004). This is because of the acellular makeup of the corneo-scleral shell. The strength of the eye comes from the collagen fibers similar to those found in ligaments. These tissues break down very slowly if kept hydrated and refrigerated. Also, the tissue was never frozen because it is sensitive to freeze-thaw cycles. Since the tissue was never frozen and was stored in refrigerated saline, the integrity of the globe was maintained prior to testing.

Combined Injury Risk Functions

The injury risk functions developed in this study can be combined with the similarly developed injury risk functions for other less severe eye injuries (Duma 2005). Using the injury risk functions reported in the previous study, combined with additional data generated during this study, injury risk functions can be compared for corneal abrasion, hyphema, lens dislocation, retinal detachment, and globe rupture.

Using normalized energy, a 50% injury risk of corneal abrasion, hyphema, lens dislocation, retinal damage, and globe rupture is found to be 1,503 J/m^2, 20,188 J/m^2, 19,194 J/m^2, 30,531 J/m^2, and 35,519 J/m^2, respectively. Overall, the results of this combined set of injury risk functions appear logical. Generally, the injury pathologies that are seen more frequently in the clinical setting occur at lower energies than the injury pathologies that are of higher severities and less frequently observed (Pearlman 2001, Kuhn 1995, Duma 1996). Pearlman *et al.* (2001) reviewed 263 cases of eye injury from automobile accidents and observed corneal abrasion and hyphema to be the two most frequently occurring eye injury types in auto accidents. In a review of 24 cases, Kuhn *et al.* (1995) found corneal abrasion and hyphema to occur in approximately 33% of automotive eye injury cases, compared to approximately 16% who suffered retinal injury. The study did not mention the incidence rate for lens dislocation and globe rupture was not observed in this study. Duma *et al.* (1996) show similar injury rates for corneal abrasion, hyphema, and retinal detachment, while showing approximately a 4% chance of globe rupture due to airbag-related eye trauma.

Future Applications

Currently, eye injury assessment tools for automobile, consumer product, sports, and military are not based on biomechanically determined injury limits. For automobile safety, anthropometric test devices (ATDs) such as the Hybrid-III dummy have no capability for measuring eye injury risk. The THOR dummy, utilizes four facial load cells to predict facial injury, but has no eye injury assessment capability. Conversely, the National Operating Committee on Standards for Athletic Equipment (NOCSAE) headform and the American National Standards Institute (ANSI) Alderson headform have detailed facial geometry including the eyes, nose, and mouth, but no instrumentation to determine eye or other head injury. Due to the lack of appropriate measurement capabilities of these headforms, it is expected that the injury risk functions presented in this paper could serve to assess the eye injury risk from potential eye impacts. However, this is only possible in cases where the specific velocity and size of impacting projectiles can be determined.

Since the injury risk functions presented in this paper are input based, they could be useful in development of a biofidelic sensor and injury thresholds for a synthetic eye sensor. Projectile tests can be conducted on an instrumented synthetic eye and the sensor outputs calibrated to the predicted injury risk based on the input parameters. This approach to injury threshold determination for ATDs may ultimately yield more accurate injury risk prediction due to the fact that a direct mapping from input energy and known injury risk are correlated to sensor output. A development such as a synthetic eye in an advanced ATD headform would allow experimental testing and evaluation of possible eye injury hazards, even in scenarios such as automobile crash testing where it may be extremely difficult to isolate and determine projectile characteristics that may assault the eye.

Limitations

Despite the fact that the present study utilizes a large amount of experimental data for the development of injury risk functions, there are several areas where further research is warranted. First, while all experimental data was pooled into two large impact databases for human and porcine eyes, it is also possible to develop projectile specific risk functions for globe rupture and

compare these to the overall injury risk functions. However, due to the large variety of objects used in the eye impact tests, an insufficient number of injury and non-injury data exists from which projectile specific injury risk functions can be determined. While it would have been possible to utilize a smaller variety of projectiles for the experimental tests, it was felt that this would negate the advantage of a sufficient variety of objects used to develop a versatile risk function for virtually any type of blunt projectile. Second, because of the rapid degradation of other internal structures of the eye, such as the retina and lens detaching from their *in-vivo* positions, it is not possible to test post-mortem eyes for injury pathologies such as lens and retinal damage. Third, due to the lack of cardiovascular pressure, it is not possible to test post-mortem eyes for hyphema. A limited amount of experimental data exists for these injuries from previously performed live animal tests. It would be desirable to have additional data in order to develop injury risk functions in a similar manner to that of the current study.

Although the current study demonstrates a clear and accurate method for determining the risk of globe rupture based on projectile characteristics, it has not presented a more typical set of experimental results of failure stress or failure strain of the corneo-scleral shell. At present, no studies have presented the failure stress or strain of the human eye due to dynamic impact. While the injury risk functions are useful in a practical sense, it is still desirable to determine these properties of the human eye, especially for use in computational models of the eye. Knowledge of the material properties of the human and the porcine eye will also have a profound effect in explaining the significant strength differences between human and porcine eyes.

CONCLUSION

Eye injuries in both the civilian and military sectors are severely debilitating and pose an enormous health cost. The relative severity of eye injuries is much greater for the military than in the civilian population. Computer models have been shown to be an effective tool in predicting eye injury response, such as globe rupture, from blunt impact. However, the use of computer models is not always practical or possible for the wide range of impact scenarios or industries in which eye injuries are a concern. Also, due to a lack of instrumentation, the prediction of eye injuries using anthropomorphic test devices is not currently possible. The

current study presents a new method to determine the risk of globe rupture to projectile impacts, based on the projectile characteristics of mass, velocity, and area of contact. A total of 183 eye impact tests were analyzed to develop injury risk functions and estimate confidence intervals for human and porcine eyes. It has been shown that porcine eyes are more resistant to globe rupture than human eyes. In the present study, a 50% risk of globe rupture was found to be 71,145 J/m^2 for porcine eyes, compared to 35,519 J/m^2 for human eyes. The results presented in this paper will be useful in estimating the risk of globe rupture when projectile parameters are known, or can be coupled with a computational or physical model for injury risk criteria that correlates with experimentally based injury response.

REFERENCES

Allison, P.D. (1999) Logistic Regression Using the SAS System: Theory and Application, Cary, NC, SAS Institute Inc.

Berger, R.E. (1978) A model for evaluating the ocular contusion injury potential of propelled objects. Journal of Bioengineering 2: 345-358.

Biehl, J.W., Valdez, J., Hemady, R.K., Steidl, S.M., Bourke, D.L. (1999) Penetrating eye injury in war. Military Medicine 164(11): 780-784.

Collett, D. (1991) Modeling Binary Data, Chapman and Hall, London.

Chisholm, L. (1969) Ocular injury due to blunt trauma. Applied Therapeutics 11(11):597-598.

Delori, F., Pomerantzeff, O., Cox, M.S. (1969) Deformation of the globe under high speed impact: its relation to contusion injuries. Investigative Ophthalmology 8:290-301.

DiDomenico, L., Nusholtz, G. (2003) Comparison of parametric and non-parametric methods for determining injury risk. Society of Automotive Engineers. 2003-01-1362.

Duma, S.M., Kress, T.A., Porta, D.J., Woods, C.D., Snider, J.N., Fuller, P.M., Simmons, R.J. (1996) Airbag-induced eye injuries: a report of 25 cases. The Journal of Trauma: Injury, Infection, and Critical Care 41(1): 114-119.

Duma, S.M., Crandall, J.R.. (2000) Eye injuries from airbags with seamless module covers. Journal of Trauma 48(4): 786-789.

Duma, S.M., Jernigan, M., Stitzel, J.D., Herring, I., Crowley, J., Brozoski, F., Bass, C. (2002) The effect of frontal air bags on eye injury patterns in automobile crashes. Archives of Ophthalmology 120(11): 1517-1522.

Duma, S.M., Ng, T.P., Kennedy, E.A., Stitzel, J..D, Herring, I.P., Kuhn, F. (2005) Determination of significant parameters for eye injury risk from projectiles. Journal of Trauma 59(4): 960-964.

Endo, S., Ishida, N., Yamaguchi, T. (2000) The BB gun is equivalent to the airsoft gun in the japanese literature. Archives of Ophthalmology 118: 732.

Endo, S., Ishida, N., Yamaguchi, T. (2001) Tear in the trabecular meshwork caused by an airsoft gun. American Journal of Ophthalmology 131: 656-657.

Eppinger, R., Sun, E., Bandak, F., Haffner, M., Khaewpong, N., Maltese, M., Kuppa, S., Nguyen, T., Takhounts, E., Tannous, R., Zhang, A., Saul, R. (1999) Development of Improved Injury Criteria for the Assessment of Advanced Automotive Restraint Systems - II. NHTSA, USA.

Fineman, M.S., Fischer, D.H., Jeffers, J.B., Buerger, D.G., Repke, C. (2000) Changing trends in paint ball sport related ocular injuries. Archives of Ophthalmology 118(1): 60-64.

Fleischhauer, J.C., Goldblum, D., Frueh, B.E., Koerner, F. (1999) Ocular injuries caused by airsoft guns. Archives of Ophthalmology 117: 1437-1439.

Galler, E.L., Umlas, J.W., Vinger, P.F., Wu, H.K. (1995) Ocular integrity after quantitated trauma following photorefractive keratectomy and automated lamellar keratectomy. Investigative Ophthalmology & Visual Science 36(4):S580.

Ghafouri, A., Burgess, S.K., Hrdlicka, Z.K., Zagelbaum, B.M. (1997) Air bag - related ocular trauma. American Journal of Emergency Medicine 15(4): 389-392.

Green, R.P., Jr., Peters, D.R., Shore, J.W., Fanton, J.W., Davis H. (1990) Force necessary to fracture the orbital floor. Ophthalmic Plastic & Reconstructive Surgery 6(3):211-217.
Hansen, G.A., Stitzel, J.D., Duma, S.M. (2003) Incidence of elderly eye injuries in automobile crashes: The effects of lens stiffness as a function of age. Association for the Advancement of Automotive Medicine, 47th Annual Proceedings, Lisbon Portugal.
Heier, J.S., Enzenauer, R.W., Wintermeyer, S.F., *et al.* (1993) Ocular injuries and diseases at a combat support hospital in support of Operations Desert Shield and Desert Storm. Archives of Ophthalmology 111: 795-798.
Kennedy, E.A., Voorhies, K.D., Herring, I.P., Rath, A.L., Duma, S.M. (2004) Prediction of severe eye injuries in automobile accidents: static and dynamic rupture pressure of the eye. The Proceedings of the 48th Association for the Advancement of Automotive Medicine Conference, Key Biscayne, Florida.
Kent, R.W., Funk, J.R. (2004) Data censoring and parametric distribution assignment in the development of injury risk functions from biomechanical data. Society of Automotive Engineers. 2004-01-0317.
Kuhn F, Collins P, Morris R, Witherspoon CD (1994) Epidemiology of motor vehicle crash-related serious eye injuries. Accident Analysis and Prevention 26(3): 385-390.
Kuhn, F., Morris, R., Witherspoon, C.D. (1995) Eye injury and the airbag. Current Opinion in Ophthalmology 6(iii): 38-44.
Kuhn F, Morris R, Witherspoon CD, *et al.* (2000) Serious fireworks-related eye injuries. Ophthalmic Epidemiology 7: 139-148.
Listman, D.A. (2004) Paintball injuries in children: more than meets the eye. Pediatrics 113(1): e15-e18.
Lueder, G.T. (2000) Airbag associated ocular trauma in children. Journal of Ophthalmology 107(8):1472-1475.
Mader, T.H.L., Aragones, J.V., Chandler, A.C., *et al.* (1993) Ocular and ocular adnexal injuries treated by United States military ophthalmologists during Operation Desert Shield and Desert Storm. Ophthalmology 100: 1462-1467.
Mertz, H.J., Prasad, P., Nusholtz, G. (1996) Head injury risk assessment for forehead impacts. SAE Transactions 960099: 26-46.
McGwin, G., Xie, A., Owsley, C. (2005) Rate of eye injury in the United States. Archives of Ophthalmology 123: 970-976.
McKnight, S.J., Fitz, J., Giangiacomo, J. (1988) Corneal rupture following keratotomy in cats subjected to BB gun injury. Ophthalmic Surgery 19(3):165-167.
Olsen, T.W., Aaberg, S.Y., Geroski, D.H., Edelhauser, H.F. (1998) Human sclera: thickness and surface area. American Journal of Ophthalmology 125(2): 237-241.
Olsen, T.W., Sanderson, S., Feng, X., Hubbard, W.C. (2002) Porcine sclera: thickness and surface area. Investigative Ophthalmology and Visual Science 43(8): 2529-2532.
Parver, L.M. (1986) Eye trauma: the neglected disorder. Archives of Ophthalmology 104: 1452-1453.
Peacock, L.W., Slade, S.G., Martiz, J., Chuang, A., Yee, R.W. (1997) Ocular integrity after refractive procedures. Ophthalmology 104(7):1079-1083.
Pearlman, J.A., AuEong, K.G., Kuhn, F., Pieramici, D.J. (2001) Airbags and eye injuries: epidemiology, spectrum of injury, and analysis of risk factors. Survey of Ophthalmology 46(3): 234-242.
Power, E.D., Stitzel, J.D., Duma, S.M., Herring, I.P., West, R.L. (2002) Investigation of ocular injuries from high velocity objects in an automobile collision. SAE Technical Paper Series 2002-01-0027: 1-8.
Rodriguez, J.O., Lavina, A.M. (2003) Prevention and treatment of common eye injuries in sports. American Family Physician 67: 1481-1488.
Scott, W.R., Lloyd, W.C., Benedict, J.V., Meredith R. (2000) Ocular injuries due to projectile impacts. Association for the Advancement of Automotive Medicine 205-217.
Stein J.D., Jaeger E.A., Jeffers J.B. (1999) Air bags and ocular injuries. Transactions American Ophthalmology Society 97: 59-82.
Stitzel, J.D., Duma, S.M., Cormier, J.M., Herring, I.P. (2002) A nonlinear finite element model of the eye with experimental validation for the prediction of globe rupture. Stapp Car Crash Journal 46:81-102.
Stitzel J.D., Hansen G.A., Herring, I.P., Duma S.M. (2005) Blunt trauma of the aging eye. Archives of Ophthalmology 123: 789-794.
Stone, W. (1950) Ocular injuries in the armed forces. Journal of the American Medical Association 142: 151-152.
Thach, A.B., Ward, T.P., Hollifield, R.D., et. al. (1999) Ocular injuries from paintball pellets. Ophthalmology 105: 533-547.
Vichnin, M.C., Jaeger, E.A., Gault, J.A., Jeffers, J.B. (1995) Ocular injuries related to air bag inflation. Ophthalmic Surgery and Lasers 26: 542-548.

Vinger, P.F. (1996) Baseball eye protection: the effect of impact by major league and reduced injury factor baseball on currently available eye protectors. International Symposium on Safety in Baseball and Softball, American Society for Testing and Materials.
Vinger, P.F., Sparks, J.J., Mussack, K.R., Dondero, J., Jeffers, J.B. (1997) A program to prevent eye injuries in paintball. Sports Vision 3:33-40.
Vinger, P.F., Duma, S.M., Crandall, J. (1999) Baseball hardness as a risk factor in eye injuries. Archives of Ophthalmology 117: 354-358.
Vinger, P.F. (2005) Understanding eye trauma through computer modeling. Archives of Ophthalmology 123: 833-834.
Weidenthal, D.T. (1964) Experimental ocular contusion. Archives of Ophthalmology 71: 111-115.
Weidenthal, D.T., Schepens, C.L. (1966) Peripheral fundus changes associated with ocular contusion. American Journal of Ophthalmology 62: 465-477.
Wong, T.Y., Smith, G.S., Lincoln, A.E., Tielsch, J.M. (2000) Ocular trauma in the United States Army: hospitalization records from 1985 through 1994. American Journal of Ophthalmology 129(5): 645-650.

CHAPTER 5:
MATCHED EXPERIMENTAL AND COMPUTATIONAL SIMULATIONS OF PAINTBALL EYE IMPACTS

ABSTRACT

Over 1200 paintball related eye injuries are treated every year in US emergency departments. These injuries can be manifested as irritation from paint splatter in the eye to catastrophic rupture of the globe. Using the Virginia Tech – Wake Forest University Eye Model, experimental paintball impacts were replicated and the experimental and computational results compared. A total of 10 paintball impacts were conducted from a range of 71.1 m/s to 112.5 m/s. All experimental tests resulted in rupture of the globe. The matched computational simulations also predicted near-failure or failure in each of the simulations, with a maximum principal stress of greater than 22.8 MPa in all scenarios, over 23 MPa for velocities above 73 m/s. Failure stress for the VT-WFU Eye Model is defined as 23 MPa. The current regulation velocity for paintballs of 91 m/s exceeds the tolerance of the eye to globe rupture and underscores the importance for eyewear in this sport.

INTRODUCTION

There are over 1.9 million eye injuries per year in the United States (McGwin 2005). Some of the most severe eye injuries are caused by high speed projectiles from fireworks, sports equipment, firearms and air-powered guns (Berger 1978, Vinger 1997, Kuhn 2000). One of the most alarming ocular injury trends in the past decade has been the proliferation of paintball guns and a proportional increase in the number of ocular eye injuries caused by paintballs (Vinger 1997, Farr 1999, Listman 2004, Vassilev 2004, Laraque 2004, Committee on Sports Medicine and Fitness 2004). The number of paintball-related eye injuries treated in US emergency medical departments more than doubled from 545 in the year 1998, to more than 1200 in the year 2000, with nearly 40% of those cases occurring in pediatric patients (Listman 2004).

Previous researchers have performed eye impact tests to determine the injury tolerance of eyes to a variety of blunt objects (Weidenthal 1964, Weidenthal 1966, Delori 1969, McKnight 1988, Green 1990, Duma 2000, Scott 2000, Stitzel 2002). Additionally, researchers have shown

computational models of the eye to be effective for analyzing the injury potential of a variety of different impact situations (Kisielewicz 1998, Uchio 1999, Uchio 2001, Power 2002, Stitzel 2002, Hansen 2003, Stitzel 2005).

The intent of both experimental models and computational models is to determine the parameters at which eye injury can be predicted. In experimental studies, researchers have used kinetic energy, velocity, mass, and normalized energy to predict the risk of eye injury (Berger 1978, Duma 2000, Scott 2000, Duma 2005, Kennedy 2006). In computational models, material level responses of stress and strain are the primary factors used to infer injury or non-injury impact scenarios (Kisielewicz 1998, Uchio 1999, Uchio 2001, Power 2002, Stitzel 2002, Hansen 2003, Stitzel 2005). In order to look more closely at the global and localized response of the eye to paintball impacts, a series of matched experimental tests and computational simulations will be performed to further develop our understanding of paintball impacts to the human eye.

METHODOLOGY

Experimental impact tests were conducted using post-mortem human eyes. Prior to testing, the eyes were pressurized to physiologic pressure through the optic nerve. All eyes were placed in a synthetic orbit designed of polycarbonate, which was then filled with a 10% gelatin solution, designed to approximate the dimensions and extraocular fatty tissue of a human orbit (Vinger 1997, Stitzel 2002, Kennedy 2007). Paintballs were fired from a distance of approximately 175 cm using a paintball gun (Kingman, Spyder TL-X, Baldwin Park, CA). Tests were conducted by firing the gun directly at the cornea of the eye in an enclosed shooting gallery. High-speed video (Vision Research, Phantom IV, Wayne, NJ) was taken of each impact event at 7400 frames per second and was used to record the impact event, and calibrated to determine the projectile velocity. Eyes were inspected for injury following each test. High speed video was used to determine the velocity of the projectile, and the kinetic and normalized energy of the projectiles were calculated. Normalized energy is defined as the kinetic energy of a projectile divided by the projected area of the projectile.

An existing finite element model of the eye, the Virginia Tech – Wake Forest University Eye Model (VT-WFU Eye Model) has been validated to predict globe rupture for dynamic blunt impacts of the eye (Stitzel 2002, Stitzel 2003, Stitzel 2005). This eye model was developed to include detailed geometry of the cornea, sclera and limbus, as well as the ciliary body, zonules and lens. The model includes both Lagrangian and Eulerian meshes to accurately represent the mechanics of both solid and fluid interactions. The model had a total of 10,020 solid and shell elements and was developed using LS-DYNA software (Livermore Software Technology Corporation, Livermore, CA). The model was set up to perform matched computational simulations of the experimental paintball impact tests. Results from the computational simulations (local response) were jointly analyzed with the experimental outcome of impact tests (global response) to compare the outcome of impacts under both testing modalities.

RESULTS

A total of 10 matched experimental tests and computational simulations were conducted. For the experimental tests, projectile velocities ranged from 71.1 m/s to 112.5 m/s (Table 16). Based on the normalized energy of the paintballs, risk of globe rupture ranged from 44% at 71.1 m/s to nearly 100% from 97.9 m/s and above. The actual experimental outcome for all tests was globe rupture. Computational modeling results showed similar likelihood of injury, with maximum principal stress at the equator of the eye ranging from 22.83 MPa to 30.01 MPa, where the VT-WFU Eye Model is validated to predicting globe rupture at a threshold of 23 MPa.

Table 16: Test results from experimental eye impact tests on porcine eyes.

Test #	Velocity (m/s)	Norm. Energy (J/m^2)	Risk of Globe Rupture	Experimental Tests		Computational Simulations	
				Duration (ms)	Outcome	Time to Max Stress (ms)	Max Principal Stress (MPa)
1	71.1	34572	44%	0.41	Globe Rupture	0.37	22.83
2	71.3	34613	44%	0.36	Globe Rupture	0.38	22.88
3	71.7	35070	47%	0.54	Globe Rupture	0.37	22.88
4	72.0	35478	50%	0.27	Globe Rupture	0.36	22.94
5	73.3	36645	57%	0.40	Globe Rupture	0.37	23.20
6	75.3	38684	69%	0.33	Globe Rupture	0.36	23.47
7	97.9	65030	100%	0.27	Globe Rupture	0.29	26.74
8	108.0	79493	100%	0.27	Globe Rupture	0.27	28.34
9	109.4	81471	100%	0.27	Globe Rupture	0.21	30.01
10	112.5	86503	100%	0.21	Globe Rupture	0.26	29.04

For three simulations conducted at initial paintball velocities of 71.1 m/s, 97.9 m/s and 112.5 m/s, the principal stress vs. time is shown (Figure 32). It is notable that each of the three simulations reach the failure threshold of 23 MPa within approximately 0.05 ms of the timing noted for rupture in experimental testing. Comparisons are presented from high-speed video and simulations (Figure 33).

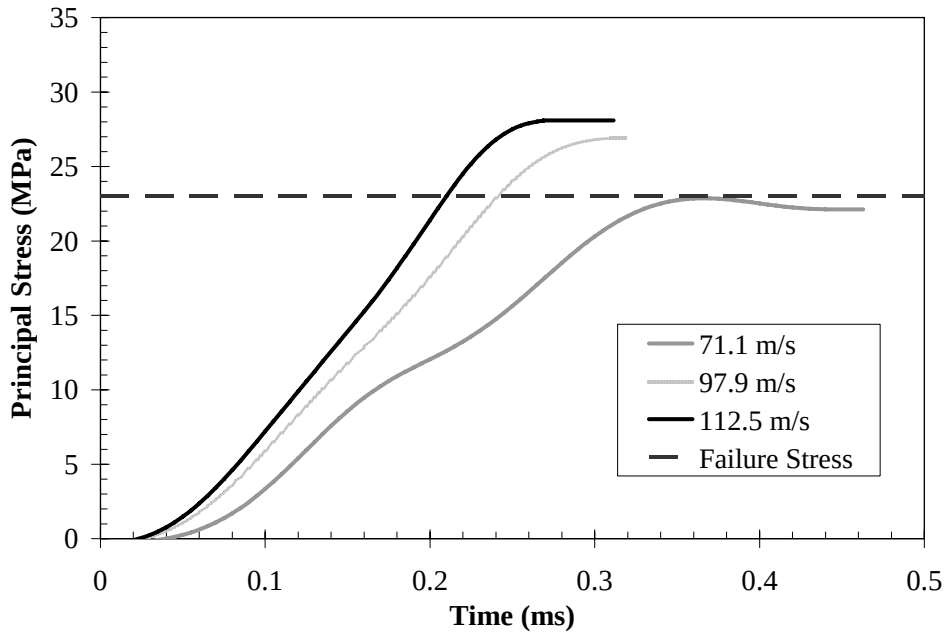

Figure 32: Principal stress vs. time for three different paintball impact scenarios.

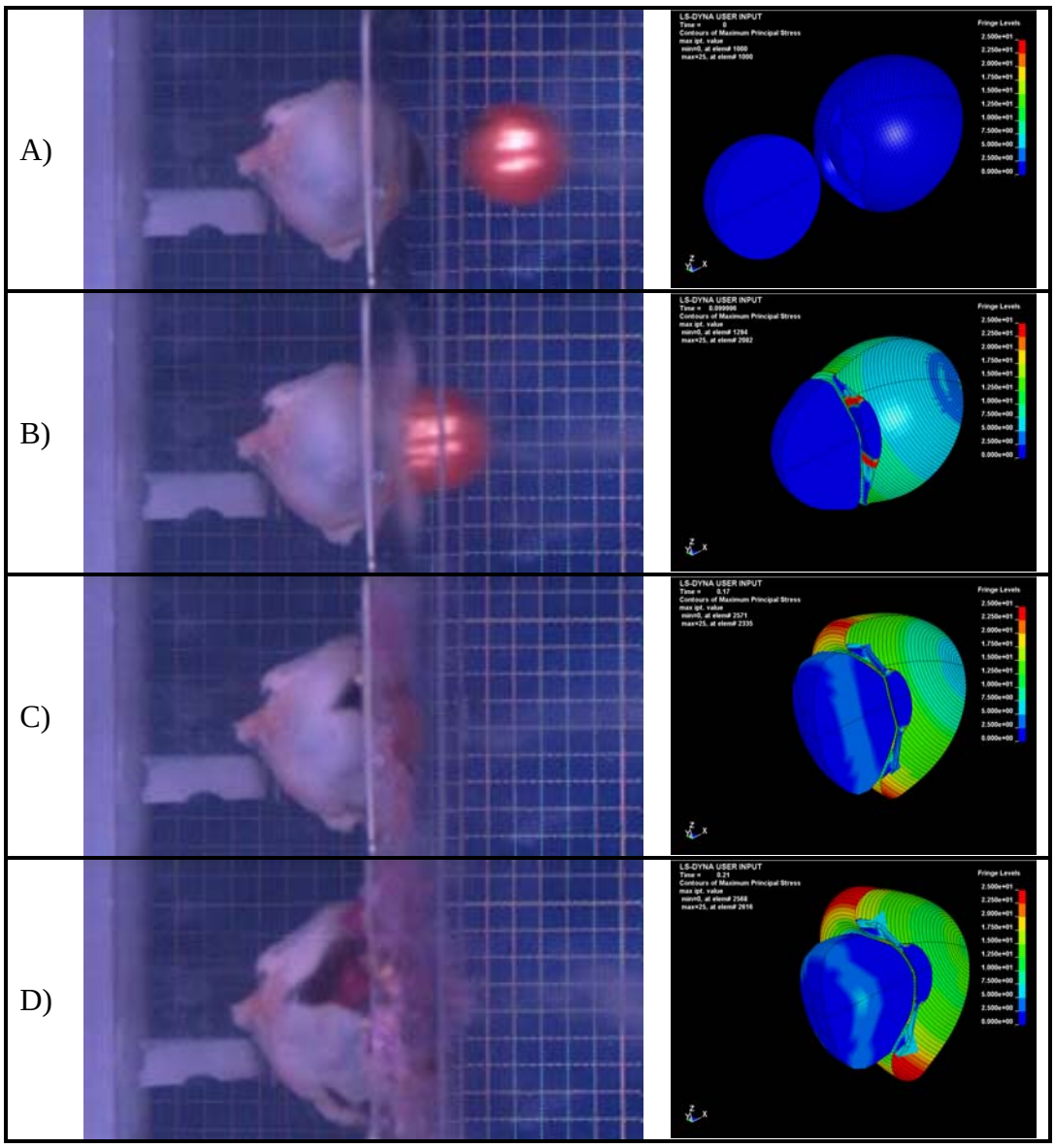

Figure 33: Experimental tests vs. computational simulation of 112.5 m/s paintball impact:
a) pre-impact condition for both experimental and computational scenarios,
b) first high-speed frame showing impact for experimental test (left), 0.1 ms into impact scenario for computational simulation (right)
c) second high-speed frame of impact shows initial signs of rupture at equator (left), 0.17 ms into impact scenario the computational model eclipses 23 MPa at corneo-scleral shell
d) third high-speed frame of impact shows catastrophic rupture of the globe, 0.21 ms into impact shows the equator of the eye well above the 23 MPa failure stress.

DISCUSSION

Based on the determination of normalized energy, the risk of globe rupture for all ten impacts is substantial, yielding a 44% risk of injury in the lowest velocity (71 m/s), to nearly 100% risk of injury at the high velocity impacts (>97 m/s). It was shown that at a velocity of 72 m/s the risk of globe rupture is 50%, indicating globe rupture for one out of two eye impacts at this velocity. Given a larger sample size, perhaps some eyes would have sustained a paintball impact without rupturing; however, the risk of injury in all scenarios was substantial. The regulation velocity for most paintball games is approximately 91 m/s.

Generally, strong agreement was observed between the experimental test results and the VT-WFU Eye Model simulation results. In experimental testing, all eyes tested resulted in globe rupture and the results from the computational modeling indicate that all tests exceeded the failure threshold or were within 0.2 MPa of the 23 MPa failure threshold. The computational model also closely replicates the actual timing of globe rupture as observed in the experimental tests.

It should be noted that in the computational simulations, failure of the eye or paintballs was not modeled. This is an important consideration when interpreting the results of the simulation. For instance, at 112.5 m/s the model predicts a maximum principal stress of 29 MPa at 0.26 ms. Upon closer inspection, the time history of the principal stress shows that the corneo-scleral shell reached the 23 MPa threshold at 0.21 ms. The peak principal stresses are therefore intended to be interpreted as indicators of the injury status of the eye, whether the failure threshold was exceeded or not. Larger peak principal stresses are representative only of the expectation of a potentially more catastrophic injury.

Since the paintballs are not designed to rupture in this model, it is possible that under certain conditions the experimental paintball could rupture, expending enough energy that the eye would not rupture. For the matched computational simulation, the computational paintball would not rupture and would continue to impact the eye and produce deformation that would lead to

predicted failure. In this study, such a scenario did not present itself; however, in such a case, it would be prudent to stop the computational simulation at the time duration where the paintball was observed to fail in the matched experimental test.

CONCLUSION

Paintball injuries are an increasingly common and potentially devastating eye injury. Using the Virginia Tech – Wake Forest University Eye Model, experimental paintball impacts were replicated and the experimental and computational results compared. A total of 10 paintball impacts were conducted from a range of 71.1 m/s to 112.5 m/s. All experimental tests resulted in rupture of the globe. The matched computational simulations also predicted near-failure or failure in each of the simulations, with a maximum principal stress of greater than 22.8 MPa in all scenarios, over 23 MPa for velocities above 73 m/s. Failure stress for the VT-WFU Eye Model is defined as 23 MPa. The current regulation velocity for paintballs of 91 m/s exceeds the tolerance of the eye to globe rupture and underscores the importance of protective eyewear in this sport.

REFERENCES

Allison, P.D. (1999) Logistic Regression Using the SAS System: Theory and Application, Cary, NC, SAS Institute Inc.

Berger RE. (1978) A model for evaluating the ocular contusion injury potential of propelled objects. Journal of Bioengineering 2: 345-358.

Collett, D. (1991) Modeling Binary Data, Chapman and Hall, London.

Committee on Sports Medicine and Fitness (2004) Protective eyewear for young athletes. Pediatrics 113: 619-622.

Delori, F., Pomerantzeff, O., Cox, M.S. (1969) Deformation of the globe under high speed impact: its relation to contusion injuries. Investigative Ophthalmology 8:290-301.

Duma S.M., Crandall J.R.. (2000) Eye injuries from airbags with seamless module covers. J Trauma. 48(4):786-9.

Duma, S.M., Ng, T.P., Kennedy, E.A., Stitzel, J..D, Herring, I.P., Kuhn, F. (2005) Determination of significant parameters for eye injury risk from projectiles. Journal of Trauma 59(4): 960-964.

Farr AK, Fekrat S. (1999) Eye injuries associated with paintball guns. International Ophthalmology 22: 169-173.

Green, R.P., Jr., Peters, D.R., Shore, J.W., Fanton, J.W., Davis H. (1990) Force necessary to fracture the orbital floor. Ophthalmic Plastic & Reconstructive Surgery 6(3):211-217.

Hansen, G.A., Stitzel, J.D., Duma, S.M. (2003) Incidence of elderly eye injuries in automobile crashes: The effects of lens stiffness as a function of age. Association for the Advancement of Automotive Medicine, 47th Annual Proceedings, Lisbon Portugal.

Kennedy EA, Ng TP, McNally C, Stitzel JD, Duma SM (2006) Risk functions for human and porcine eye rupture based on projectile characteristics of blunt objects. Stapp Car Crash Journal 50.

Kennedy EA, McNally C, Duma SM (2007) Experimental techniques for measuring the biomechanical response of the eye during impact. Biomedical Sciences Instrumentation 43: 7-12

Kisielewicz LT, Kodama N, Ohno S, Uchio E (1998) Numerical prediction of airbag caused injuries on eyeballs after radial keratotomy. Society of Automotive Engineers.

Kuhn F, Morris R, Witherspoon CD, *et al.* (2000) Serious fireworks-related eye injuries. Ophthalmic Epidemiology 7: 139-148.
Laraque D, and the Committee on Injury, Violence, and Poison Prevention. (2004) Injury risk of nonpowder guns. Pediatrics 114: 1357-1361.
Listman DA. (2004) Paintball injuries in children: more than meets the eye. Pediatrics 113: e15-e18.
McGwin G, Xie A, Owsley C (2005) Rate of eye injury in the United States. Archives of Ophthalmology 123: 970-976.
McKnight S.J., Fitz J., Giangiacomo J. (1988) Corneal rupture following keratotomy in cats subjected to BB gun injury. Ophthalmic Surgery. 19(3):165-167.
Power E, Duma S, Stitzel J, Herring I, West R, Bass C, Crowley J, Brozoski F. (2002) Computer modeling of airbag induced ocular injury in pilots wearing night vision goggles. Aviation Space and Environmental Medicine 73: 1000-1006.
Power, E.D., Stitzel, J.D., Duma, S.M., Herring, I.P., West, R.L. (2002) Investigation of ocular injuries from high velocity objects in an automobile collision. SAE Technical Paper Series 2002-01-0027: 1-8.
Scott, W.R., Lloyd, W.C., Benedict, J.V., Meredith R. (2000) Ocular injuries due to projectile impacts. Association for the Advancement of Automotive Medicine 205-217.
Stitzel J.D., Hansen G.A., Herring, I.P., Duma S.M. (2005) Blunt trauma of the aging eye. Archives of Ophthalmology 123: 789-794.
Stitzel J.D., Hansen, G.A., Duma S.M. (2003) Modeling elderly eye injuries in automobile crashes. Proceedings of ASME International Mechanical Engineering Congress 2003, Washington D.C. IMECE2003-43454.
Stitzel J.D., Duma S.M., Cormier J.M., Herring I.P. (2002) A nonlinear finite element model of the eye with experimental validation for the prediction of globe rupture. Stapp Car Crash Journal. 46:81-102.
Uchio E, Ohno S, Kudoh J, Aoki K, Kisielewicz LT. (1999) Simulation model of an eyeball based on finite element analysis on a supercomputer. British Journal of Ophthalmology 83: 1106-1111.
Uchio E. Ohno S, Kudoh J, Kadanosono K, Andoh K, Kisielewicz LT. (2001) Simulation of air-bag impact on post-radial keratotomy eye using finite element analysis. Journal of Cataract Refractive Surgery 27: 1847-1853.
Vassilev Z.P., Marcus, S.M. (2004) Paintball injuries in children: the cases managed out of hospitals. Pediatrics 113: 1468.
Vinger, P.F., Sparks, J.J., Mussack, K.R., Dondero, J., Jeffers, J.B. (1997) A program to prevent eye injuries in paintball. Sports Vision 3:33-40.
Weidenthal, D.T. (1964) Experimental ocular contusion. Archives of Ophthalmology 71: 111-115.
Weidenthal, D.T., Schepens, C.L. (1966) Peripheral fundus changes associated with ocular contusion. American Journal of Ophthalmology 62: 465-477.

CHAPTER 6:
DEVELOPMENT AND VALIDATION OF THE SYNTHETIC EYE AND ORBIT FOR THE FOCUS HEADFORM

ABSTRACT

The Facial and Ocular CountermeasUre Safety (FOCUS) headform is intended to aid safety equipment design in order to reduce the risk of eye and facial injuries. The purpose of this paper is to present a three part study that details the development and validation of the FOCUS synthetic eye and orbit and the corresponding eye injury criteria. The synthetic eye and orbit were designed to simulate the force-deflection response to *in-situ* dynamic impacts. In part I, the force-deflection response of the eye was determined based on dynamic blunt impact tests with human eyes. These data were used to validate the appropriate material for a biofidelic synthetic eye. In part II, force-deflection corridors developed from ten dynamic *in-situ* eye impacts were used to validate the design and material selections for the synthetic orbit assembly. In part III, 82 experimental tests on the FOCUS headform were conducted using steel BB projectiles to develop a conservative injury risk criteria for the FOCUS headform based on the response of the eye load cell. Injury criterion for globe rupture is strongly correlated to the data from the FOCUS eye load cell ($R^2 = 0.995$). Based on the response of the FOCUS eye load cell, a 50% risk of globe rupture is shown to be 107 N. With a biofidelic synthetic eye and headform-specific injury criteria, the FOCUS headform can be used to evaluate the effectiveness of eye injury countermeasures in military, sports, and automotive safety systems to prevent eye injuries.

INTRODUCTION

There are over 1.9 million eye injuries each year in the United States (McGwin 2005). The incidence of severe eye injuries is on the same order of magnitude of the number of passengers killed in vehicle crashes every year, with approximately 30,000 Americans left blind in one eye as a result of trauma (Parver 1986). Some of the most severe eye injuries can occur in automobile accidents, from sports related impacts, in the workplace and even at home (Figure 34) (Chisholm 1969, Berger 1978, Mader 1993, Duma 1996, Vinger 1997, Kuhn 2000, Duma 2002, Rodriguez 2003, McGwin 2005). Blunt impacts are the largest single cause of eye injuries at approximately one half of all civilian eye injuries (Figure 35) (McGwin 2005).

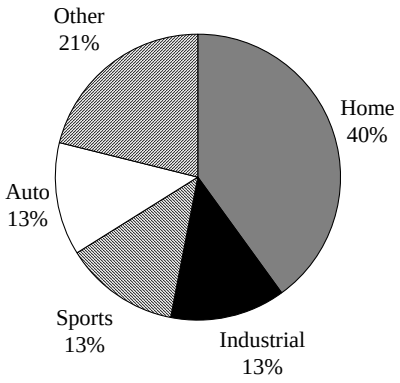

Figure 34: Location where eye injuries are suffered in the civilian sector
(Data in this figure are from McGwin 2005).

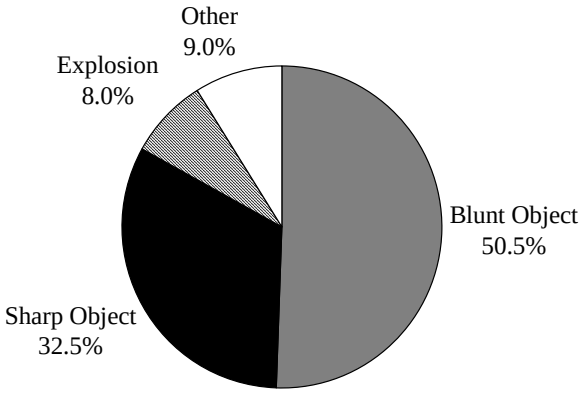

Figure 35: Type of insult which resulted in eye injury in the civilian sector
(Data in this figure are from McGwin 2005).

In combat, the rate of eye injuries has dramatically increased during the past 90 years from approximately 2% during World War I and World War II, to nearly 13% during Operation Desert Storm (Heier 1993, Wong 2000). While many of the conflict-related eye injuries are caused by shrapnel and other debris, nearly 25% of the injuries are also caused by blunt trauma from motor vehicle and helicopter crashes, falling, and direct hits from blunt objects (Mader 1993, Biehl 1999). One reason for the increase in eye injuries in modern day military conflicts is a lack of modernization of protective goggles and face shields to keep up with advances in weaponry (Biehl 1999).

Eye Injury Prediction Tools

In order to develop safety countermeasures effective at preventing these eye injuries, as well as evaluate the eye injury potential of different impacts, it is desirable to have the capability for distinguishing between injurious and non-injurious eye impacts. Computational models of the eye have been developed for predicting eye injury, but their implementation is complex and requires specialized training (Stitzel 2002, Stitzel 2005, Vinger 2005). Current anthropometric test device (ATD) headforms lack instrumentation and facial features to allow detailed assessment of eye or discrete facial injuries. The current ATD headform used for most impact biomechanics testing is the Hybrid-III headform developed by Hubbard and McLeod (1974).

The Hybrid-III headform is typically instrumented with a tri-axial accelerometer mounted at the center of gravity of the head, as well as a six-axis upper-neck load cell mounted at the base of the ATD headform. The resultant linear acceleration of the head center of gravity over time has been used to calculate head injury measures, but cannot be used for eye injury assessment. Additionally, because of the basic design of the Hybrid-III with no detailed anatomical representation of eyes, there is no way of detecting impact to the eyes or assessing eye injury risk.

The American National Standards Institute (ANSI) standards are written for protection designed for occupational and recreational uses (ANSI Z87.1-2003). These include goggles, face shields, and welding helmets. Two different impact test methodologies are used to assess the efficacy of the safety glasses. The lens cannot detach from the frame and the lens cannot fracture or be penetrated by the projectile. Contact paste is used to determine if there is contact between the protection and the eye. No contact is allowed for the protection to pass the test.

The National Operating Committee on Standards for Athletic Equipment (NOCSAE) standards focus on only athletic equipment protective gear (NOCSAE 1998, 2003a, 2003b, 2004a, 2004b, 2004c). For facial protection the NOCSAE standard requires several impacts to the facemask region with the correct projectile for that sport. All NOCSAE impact tests use the NOCSAE standard headform, and no contact is permitted with the ocular region and only limited contact is allowed for the surrounding face region. The American Society for Testing and Materials (ASTM) also conducts tests for the purposes of evaluating sports injury protective equipment (ASTM 1998, 1999, 2000, 2001, 2003, 2004). As in the NOCSAE tests, a paste is used to determine contact between the protective equipment and the eye of the headform. These tests are performed on hockey, ski, youth baseball and other sports equipment. With all of the aforementioned standards, there is no direct measurement of any specific eye injury impact severity or corresponding injury risk.

An experimental model which attempted to correlate force to eye injury was developed by Nakai *et al.* (2003). This model used an arrangement of load cells around the perimeter of a 2 x 2

arrangement of porcine eyes, which were mounted in simulated orbits filled with gelatin. The authors were unable to present a strong correlation between loads measured by the load cells and endothelial cell damage, but were able to show the influence of airbag folding patterns on the distribution of the load. This arrangement of load cells for the purposes of predicting ocular injury is not ideal. The load cells are positioned approximately at what would anatomically be the orbital rim, and measure the forces that would be exerted on the orbit. They are not a direct measurement of the force imparted on the eye. Therefore, this is not a preferred approach to predicting ocular injury. Additionally, this model only predicts a relatively low severity injury of endothelial cell loss, and does not attempt to predict the most severe eye injuries such as globe rupture.

Empirical eye injury prediction techniques have been proposed by several researchers (Berger 1978, Duma 2000, Scott 2000, Duma 2005, Kennedy 2006). An ocular injury assessment tool was developed by Berger (1978) to predict the occurrence of an eye injury based on a mathematical model of contact forces from projectiles impacting the eye. The contact force was estimated based on projectile characteristics, such as velocity, diameter, and mass, as well as assumed material properties of the eye. Berger developed an analytical model to predict the maximum force as well as the time to maximum force, and then used this model to plot binary injury and no injury data on a force versus time to maximum force plot. This injury model was reported to correlate well with known experimental test data. However, present knowledge that under dynamic loading the eye is significantly stronger than under static loading (Kennedy 2004) would indicate that this model is inaccurate and unsuitable for injury prediction.

An empirical technique for predicting eye injury risk has been presented based on the normalized energy of the projectile impacting the eye (Duma 2005, Kennedy 2006). This metaanalysis and projectile based risk determination yields a 50% injury risk of corneal abrasion, hyphema, lens dislocation, retinal damage, and globe rupture at normalized energy levels of 1,503 J/m^2, 20,188 J/m^2, 19,194 J/m^2, 30,531 J/m^2, and 35,519 J/m^2, respectively. However, this approach and Berger's assumes that the diameter, mass and velocity of the impacting projectile are known, which is information that sometimes is unknown for a given impact scenario.

In none of the aforementioned standards tests or eye injury prediction techniques, is the eye injury potential determined from a quantified impact force on the eyes. Therefore, the purpose of this study is to present the development and validation of the Facial and Ocular CountermeasUre Safety (FOCUS) headform's synthetic eye and orbit and corresponding eye injury risk criteria for globe rupture.

In order to assess the capability of protective equipment in reducing eye and facial injuries, a new advanced headform has been developed that can predict fracture of facial bones, as well as eye injury from impact loading. In order to predict facial bone fracture and ocular injuries, the FOCUS headform is designed with discrete load cells capable of measuring local impact forces (Figure 36).

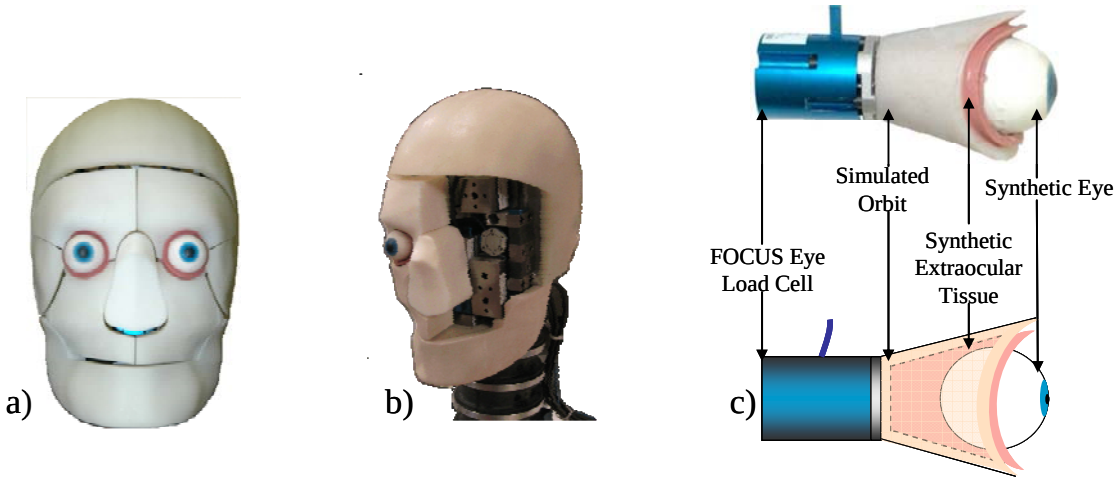

Figure 36: The FOCUS headform:
a) individual skull segments are shown with the headform skin removed
b) a cutaway view of the FOCUS headform with the left facial bone segments and synthetic eye/orbit removed, in this picture the underlying instrumentation can be seen
c) schematic of the synthetic eye and instrumentation arrangement used in the FOCUS headform.

METHODOLOGY

This study is comprised of three parts: In Part I, the force-deflection response of the eye was characterized in order to determine the response of the human eye to high-rate blunt loading. Next, surrogate eyes were manufactured and tested to determine the most suitable biofidelic

material for the synthetic eye. For Part II, the force-deflection response of the *in-situ* human eye was determined based on impact tests on human cadavers. This data was used to test different modular orbit designs for the FOCUS headform and select materials based on the most biofidelic response possible. In Part III, experimental eye impact tests were performed using the FOCUS headform. These impact tests corresponded to eye impact data reported in the literature and the injury outcome from those experimental tests were correlated to the output of the FOCUS headform. This data was used to generate injury risk functions for globe rupture specific to the FOCUS headform.

Part I: Biofidelity of the Eye

A total of four human eyes were tested to characterize the force-deflection response of the eyes under blunt impact, and then a urethane synthetic eye was tested for comparison. All tests were conducted using a spring powered impactor at approximately 10 m/s (Figure 37) and the force-deflection response for *ex-vivo* human eyes as well as synthetic eyes were determined.

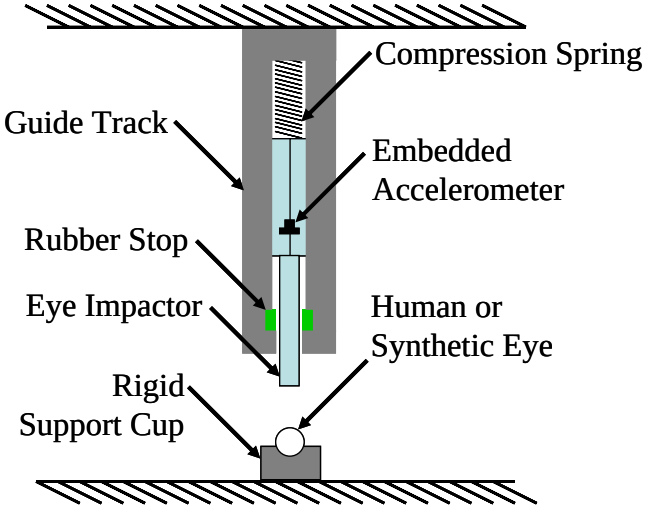

Figure 37: Spring-powered impactor setup to measure force-deflection response of human and synthetic eyes.

In order to provide a broad, blunt surface to determine the force-deflection response of the eye, a 19 mm diameter impactor tip was used. The impactor was accelerated to approximately 10 m/s by the compression spring and had approximately 49 mm of free travel prior to striking the eye.

After making initial contact with the eye, the impactor had approximately 6 mm of free travel prior to striking the rubber stops.

Prior to testing, human eyes were enucleated within 24 hours of death. Hydration of the eyes was maintained by storage in a saline filled specimen jar and refrigerated fresh prior to testing. For testing, the eyes were removed from refrigeration and kept hydrated as they returned to room temperature just prior to the actual testing. Immediately prior to testing, the eyes were pressurized to physiologic conditions by insertion of a needle through the optic nerve (Klein 1992, Kennedy 2004). All test procedures were reviewed and approved by the Virginia Tech Institutional Review Board.

Each eye was placed in a rigid support cup milled out to the radius of the human eye. The cup was approximately 4 mm in depth to keep the eye in position during the impact test. The eye was impacted with the impactor piston with embedded accelerometer (Endevco 7264B-2000, Endevco Corp., San Juan Capistrano, CA) and the impact filmed using a high-speed video camera (Phantom 4, Vision Research, Inc., Wayne, NJ). Acceleration data was filtered to CFC 1000, then double-integrated to determine impactor tip displacement and also multiplied by the impactor mass (104.05 g) to determine impactor force (Nyquist 1986, Kennedy 2007). This data was used to determine the force-deflection characteristics of the eyes. The synthetic eyes were tested using the same experimental test method.

Part II: Biofidelity of the Eye and Orbit

A total of 10 tests were performed on five human cadaver heads. All tests were performed on fresh refrigerated cadavers which were never frozen. All test procedures were reviewed and approved by the Virginia Tech Institutional Review Board. In order to make a comparison on the effects of the extraocular muscles, in each head the extraocular muscles were left intact on one eye and transected on the contralateral eye. The post-mortem human head was mounted in a rigid plastic container using expandable foam. The impact tests were performed using a spring-powered dynamic impactor, which was accelerated to a velocity of approximately 10 m/s before

it impacted the eye (Figure 38). As in Part I, the impactor tip for these tests was 19 mm in diameter. The impactor had approximately 30 mm of free travel prior to impacting the eye and, after contacting the eye, had approximately 25 mm of travel prior to striking the rubber stops.

An embedded accelerometer (Endevco 7264B-2000, Endevco Corp., San Juan Capistrano, CA) was used to collect data at a sampling rate of 100 kHz for the duration of the test on each eye. Acceleration data was filtered to CFC 1000, then double-integrated to determine impactor tip displacement and also multiplied by the impactor mass (104.05 g) to determine impactor force, this data was used to determine the force-deflection characteristics of the *in-situ* eyes.

For both test conditions, muscles intact and muscles transected, the characteristic average response was determined using a method similar to that described by Lessley *et al.* (2004). Additionally, force-deflection corridors were calculated using the average force-deflection response plus or minus the standard deviation of the force at each displacement step. For the human *in-situ* eyes, force-deflection curves were cutoff at the peak force. This will be further addressed in the discussion section.

Using the corridor of the human orbit as a guideline, the synthetic orbit assembly for the FOCUS headform was tested using the same test setup (Figure 39). The response was compared to the characteristic response of the *in-situ* tests to ensure an accurate biofidelic response.

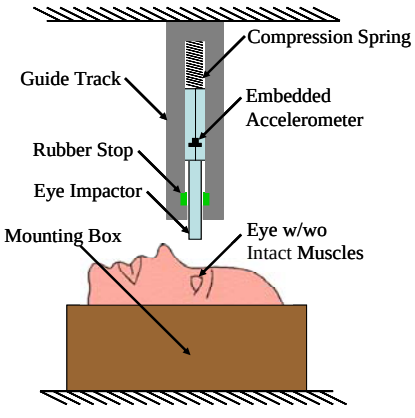

Figure 38: Test setup for spring-powered dynamic impactor used for *in-situ* eye

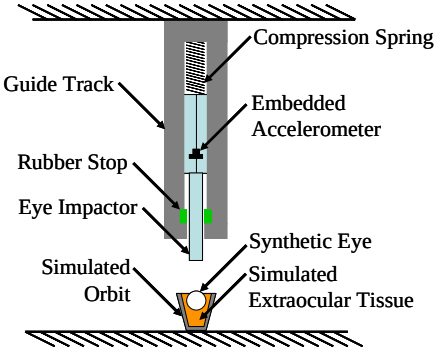

Figure 39: Test setup for spring-powered dynamic impactor used for synthetic orbit development and validation tests.

impact tests.

Part III: FOCUS Eye Risk Functions

The results from Part I and Part II were used to determine the most biofidelic synthetic eye on the basis of matching the *in-situ* force-deflection profile of a human eye. Using this selection, eye impact tests were conducted on the FOCUS headform assembly (Figure 40).

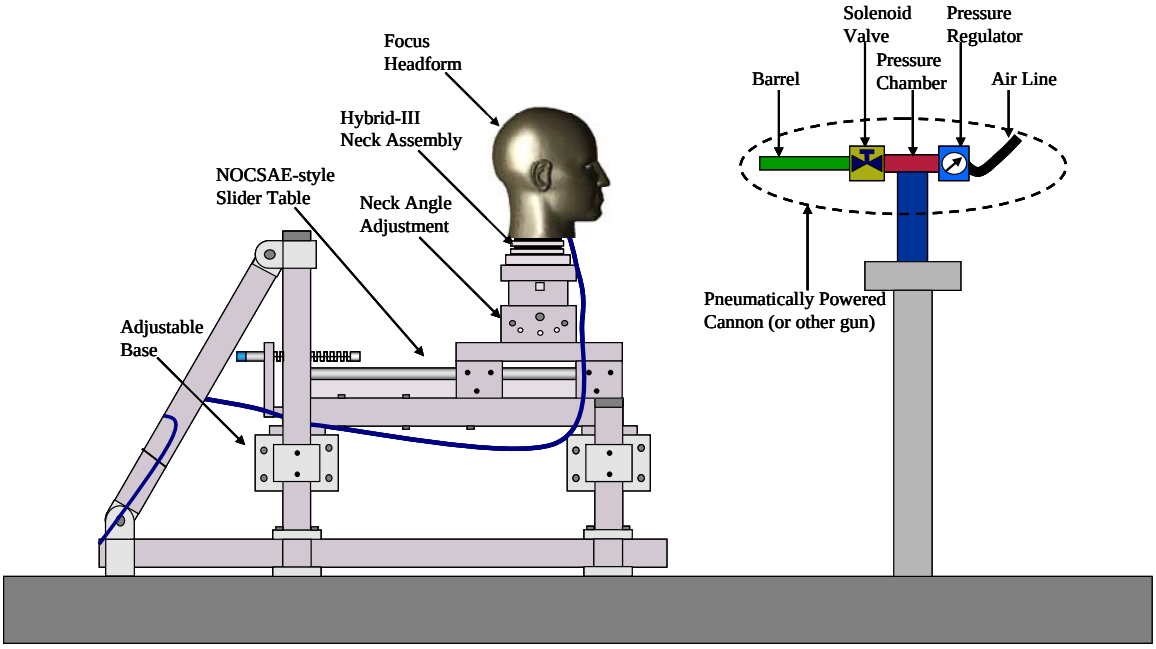

Figure 40: Experimental test configuration for Part III with the FOCUS headform. Experimental testing was performed from a distance of 175 mm, the FOCUS headform was on a NOCSAE style slider table (NOCSAE 1998, 2003a, 2003b, 2004a, 2004b, 2004c).

A total of 82 impact tests were conducted using steel BB projectiles impacting the eye of the FOCUS headform. All tests were conducted by striking the cornea directly in center, with all projectiles fired along the negative X-axis of the headform using the SAE J211 coordinate system. Tests were conducted in three separate testing series, with Series 1 and Series 2 sharing the same synthetic eye specimen. For Series 3, a new synthetic eye specimen was used. The BBs were selected as the basis for eye injury criteria because they will result in a conservative

injury criterion. Objects larger than a BB will distribute their load over a larger area than the BB and therefore would pose a lower relative risk of injury.

A uni-axial load cell (8060JFL, Robert A. Denton, Inc., Rochester Hills, MI) at the posterior of the modular orbit will measure impact loads transmitted through the eye and surrounding soft tissue. Data was collected from the load cell at 50 kHz and was filtered to 3500 Hz using a Butterworth 4-pole phaseless digital filter.

High-speed video (Phantom 4, Vision Research, Inc., Wayne, NJ) at 7400 frames/second was used to visualize the response of the eye as it was impacted by oncoming projectiles, as well as to calculate the velocity of the projectile when it was approximately 10 mm to 30 mm from striking the eye. Based on the data from a previous study (Kennedy 2006) the velocity of the projectile, the kinetic energy, and the normalized energy (J/m^2) of the striking projectile was calculated and the corresponding risk of globe rupture was calculated based on the normalized energy of the projectile. The normalized energy of the projectile is the kinetic energy of the projectile divided by the cross-sectional area of the projectile or the cross-sectional area of a spherical projectile (Eq. 1).

$$Normalized\ Energy\ \left(\frac{J}{m^2}\right) = \frac{Kinetic\ Energy}{Projected\ Area} = \frac{\frac{1}{2}mv^2}{\pi r^2} (\ for\ a\ sphere\ ) \qquad \text{Eq. (1)}$$

The impact tests were designed to impact the eye with a large range of velocities, which would result in normalized energy levels that varied from approximately 1,000 J/m^2 up to approximately 60,000 J/m^2, and corresponding risk of globe rupture of nearly 0% risk up to nearly 100% risk of injury (Kennedy 2006).

From each test, peak loads from the eye load cells were matched to the corresponding risk of globe rupture. Statistical analysis software (NCSS 2004, NCSS, Inc., Kaysville, UT) was used to determine the coefficients for a logistical regression injury risk function based on this data.

A general form of the logistic regression injury risk function (Equation 2) can be used to develop a FOCUS headform-specific injury risk function based on the peak impact load. The variable "x" refers to the level of input (such as peak load) of the projectile onto the eye. The variables "a" and "b" are constants determined from the logistic regression.

$$\text{Probability of Injury}\,(\%) = \frac{1}{1+e^{a-bx}} \qquad \text{Eq. (2)}$$

Additionally, confidence intervals developed by Kennedy *et al.* (2006) were incorporated into the injury risk function. Confidence intervals from 5% to 95% were calculated assuming a logistic distribution.

RESULTS

Part I: Biofidelity of the Eye

Impact tests on the human eye resulted in an average of 5.5 mm of displacement and 510 N of load at rupture. The force-deflection curves for all four *ex-vivo* human eye tests are shown (Figure 41). All human eyes tested resulted in equatorial globe rupture at the peak load shown on the figures.

A molded urethane eye was tested in the same manner to compare the force deflection response to that of the human eyes (Table 17) (Figure 42). The force-deflection response of the urethane eye was found to compare favorably through 5.5 mm of displacement, although the synthetic eyes did not rupture and therefore were subjected to higher overall peak loads.

Table 17: Summary of peak displacement and peak force from force-deflection of human eyes and synthetic eye materials.

	Peak Displacement (mm)	**Peak Load (N)**
Human Eye	5.5	510
Synthetic Urethane Eye	6.0	570

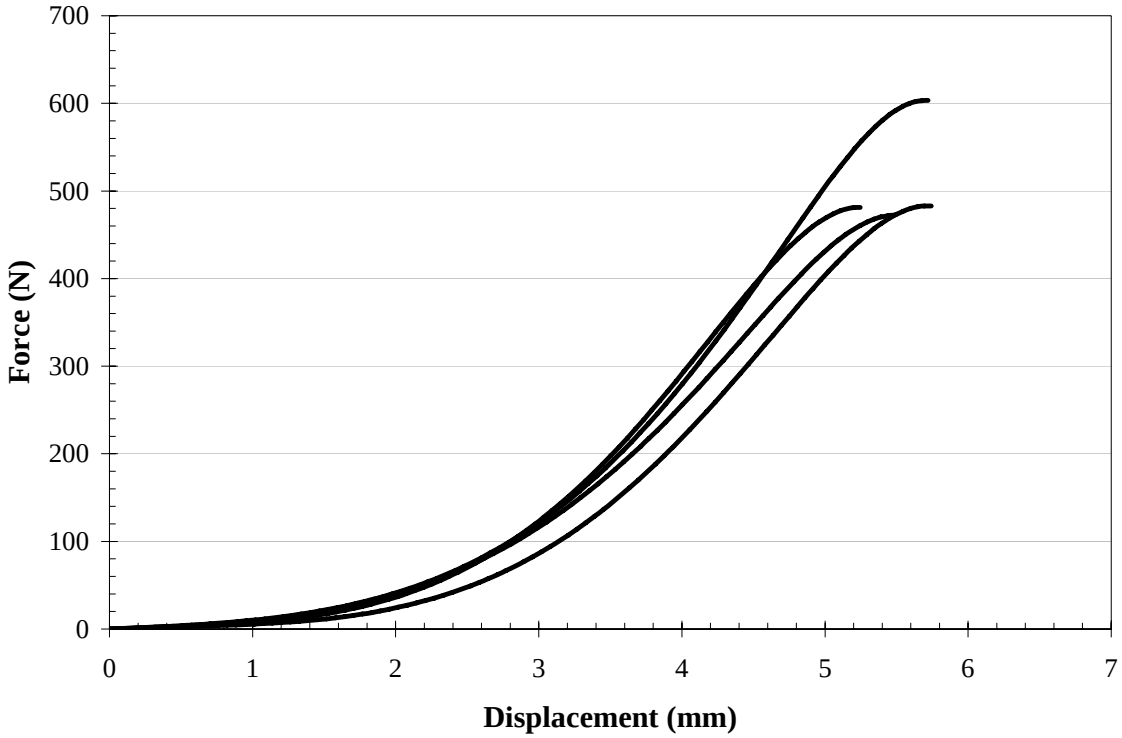

Figure 41: Force-deflection of the human eye for all four eyes.

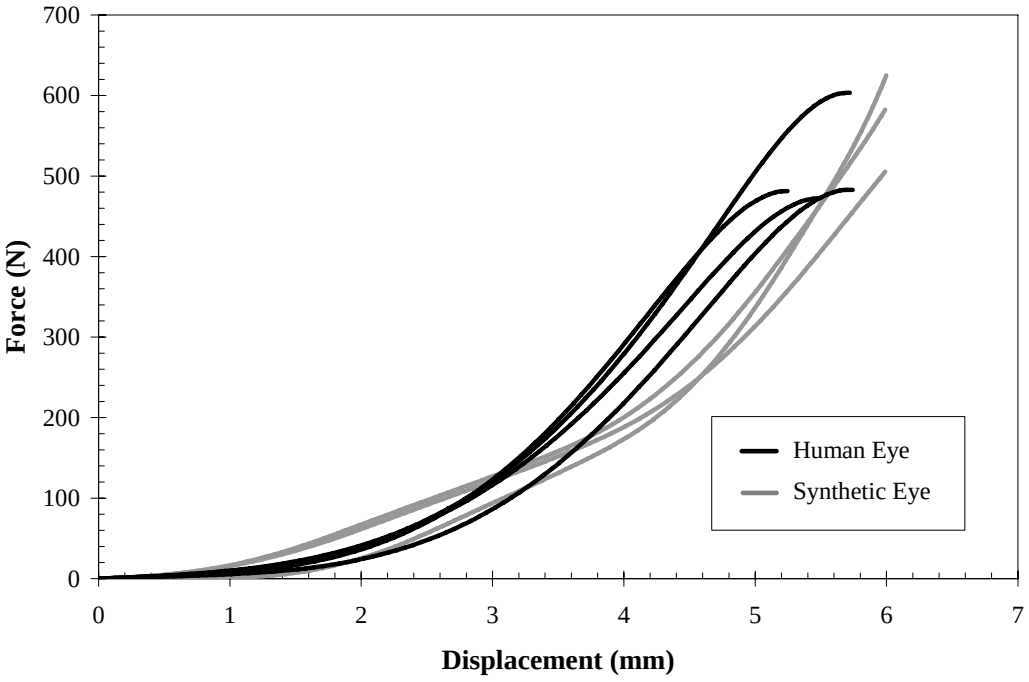

Figure 42: Force-deflection response of molded urethane synthetic eye versus human eye.

Part II: Biofidelity of the Eye and Orbit

A total of 10 dynamic blunt eye impact tests were conducted on five human heads. The force-deflection results for impact tests conducted with the extraocular muscles intact and with the muscles transected are shown (Figure 43). Curves are cutoff at the peak load which coincides with the time of globe rupture. The displacement when injuries were observed was consistent with the results of other studies, which show a displacement of approximately 6 mm to 8 mm at the time of injury (Stitzel 2002, Kennedy 2006). Further discussion on the injury tolerance of these eyes using the blunt impactor is presented in the discussion section.

The characteristic average response of the test condition with the extraocular muscles intact had a peak force of 268 N at a displacement of 7.5 mm. The characteristic average with the muscles transected had an average peak force of 267 N at a displacement of 7.5 mm. The force-deflection corridors were generated using the average force-deflection response plus or minus the standard deviation of the force at each displacement step and are shown (Figure 44).

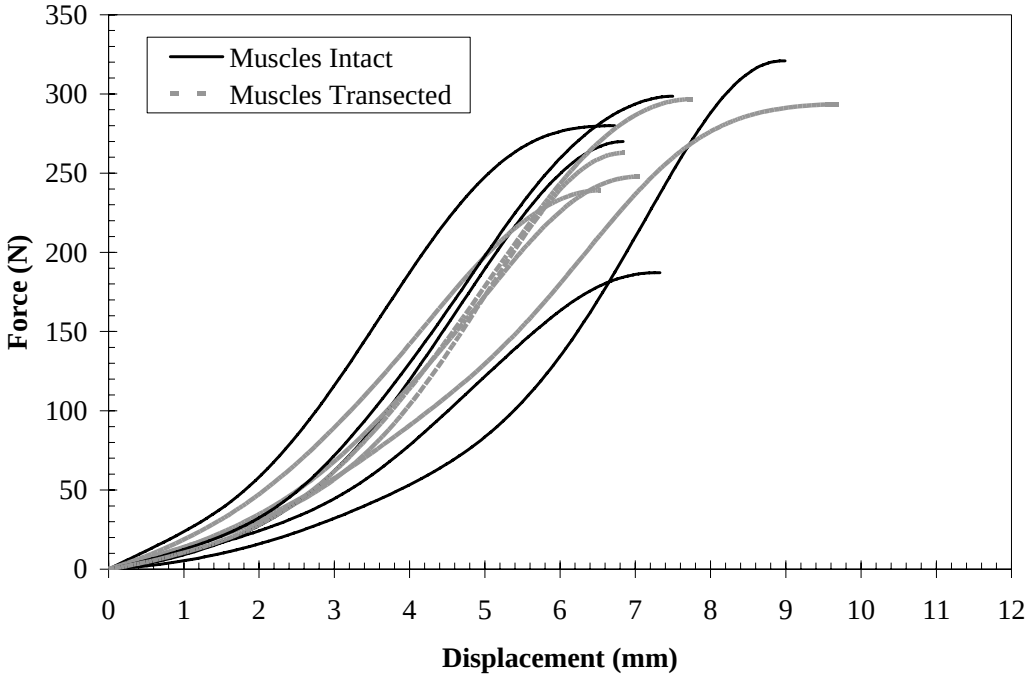

Figure 43: Force-deflection response of human eyes *in-situ* with extraocular muscles intact and with extraocular muscles transected.

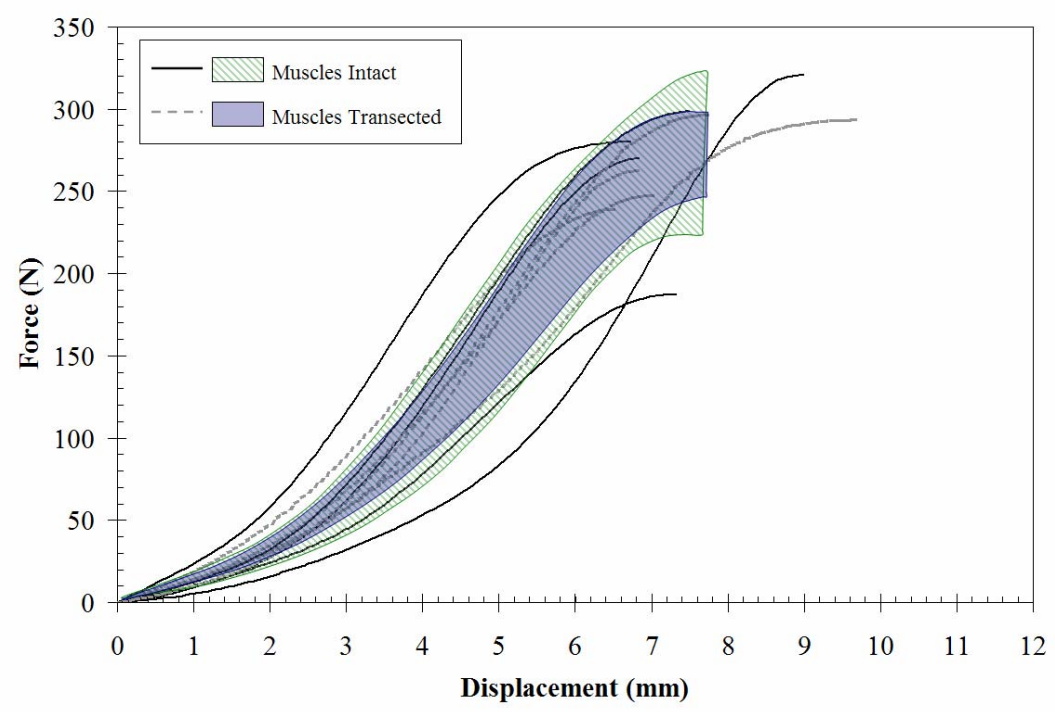

Figure 44: Force-deflection corridors generated to reflect the typical response from a dynamic impact, corridors for the extraocular muscles intact and the extraocular muscles transected are shown.

Using the synthetic urethane eye from Part I, dynamic impact tests were conducted on the FOCUS synthetic orbit assembly. The force-deflection response of the synthetic orbit assembly was determined and compared to the results from the *in-situ* impact tests. The response of the system for three impacts is plotted against the corridors developed for the force-deflection of human eyes *in-situ* (Figure 45). The response can be seen to fall entirely within the corridors to the cutoff at 7.5 mm and, as such, was determined to be representative of human eye response to dynamic impact because this is where globe rupture is typically observed (Stitzel 2002, Kennedy 2006).

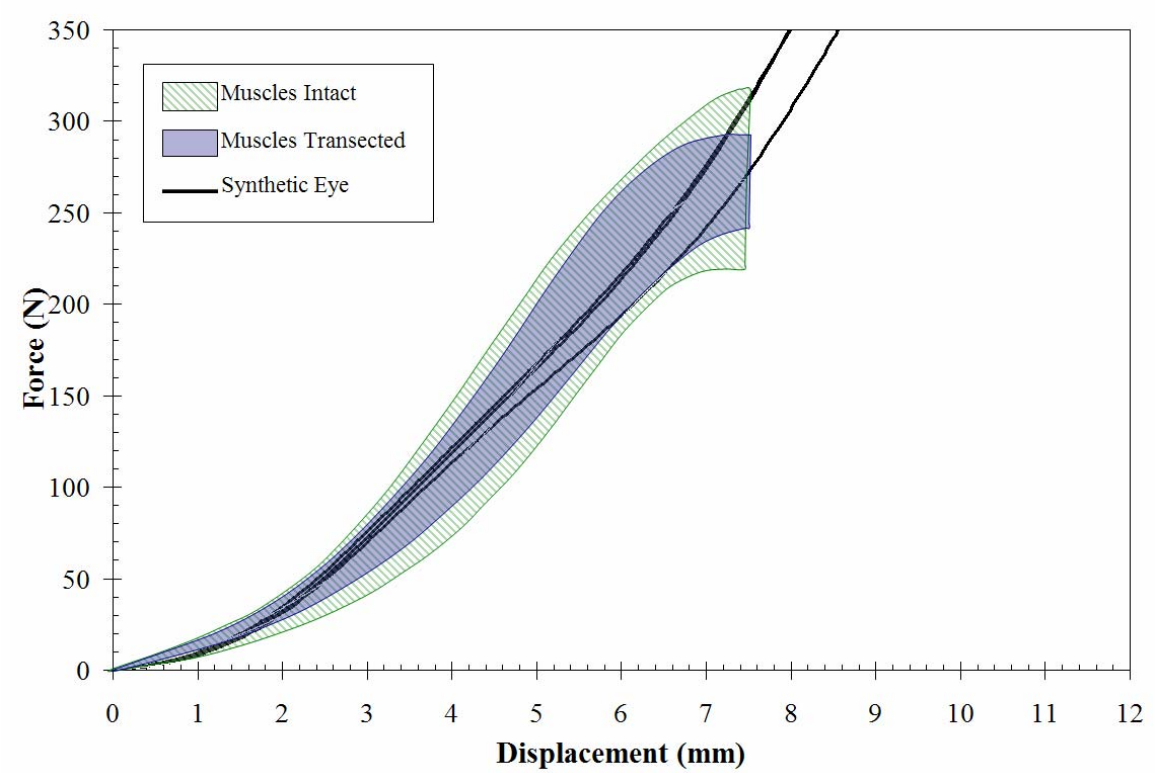

Figure 45: Force-deflection results from impacts performed on a simulated orbit with a urethane synthetic eye and silicone synthetic extraocular tissue.

Part III: FOCUS Eye Risk Functions

A total of 82 impact tests were conducted using steel BB projectiles impacting the eye of the FOCUS headform (Table 18). The BBs were selected as the basis for eye injury criteria development because they will result in a conservative injury criterion. To investigate repeatability, tests were conducted in three separate testing series, with series 1 and series 2 sharing the same synthetic eye specimen. For test series 3, a new synthetic eye specimen was used. Based on the data from a previous study (Kennedy 2006) the velocity of the projectile, the kinetic energy, and the normalized energy of the striking projectile was calculated and the corresponding risk of globe rupture was calculated based on the normalized energy of the projectile. Tests were conducted using a projectile velocity ranging from 12.0 m/s to 73.8 m/s, which equates to a range of normalized energy levels of 1,594 J/m^2 to 59,764 J/m^2. Based on risk functions for globe rupture from Kennedy *et al.* (2006), the corresponding globe rupture risk

was determined to range from 0.02% risk to 99.80%. These impacts resulted in measured peak loads from 11.5 N to 153.1 N at the FOCUS eye load cell.

Table 18: Test results from experimental FOCUS synthetic eye impact tests matched to human eye tests.

Test	Series	Eye Specimen	Object	Projectile Diameter (mm)	Projectile Mass (g)	Projectile Velocity (m/s)	Kinetic Energy (J)	Normalized Energy (J/m^2)	Peak Force (N)	Globe Rupture Risk from Normalized Energy
FOCUS-BB-01	1	A	Steel BB	4.5	0.340	49.4	0.42	26839	88.3	9.71%
FOCUS-BB-02	1	A	Steel BB	4.5	0.340	49.1	0.41	26483	85.1	8.94%
FOCUS-BB-03	1	A	Steel BB	4.5	0.340	49.8	0.42	27198	87.2	10.55%
FOCUS-BB-04	1	A	Steel BB	4.5	0.340	50.1	0.43	27560	90.8	11.46%
FOCUS-BB-05	1	A	Steel BB	4.5	0.340	49.4	0.42	26839	88.5	9.71%
FOCUS-BB-06	1	A	Steel BB	4.5	0.340	37.8	0.24	15707	57.0	0.61%
FOCUS-BB-07	1	A	Steel BB	4.5	0.340	35.3	0.21	13683	53.6	0.37%
FOCUS-BB-08	1	A	Steel BB	4.5	0.340	35.6	0.22	13901	52.6	0.39%
FOCUS-BB-09	1	A	Steel BB	4.5	0.340	32.8	0.18	11798	48.2	0.23%
FOCUS-BB-10	1	A	Steel BB	4.5	0.340	31.9	0.17	11200	46.4	0.19%
FOCUS-BB-11	1	A	Steel BB	4.5	0.340	28.6	0.14	8967	39.0	0.11%
FOCUS-BB-12	1	A	Steel BB	4.5	0.340	29.4	0.15	9502	40.6	0.13%
FOCUS-BB-13	1	A	Steel BB	4.5	0.340	25.5	0.11	7137	32.7	0.07%
FOCUS-BB-14	1	A	Steel BB	4.5	0.340	26.9	0.12	7943	35.3	0.08%
FOCUS-BB-15	1	A	Steel BB	4.5	0.340	23.2	0.09	5937	28.8	0.05%
FOCUS-BB-16	1	A	Steel BB	4.5	0.340	21.3	0.08	4978	26.0	0.04%
FOCUS-BB-17	1	A	Steel BB	4.5	0.340	19.0	0.06	3985	22.6	0.03%
FOCUS-BB-18	1	A	Steel BB	4.5	0.340	23.0	0.09	5795	27.9	0.05%
FOCUS-BB-19	1	A	Steel BB	4.5	0.340	16.2	0.04	2899	17.2	0.02%
FOCUS-BB-20	1	A	Steel BB	4.5	0.340	17.6	0.05	3421	19.9	0.03%
FOCUS-BB-21	1	A	Steel BB	4.5	0.340	14.8	0.04	2421	15.7	0.02%
FOCUS-BB-22	1	A	Steel BB	4.5	0.340	25.5	0.11	7137	33.0	0.07%
FOCUS-BB-23	1	A	Steel BB	4.5	0.340	35.3	0.21	13683	54.1	0.37%
FOCUS-BB-24	1	A	Steel BB	4.5	0.340	39.5	0.27	17134	61.9	0.88%
FOCUS-BB-25	1	A	Steel BB	4.5	0.340	39.8	0.27	17378	63.6	0.94%
FOCUS-BB-26	1	A	Steel BB	4.5	0.340	41.5	0.29	18878	67.8	1.37%
FOCUS-BB-27	1	A	Steel BB	4.5	0.340	42.6	0.31	19912	70.3	1.78%
FOCUS-BB-28	1	A	Steel BB	4.5	0.340	42.6	0.31	19912	71.4	1.78%
FOCUS-BB-29	1	A	Steel BB	4.5	0.340	47.2	0.38	24447	86.7	5.50%
FOCUS-BB-30	1	A	Steel BB	4.5	0.340	48.6	0.40	25893	87.8	7.78%
FOCUS-BB-31	1	A	Steel BB	4.5	0.340	50.7	0.44	28290	92.7	13.50%
FOCUS-BB-32	2	A	Steel BB	4.5	0.340	52.2	0.46	29896	90.4	19.09%
FOCUS-BB-33	2	A	Steel BB	4.5	0.340	54.3	0.50	32353	95.4	30.71%
FOCUS-BB-34	2	A	Steel BB	4.5	0.340	56.4	0.54	34935	102.3	46.25%
FOCUS-BB-35	2	A	Steel BB	4.5	0.340	57.9	0.57	36810	108.8	58.21%
FOCUS-BB-36	2	A	Steel BB	4.5	0.340	26.1	0.12	7454	31.2	0.07%
FOCUS-BB-37	2	A	Steel BB	4.5	0.340	36.7	0.23	14790	55.0	0.48%
FOCUS-BB-38	2	A	Steel BB	4.5	0.340	56.8	0.55	35399	107.7	49.22%

Table 18 (cont.): Test results from experimental FOCUS synthetic eye impact tests matched to human eye tests.

Test	Series	Eye Specimen	Object	Projectile Diameter (mm)	Projectile Mass (g)	Projectile Velocity (m/s)	Kinetic Energy (J)	Normalized Energy (J/m^2)	Peak Force (N)	Globe Rupture Risk from Normalized Energy
FOCUS-BB-39	2	A	Steel BB	4.5	0.340	17.6	0.05	3421	18.8	0.03%
FOCUS-BB-40	2	A	Steel BB	4.5	0.340	12.0	0.02	1594	11.5	0.02%
FOCUS-BB-41	2	A	Steel BB	4.5	0.340	19.6	0.07	4223	21.4	0.03%
FOCUS-BB-42	2	A	Steel BB	4.5	0.340	19.9	0.07	4345	21.9	0.03%
FOCUS-BB-43	2	A	Steel BB	4.5	0.340	19.3	0.06	4103	21.4	0.03%
FOCUS-BB-44	2	A	Steel BB	4.5	0.340	19.9	0.07	4345	21.9	0.03%
FOCUS-BB-45	2	A	Steel BB	4.5	0.340	18.8	0.06	3869	21.2	0.03%
FOCUS-BB-46	2	A	Steel BB	4.5	0.340	49.8	0.42	27198	83.9	10.55%
FOCUS-BB-47	2	A	Steel BB	4.5	0.340	50.4	0.43	27923	88.3	12.44%
FOCUS-BB-48	2	A	Steel BB	4.5	0.340	50.4	0.43	27923	89.1	12.44%
FOCUS-BB-49	2	A	Steel BB	4.5	0.340	50.7	0.44	28290	89.5	13.50%
FOCUS-BB-50	2	A	Steel BB	4.5	0.340	50.7	0.44	28290	88.8	13.50%
FOCUS-BB-51	2	A	Steel BB	4.5	0.340	59.0	0.59	38249	113.9	66.84%
FOCUS-BB-52	2	A	Steel BB	4.5	0.340	59.0	0.59	38249	114.3	66.84%
FOCUS-BB-53	2	A	Steel BB	4.5	0.340	64.8	0.72	46159	132.8	93.89%
FOCUS-BB-54	2	A	Steel BB	4.5	0.340	65.9	0.74	47751	125.2	95.86%
FOCUS-BB-55	2	A	Steel BB	4.5	0.340	70.0	0.84	53865	146.6	99.11%
FOCUS-BB-56	2	A	Steel BB	4.5	0.340	69.4	0.82	52875	146.8	98.85%
FOCUS-BB-57	2	A	Steel BB	4.5	0.340	73.8	0.93	59764	153.1	99.80%
FOCUS-BB-58	3	B	Steel BB	4.5	0.340	37.6	0.24	15561	57.0	0.59%
FOCUS-BB-59	3	B	Steel BB	4.5	0.340	39.4	0.27	17078	63.5	0.87%
FOCUS-BB-60	3	B	Steel BB	4.5	0.340	41.7	0.30	19139	67.5	1.47%
FOCUS-BB-61	3	B	Steel BB	4.5	0.340	43.9	0.33	21206	72.5	2.47%
FOCUS-BB-62	3	B	Steel BB	4.5	0.340	45.4	0.35	22608	74.8	3.50%
FOCUS-BB-63	3	B	Steel BB	4.5	0.340	47.9	0.39	25213	86.0	6.62%
FOCUS-BB-64	3	B	Steel BB	4.5	0.340	50.3	0.43	27797	88.5	12.09%
FOCUS-BB-65	3	B	Steel BB	4.5	0.340	52.2	0.46	29904	94.1	19.12%
FOCUS-BB-66	3	B	Steel BB	4.5	0.340	54.8	0.51	32927	99.3	33.94%
FOCUS-BB-67	3	B	Steel BB	4.5	0.340	55.8	0.53	34143	107.1	41.25%
FOCUS-BB-68	3	B	Steel BB	4.5	0.340	57.9	0.57	36847	110.6	58.44%
FOCUS-BB-69	3	B	Steel BB	4.5	0.340	49.1	0.41	26489	88.2	8.95%
FOCUS-BB-70	3	B	Steel BB	4.5	0.340	48.5	0.40	25868	85.3	7.73%
FOCUS-BB-71	3	B	Steel BB	4.5	0.340	49.1	0.41	26489	85.6	8.95%
FOCUS-BB-72	3	B	Steel BB	4.5	0.340	48.3	0.40	25635	83.5	7.32%
FOCUS-BB-73	3	B	Steel BB	4.5	0.340	47.9	0.39	25190	83.6	6.58%
FOCUS-BB-74	3	B	Steel BB	4.5	0.340	59.9	0.61	39395	116.2	73.01%
FOCUS-BB-75	3	B	Steel BB	4.5	0.340	60.2	0.62	39856	117.5	75.28%
FOCUS-BB-76	3	B	Steel BB	4.5	0.340	62.0	0.66	42210	121.6	84.79%
FOCUS-BB-77	3	B	Steel BB	4.5	0.340	62.5	0.67	42962	121.9	87.12%
FOCUS-BB-78	3	B	Steel BB	4.5	0.340	63.3	0.68	44079	124.1	90.01%

Table 18 (cont.): Test results from experimental FOCUS synthetic eye impact tests matched to human eye tests.

Test	Series	Eye Specimen	Object	Projectile Diameter (mm)	Projectile Mass (g)	Projectile Velocity (m/s)	Kinetic Energy (J)	Normalized Energy (J/m^2)	Peak Force (N)	Globe Rupture Risk from Normalized Energy
FOCUS-BB-79	3	B	Steel BB	4.5	0.340	64.7	0.71	45988	128.5	93.64%
FOCUS-BB-80	3	B	Steel BB	4.5	0.340	66.3	0.75	48292	131.8	96.38%
FOCUS-BB-81	3	B	Steel BB	4.5	0.340	69.3	0.82	52793	137.3	98.83%
FOCUS-BB-82	3	B	Steel BB	4.5	0.340	73.5	0.92	59386	143.7	99.78%

Two impacts of varying impact severities are shown, where the 25.5 m/s impact results in a peak force of 33.0 N and the 57.9 m/s impact results in a peak force of 110.6 N (Figure 46). Impact durations were similar for all impacts throughout all of the three impact test series on the FOCUS headform.

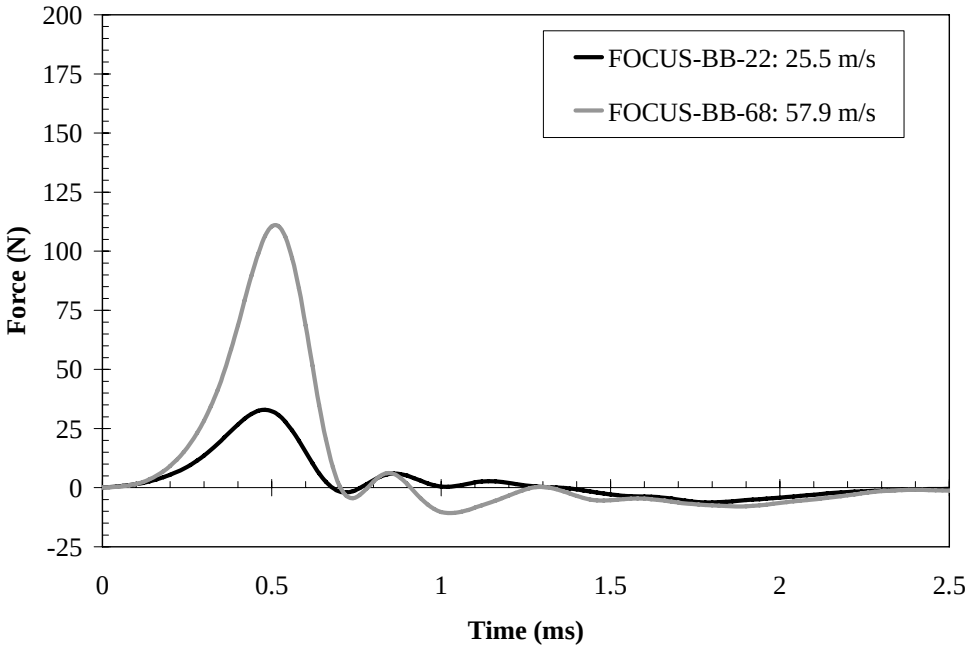

Figure 46: Force vs. time history for two sample impacts of varying impact velocities.

To demonstrate repeatability, multiple impacts were conducted at similar velocities throughout the three test series. Three similar impacts from series 1, series 2 and series 3 are shown to demonstrate repeatability (Figure 47). Impact velocities for three tests conducted during each of the three test series are shown for impact velocities of 49.4 m/s, 49.8 m/s, and 49.1 m/s resulting in peak forces of 88.5 N, 83.9 N, and 88.2 N respectively. Overall, for all seven impacts conducted between 49.1 m/s and 49.8 m/s the coefficient of variation for peak load was determined to be 2.1% (Table 19).

Table 19: Repeat impacts conducted between 49.1 m/s and 49.8 m/s.
The coefficient of variation was found to be 2.1%.

Test	Series	Eye Specimen	Projectile Velocity (m/s)	Peak Force (N)
FOCUS-BB-01	1	A	49.4	88.3
FOCUS-BB-02	1	A	49.1	85.1
FOCUS-BB-03	1	A	49.8	87.2
FOCUS-BB-05	1	A	49.4	88.5
FOCUS-BB-46	2	A	49.8	83.9
FOCUS-BB-69	3	B	49.1	88.2
FOCUS-BB-71	3	B	49.1	85.6
Average (Standard Deviation)			49.4 (0.3)	86.7 (1.8)
Coefficient of Variation (CV)				2.1%

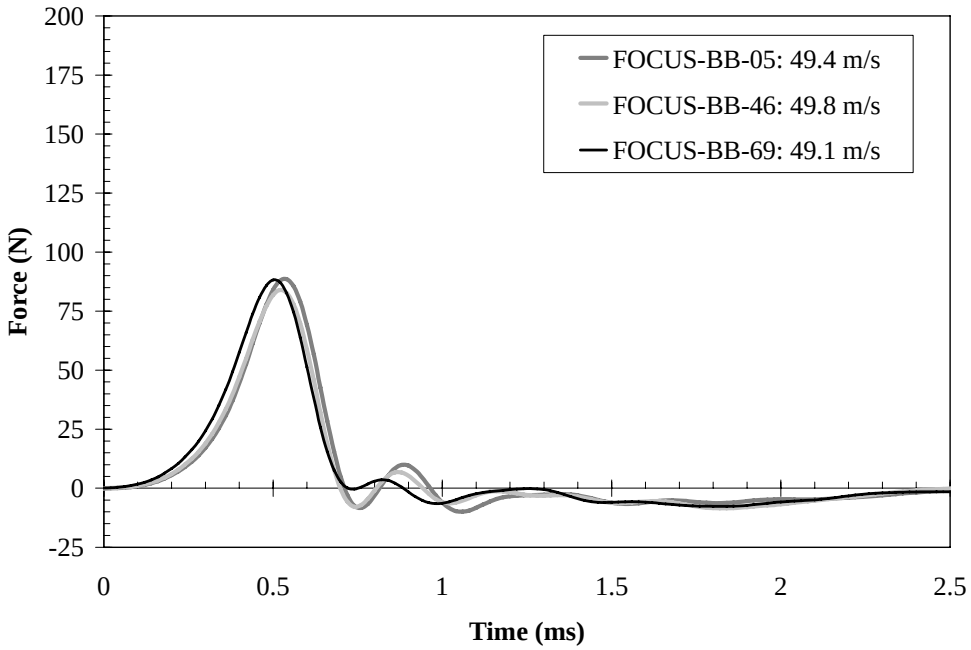

Figure 47: Force vs. time history for three sample impacts to show repeatability.
FOCUS-BB-05 was conducted during test series 1, using eye specimen A.
FOCUS BB-46 was conducted during test series 2, using eye specimen A.
FOCUS-BB-69 was conducted during test series 3, using eye specimen B.

Because all projectiles used in this study were precision ground BBs of the same type, the mass and diameter of the impacting projectiles was constant for all tests. This resulted in equivalent correlations for peak force and the parameters of velocity, kinetic energy, and normalized energy of the projectile (R^2 = 0.996). Given the significance of the normalized energy in predicting

globe rupture (Kennedy 2006), a risk function using the generalized logistic regression equation was fit between peak force and risk of globe rupture based on normalized energy of the impacting BB. Using peak force as a predictor of injury, the coefficients for the injury risk function (Eq. 2) were determined to be as shown (Table 20) (Eq. 3). This demonstrated a strong correlation between the parameters of peak force and injury risk with an R^2 value of 0.995. A risk function of this form can be used to determine the probability of sustaining globe rupture based on the impact force measured by the FOCUS headform. A 50% risk of globe rupture is shown to be 107 N (Figure 48).

Table 20: Injury risk function coefficients for globe rupture of both porcine and human eyes, using peak force from the FOCUS headform.

	Parameter "A"	**Parameter "B"**	**R^2**
Peak Force	11.93882	0.1118708	0.995

$$Probability\ of\ \ Injury\ (\%) = \frac{1}{1+e^{11.93882-(0.1118708)(Peak\ Load)}} \qquad \text{Eq. 3}$$

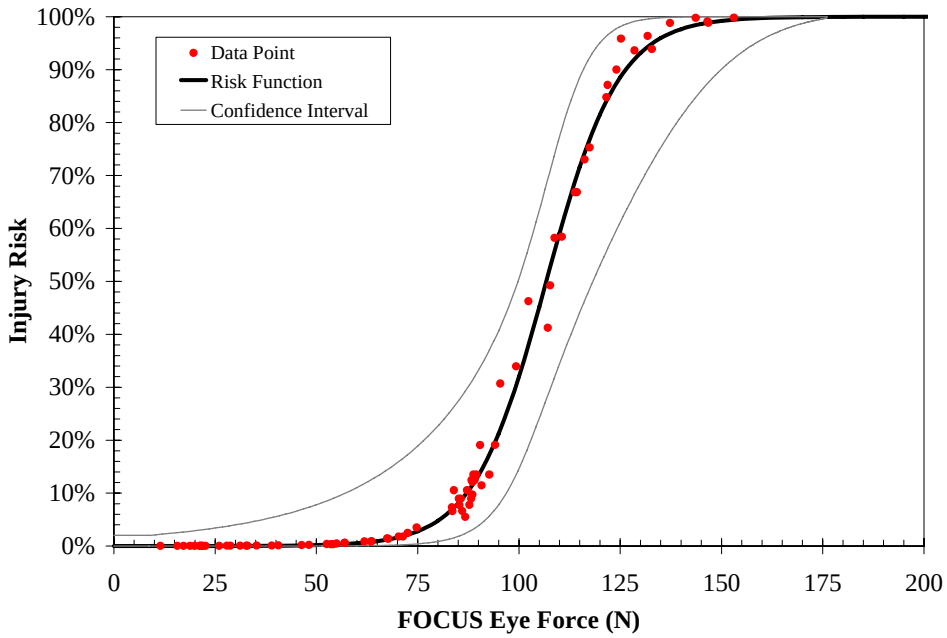

Figure 48: Injury risk curves for globe rupture with confidence intervals calculated from peak force of FOCUS eye load cells.

DISCUSSION

Extraocular Muscles

In addition to allowing for biofidelic evaluation, the dynamic impact tests on *in-situ* human eyes allowed a comparison of the effects of the extraocular muscles on eye impact response. For the two scenarios, with the extraocular muscles transected and with the extraocular muscles intact, the average force deflection response was nearly identical. The corridor generated to represent the scenario with the extraocular muscles transected was fully contained in the corridor with the extraocular muscles intact (Figure 44). This suggests that it is not necessary that the synthetic eye be constrained by surrogate extraocular muscle attachments in order to provide a biofidelic response to impact. The finding that extraocular muscles have little influence on dynamic force-deflection response is consistent with other researchers (Cirovic 2005). Additional research into cause of the greater variation seen among tests with the extraocular muscles intact is warranted.

Biofidelity

A large portion of the development work for the synthetic eye in the FOCUS headform was centered on matching the force-deflection response of the *in-situ* human eye when subjected to a dynamic impact. As such, impact tests were conducted on enucleated human eyes and human eyes *in-situ* to develop force-deflection characteristics of the eye subjected to blunt impact. This data allowed for testing of various materials considered for use in the FOCUS headform until the most appropriate material selections were identified. The resulting synthetic orbit is shown to very closely replicate the force-deflection response of human eye from a blunt impact (Figure 45). The linear response of this force-deflection also suggests that an increase in impact severity will result in a linear increase in measured impact force, which simplifies the translation of impact force into expected injury risk.

Another issue is the cutoff displacement for the force-deflection corridors from the *in-situ* tests. Based on results observed in previous studies (Stitzel 2002, Kennedy 2006), the displacement of the eye at rupture is approximately 6 mm to 8 mm. For this reason, the force-deflection corridors developed from the *in-situ* tests were cutoff at approximately 7.5 mm of displacement, which not

only fell within the 6 mm to 8 mm region of interest, but corresponded with the observed peak force and the displacement where globe ruptures were observed.

Finally, it was observed during the force-deflection tests in Part I and Part II, that it would appear that the eye can withstand a much greater load prior to rupture than what is presented in the globe rupture risk function (Figure 48). This is due to the disparity in size between the blunt 19 mm diameter impactor used in Part I and Part II, and the 4.5 mm BBs used in Part III. The blunt impactor has over 18 times the surface area than the BB and therefore a much lower risk of injury. Based on data presented by Kennedy *et al.* (2006), the normalized energy of the blunt impactor would pose less than a 10% risk of globe rupture, whereas a BB of the same energy level would have nearly a 100% risk of injury. This serves as an example of the use of BBs resulting in a conservative estimate of injury potential.

Repeatability

One factor to consider with all surrogates used for impact testing is repeatability. In this case, the FOCUS headform's synthetic eyes must consistently respond to similar impact events. During biofidelity testing in parts I and II, repeated impacts were made on the materials used in the synthetic eyes, responses from these impact tests show consistent results between tests (Figure 42 and Figure 45). More importantly, given the intended use of the headform, repeatability in the response of the eye to projectile impacts was also tested. Data presented in Figure 47 shows the response in the force-time history of the FOCUS eye load cells, as well as the overall trends of the data tested in three separate testing series and using two different synthetic eyes. It can be seen that the impact response measured by the FOCUS eye load cell is consistent and highly correlated to increasing levels of impact severity. Under repeat impact scenarios conducted at various times in the test series, the coefficient of variation of the peak force measured by the eye load cell was determined to be 2.1%, indicating a high degree of repeatability for an ATD response (Foster 1977, Maugh 1983, Hultman 1991, Shaw 2002).

It was noted, however, that exceeding 150 N at the eye load cell was indicative of potential local failure at the anterior surface of the synthetic eye. This was observed as a lowering of the transmitted load to the load cell by as much as 25 N for a given impact. It is hypothesized that the concentration of impact forces on such a small localized area of the synthetic eye led to micro-failure with no observable symptoms of mechanical failure. This is an issue that deserves additional attention, and for this reason, it is recommended that the synthetic eye alone, be replaced for each 100 impacts or after any impact resulting in a measured peak load of 150 N or greater.

Inertial Effects on Eye Load

An important consideration for the design of the FOCUS headform is the placement of the load cells measuring the forces from eye impact. The forces reported from the FOCUS eye load cells are not meant to infer that the forces measured are the actual biomechanical loads that result in injury. The load transmitted to the eye from the impacting projectile would theoretically be greater than the load measured by the eye load cell. This is because the eye has been designed for a biofidelic force-deflection response to impact. Some of the load exerted on the eye from the projectile results in the acceleration of the mass of the eye into the synthetic orbit. Because of this deformation, the measurement at the posterior end of the orbit will be less than the load exerted on the eye from the projectile. It is important to consider that multiple factors went into the selection of this synthetic eye as an appropriate surrogate for measuring eye impact and predicting injury. This particular design was selected as the final version of the FOCUS eye due to its ability to predict injury, the repeatability of results under similar impacts, and the biofidelic force-deflection response of the eye.

The impact events presented in this study are direct impacts to the eyes of the headform and as such loads transmitted through the eyes are responsible for the entire inertial response of the FOCUS headform. If the headform were used in other scenarios, such as helmet impacts, goggle impacts, airbag interaction tests, etc. it is possible that other load paths would result in an inertial response of the FOCUS headform. This response of the headform will result in observed inertial loads from the eye load cells. In cases such as this, where the eyes are not directly impacted or

are not the only load path to the head, additional inertial compensation routines would need to be observed for accurate interpretation of the results. Otherwise, the load reported from the eye load cells may be misinterpreted to infer eye injury when none would have occurred.

Potential Applications

The ability of the FOCUS headform to predict eye injuries will give it a unique capability that no current ATD headform currently possesses. The potential applications of this headform include automobile, consumer product, sports, and military injury risk assessments. Projectile tests can be conducted on this instrumented headform and the output will reflect the magnitude of the eye impact event. This can be equated to a risk for potential eye injury and also could serve as a means of comparing the relative benefits of different types of protective eyewear in preventing eye injury.

Also, although alternative eye injury risk functions have been presented based on projectile characteristics (Berger 1978, Scott 2000, Duma 2000, Duma 2005, Kennedy 2006), it is impossible to utilize these risk functions if the mass, velocity, and size of the projectile impacting the eye cannot be determined. Therefore, in complex impact scenarios, where it is difficult or impossible to know what type of eye interaction occurred, a tool such as the FOCUS headform will be able to provide experimentally determined data that can be used to predict eye injury risk.

Prediction of Other Eye Injuries

Although not discussed in this study, it is possible that injury risk functions can be developed for the FOCUS headform that are specific to lesser severity eye injuries, such as corneal abrasion, hyphema, lens damage, and retinal damage. Injury risk functions based on projectile characteristics have been presented for these injury types by Duma *et al.* (2005). Using the same methodology as that employed in Part III of this study, it is believed that headform specific injury risk functions can be developed to reflect these other injury types. Globe rupture was selected as the target injury for this paper based on the relative severity of the injury as well as

the availability of globe rupture data from other studies (Delori 1969, Scott 2000, Duma 2000, Stitzel 2002, Duma 2005, Kennedy 2006).

Conservative Injury Criteria

The choice of using a steel BB as the basis for eye injury risk functions for globe rupture from the FOCUS headform yields a conservative estimate for eye injury risk. In previous eye injury studies by Duma *et al.* (2005) and Kennedy *et al.* (2006) the size of the projectile was shown to have a significant effect on the effectiveness of the eye injury risk function. Normalized energy, which accounts for not only the kinetic energy of the projectile, but also the size of the projectile impacting the eye was shown to have a greater statistical significance and higher correlation to injury. By definition, smaller objects have higher normalized energy levels and therefore higher injury risk than larger objects with the same amount of kinetic energy. An object such as a BB has a high ratio of normalized to kinetic energy and is smallest of the objects commonly classified as blunt, with regard to eye injuries (Weidenthal 1966, Delori 1969, McKnight 1988, Stitzel 2002, Duma 2005, Kennedy 2006).

The peak load measured by the FOCUS eye load cell is highly correlated to the kinetic energy of the steel BBs used in this test ($R^2 = 0.996$); however, it is known from previous developmental tests that the peak force is not sensitive to changes in size of impacting objects, and therefore not highly correlated to variation in normalized energy. Since the BB is a small object with high normalized energy, risk functions developed from BB impacts are intended to be conservative estimates of injury risk. For instance, if an object with the same energy but twice the cross sectional area of a BB were to strike the eye, the actual normalized energy of the impact would be one half that of a BB impact. Because the injury risk functions presented in this paper assume all projectiles to be the size of a BB, the predicted injury risk will be overestimated.

Limitations

The recommendation of the eye injury criteria based on peak force is not without limitations. The FOCUS headform is more suited to testing in the common situation where the projectile

characteristics in terms of interaction with the eye are not known. In the circumstance where the size, velocity, and mass of an impacting object are known, it is recommended that injury risk is determined based on the specific projectile characteristics, such as those presented by Duma *et al.* (2005) or Kennedy *et al.* (2006).

It would be possible to apply marking grease or other material to the eye that would show the approximate contact area; however, this methodology would add complexity and alternative miscalculations into the determination of eye injury risk. For example, if an object were to sustain a glancing blow across the eye, the mark would be artificially large and would result in an underestimation of injury risk. Testing conducted to determine the area of the impact was performed on the FOCUS headform but it was found that it was not possible to take reliable measurements of the impactor size based on the markings left on the FOCUS synthetic eye. Also, double-impact events from complex crash events will render this method ineffective since the markings left on the eye will only indicate the area of the eye that were impacted during the test sequence. For these practical limitations and the strong correlation with peak force in the FOCUS data, injury risk functions have been developed to be conservative estimates of injury risk. If testing for injury outcome was to be conducted with projectiles of a size larger than that of a steel BB, customized injury risk functions could be developed in order to more closely estimate the actual injury potential of these objects.

CONCLUSION

This study presents tests used in the development and validation of the eye and orbit of the Facial and Ocular CountermeasUre Safety (FOCUS) headform, a new anthropometric test device capable of measuring the impact forces to the eyes and facial bones. To develop a biofidelic synthetic eye, impact tests were conducted on enucleated human eyes and *in-situ* human eyes to determine the force-deflection characteristics of the eye and orbit under impact. Using this data, a synthetic eye and orbit were developed that accurately match the force-deflection response of the human eye. Next, the FOCUS headform was subjected to a total of 82 experimental eye impact tests with steel BBs. These impact tests were designed to match the FOCUS headform's eye load cell response with calculated injury risk based on previous publications. A risk function for predicting globe rupture was developed based on peak load from the FOCUS eye load cell. A 50% risk of globe rupture is determined to result from a measured 107 N peak impact force (R^2 = 0.995). This risk function will offer a conservative estimate of injury risk if objects of larger cross-sectional area (>4.5 mm) impact the eye. This headform will be useful not only for the military to evaluate protective equipment prior to deployment, but also will be useful in the civilian population for evaluation of various eye impact scenarios, such as sports, automotive, and consumer product applications.

REFERENCES

Allison, P.D. (1999) Logistic Regression Using the SAS System: Theory and Application, Cary, NC, SAS Institute Inc.

Allsop DL and Kennett KB. (2001) Skull and facial bone trauma. In Accidental Injury: Biomechanics and Prevention. 2nd ed., Ch. 12. Springer-Verlag, NY.

American National Standard, *Occupational and educational personal eye and face protection devices,* (ANSI Z87.1-2003), ASSE.

ASTM Standards: F 1587-99, *Standard specification for head and face protection equipment for ice hockey goaltenders.*

ASTM Standards: F 513-00, *Standard safety specification for eye and face protection equipment for hockey players.*

ASTM Standards: F 659-98, *Standard specification for skier goggles and face shields.*

ASTM Standards: F 803-03, *Standard specification for eye protectors for selected sports.*

ASTM Standards: F 910-04, *Standard specification for face guards for youth baseball.*

ASTM Standards: F1776-01, *Standard specification for eye protective devices for paintball sports.*

Berger, R.E. (1978) A model for evaluating the ocular contusion injury potential of propelled objects. Journal of Bioengineering 2: 345-358.

Biehl, J.W., Valdez, J., Hemady, R.K., Steidl, S.M., Bourke, D.L. (1999) Penetrating eye injury in war. Military Medicine 164(11): 780-784.

Chisholm, L. (1969) Ocular injury due to blunt trauma. Applied Therapeutics 11(11):597-598.

Cirovic S., Bhola R.M., Hose D.R., Howard I.C., Lawford P.V., Parsons M.A. (2005) A computational study of the passive mechanics of eye restraint during head impact trauma. Computer Methods in Biomechanics and Biomedical Engineering 8(1): 1-6.

Collett, D. (1991) Modeling Binary Data, Chapman and Hall, London.

Delori, F., Pomerantzeff, O., Cox, M.S. (1969) Deformation of the globe under high speed impact: its relation to contusion injuries. Investigative Ophthalmology 8:290-301.

Duma SM, Ng TP, Kennedy EA, Stitzel JD, Herring IP, Kuhn F. (2005) Determination of significant parameters for eye injury risk from projectiles. Journal of Trauma 59(4): 960-964.

Duma, S.M., Crandall, J.R.. (2000) Eye injuries from airbags with seamless module covers. Journal of Trauma 48(4): 786-789.

Duma, S.M., Jernigan, M., Stitzel, J.D., Herring, I., Crowley, J., Brozoski, F., Bass, C. (2002) The effect of frontal air bags on eye injury patterns in automobile crashes. Archives of Ophthalmology 120(11): 1517-1522.

Duma, S.M., Kress, T.A., Porta, D.J., Woods, C.D., Snider, J.N., Fuller, P.M., Simmons, R.J. (1996) Airbag-induced eye injuries: a report of 25 cases. The Journal of Trauma: Injury, Infection, and Critical Care 41(1): 114-119.

Duma, S.M., Ng, T.P., Kennedy, E.A., Stitzel, J..D, Herring, I.P., Kuhn, F. (2005) Determination of significant parameters for eye injury risk from projectiles. Journal of Trauma 59(4): 960-964.

Eppinger, R., Sun, E., Bandak, F., Haffner, M., Khaewpong, N., Maltese, M., Kuppa, S., Nguyen, T., Takhounts, E., Tannous, R., Zhang, A., Saul, R. (1999) Development of Improved Injury Criteria for the Assessment of Advanced Automotive Restraint Systems - II. NHTSA, USA.

Foster, J., Kortge, J., Wolamin, M. (1977) Hybrid-III – a biomechanically-based crash test dummy. SAE International Congress and Exposition, SAE 770938.

Heier JS, Enzenauer RW, Wintermeyer SF, Delaney M, LaPiana FP. (1993) Ocular injuries and diseases at a combat support hospital in support of Operations Desert Shield and Desert Storm. Archives of Ophthalmology 111: 795-798.

Hubbard, R.P. and McLeod, D.G. (1974) Definition and development of a crash dummy head. 18th Stapp Car Crash Conference.

Hultman, R., Laske, T., Chou, C., Lim, G., Chrobak, E., Vecchio, M. (1991) NHTSA passenger car side impact dynamic test procedure – test-to-test variability estimates. SAE International Congress and Exposition, SAE 910603.

Kennedy E.A., McNally C., Duma S.M. (2007) Experimental techniques for measuring the biomechanical response of the eye during impact. Biomedical Sciences Instrumentation 43: 7-12

Kennedy E.A., Ng T.P., McNally C., Stitzel J.D., Duma S.M. (2006) Risk functions for human and porcine eye rupture based on projectile characteristics of blunt objects. Stapp Car Crash Journal 50.

Kennedy, E.A., Voorhies, K.D., Herring, I.P., Rath, A.L., Duma, S.M. (2004) Prediction of severe eye injuries in automobile accidents: static and dynamic rupture pressure of the eye. The Proceedings of the 48th Association for the Advancement of Automotive Medicine Conference, Key Biscayne, Florida.

Klein BEK, Klien R, Linton KLP (1992) Intraocular pressure in an american community. Investigative Ophthalmology & Visual Science 33(7): 2224-2228.
Kuhn F, Morris R, Witherspoon CD, *et al.* (2000) Serious fireworks-related eye injuries. Ophthalmic Epidemiology 7: 139-148.
Lessley D, Crandall JR, Shaw CG, Kent RW, Funk JR (2004) A normalization technique for developing corridors from individual subject responses. SAE 2004-01-0288.
Mader THL, Aragones JV, Chandler AC, Hazlehurst JA, Heier J, Kingham JD, Stein E. (1993) Ocular and ocular adnexal injuries treated by United States military ophthalmologists during Operation Desert Shield and Desert Storm. Ophthalmology 100: 1462-1467.
Maugh, R. (1983) Ford Motor Company's response to requests for comments on NHTSA's crash test repeatability program. NHTSA Docket No. 83-03, Notice 1. Ford Motor Company, Dearborn, MI.
McGwin, G., Xie, A., Owsley, C. (2005) Rate of eye injury in the United States. Archives of Ophthalmology 123: 970-976.
McKnight S.J., Fitz J., Giangiacomo J. (1988) Corneal rupture following keratotomy in cats subjected to BB gun injury. Ophthalmic Surgery. 19(3):165-167.
Mertz, H.J., Prasad, P., Nusholtz, G. (1996) Head injury risk assessment for forehead impacts. SAE Transactions 960099: 26-46.
Nakai T., Suzuki K., Tobari T., Suzuki N., Nakahama R., Takizawa Y., Yabe H., Takahashi K. (2003) Airbag deployment and ocular injuries of occupants. Eighteenth International Technical Conference on the Enhanced Safety of Vehicles, #141.
National Operating Committee on Standards for Athletic Equipment, *Standard projectile impact test method and equipment used in evaluating the performance characteristics of protective headgear, faceguards or projectiles,* (NOCSAE Doc (ND) 021-98m05), NOCSAE.
National Operating Committee on Standards for Athletic Equipment, *Standard performance specification for newly manufactured baseball/softball catcher's helmets with faceguard,* (NOCSAE Doc (ND) 024-03m04), NOCSAE.
National Operating Committee on Standards for Athletic Equipment, *Standard performance specification for newly manufactured hockey face protectors,* (NOCSAE Doc (ND) 035-04m04), NOCSAE.
National Operating Committee on Standards for Athletic Equipment, *Standard performance specification for newly manufactured lacrosse face protectors,* (NOCSAE Doc (ND) 045-04m04b), NOCSAE.
National Operating Committee on Standards for Athletic Equipment, *Standard performance specification for helmet mounted polo eye protection,* (NOCSAE Doc.055-03m05), NOCSAE.
National Operating Committee on Standards for Athletic Equipment, *Standard performance specification for newly manufactured baseball/softball batter's helmet mounted face protection,* (NOCSAE Doc (ND) 072-04m05a), NOCSAE.
Nyquist GW, Cavanaugh JM, Goldberg SJ, King AI. (1986) Facial impact tolerance and response. 30th Stapp Car Crash Conference. SAE 861896.
Parver, L.M. (1986) Eye trauma: the neglected disorder. Archives of Ophthalmology 104: 1452-1453.
Rodriguez, J.O., Lavina, A.M. (2003) Prevention and treatment of common eye injuries in sports. American Family Physician 67: 1481-1488.
Scott, W.R., Lloyd, W.C., Benedict, J.V., Meredith R. (2000) Ocular injuries due to projectile impacts. Association for the Advancement of Automotive Medicine 205-217.
Shaw G, Rudd, R.W., Crandall, J.R., Luo, F. (2002) Comparative evaluation of dummy response with Thor-Lx/HIIIr and Hybrid-III lower extremities. SAE International Congress and Exposition, SAE 2002-01-0016.
Stitzel, J.D., Duma, S.M., Cormier, J.M., Herring, I.P. (2002) A nonlinear finite element model of the eye with experimental validation for the prediction of globe rupture. Stapp Car Crash Journal 46:81-102.
Stitzel J.D., Hansen G.A., Herring, I.P., Duma S.M. (2005) Blunt trauma of the aging eye. Archives of Ophthalmology 123: 789-794.
Vinger, P.F., Sparks, J.J., Mussack, K.R., Dondero, J., Jeffers, J.B. (1997) A program to prevent eye injuries in paintball. Sports Vision 3:33-40.
Vinger, P.F. (2005) Understanding eye trauma through computer modeling. Archives of Ophthalmology 123: 833-834.
Weidenthal D.T., Schepens C.L. (1966) Peripheral fundus changes associated with ocular contusion. Am J Ophthalmol. 62:465-477.
Wong, T.Y., Smith, G.S., Lincoln, A.E., Tielsch, J.M. (2000) Ocular trauma in the United States Army: hospitalization records from 1985 through 1994. American Journal of Ophthalmology 129(5): 645-650.

CHAPTER 7:
SUMMARY OF RESEARCH PROGRAM AND MAJOR CONTRIBUTIONS TO THE FIELD OF BIOMECHANICS

RESEARCH SUMMARY

As stated in the introduction, this dissertation has yielded several new and significant contributions to the field of injury biomechanics. The research objectives from these studies were designed for the purpose of developing an ATD headform to be capable of measuring impacts to the eyes and assessing injury risk for a number of different types of eye injuries. This headform is able to be used both to evaluate the risk of an object directly causing an eye injury, and also is applicable for testing for indirect injuries, such as evaluating protective equipment's ability to prevent an eye injury from occurring. Although not the focus of discussion within this document, the headform is also be able to measure and predict the risk of injuries due to impacts to the facial region of the skull.

At the conclusion of this research program, multiple research objectives have been realized:

1. The effects of post-mortem extraocular muscles on the force-deflection and injury response of the eye to blunt trauma have been determined.
2. The projectile characteristics which are the most significant predictors of eye injury have been determined and used to generate injury risk curves to predict the likelihood of eye injuries from specific impacts.
3. The amount of experimental data on globe rupture has been increased through additional experimental tests, and injury risk functions for globe rupture from blunt projectile impacts have been determined.
4. The relationship between projectile parameters and resultant tissue level response of the eye by use of a computational model of the eye have been demonstrated.
5. A biofidelic synthetic eye for use in the FOCUS headform has been developed, tested and validated for measuring eye impact scenarios and predicting injury risk.

Determining the effects of the extraocular muscles on eye injury response helps to validate the experimental test conditions that researchers have used for over 40 years of eye impact testing. Additionally, the research presented in this dissertation has yielded the most comprehensive set of experimental eye injury data available from which statistically significant eye injury risk functions have been developed, for injury types of corneal abrasion, lens dislocation, hyphema, retinal damage, and globe rupture. This data is useful in determining the relationship between

projectile characteristics such as mass, velocity, energy and normalized energy, and tissue level responses such as stress and strain. Additionally, data generated from experimental tests in this research program were used to develop the boundary conditions and force-deflection characteristics of human eyes *in-situ*. This data was used to develop an appropriately biofidelic synthetic eye for the purposes of predicting eye injury from blunt trauma. Finally, the physical models of the FOCUS headform that includes this instrumented eye was developed such that it can be used to effectively evaluate the risk of eye injury from impact. These new injury criteria, along with the physical headform, will allow researchers and engineers an unprecedented capability to evaluate products and blunt impacts to the eye to determine the specific likelihood for obtaining an eye injury.

EXPECTED PUBLICATIONS

Ultimately, the research outlined in this dissertation has attempted to answer multiple scientific questions that have never before been addressed. As each of these research objectives have been reached, it is expected that these research hypotheses and their related findings will be published in various scientific journals, and presented at relevant scientific conferences. Currently, it is expected that the research outlined in chapters two through six will be published as shown (Table 21).

Table 21: Publications plan for research hypotheses outlined in this dissertation.

Dissertation Chapter	Topic	Journal Submission (Auxiliary Conference Presentations)
Chapter 2	The Effects of the Extraocular Muscles on Eye Injury Biomechanics	Archives of Ophthalmology (American Society of Biomechanics) (NHTSA Human Subjects Workshop)
Chapter 3	Determination of Significant Parameters for Eye Injury Risk from Projectile Characteristics	Journal of Trauma (Biomedical Sciences Instrumentation)
Chapter 4	Risk Functions for Globe Rupture Based on Projectile Characteristics of Blunt Objects	Stapp Car Crash Journal
Chapter 5	Matched Experimental and Computational Simulations of Paintball Eye Impact	Biomedical Sciences Instrumentation
Chapter 6	Design and Validation of the Advanced FOCUS Headform for the Prediction of Eye Injuries	Stapp Car Crash Journal (Army Science Conference) (American Society of Biomechanics)

CURRENT PUBLICATION STATUS:

Journal Publications:

1. Kennedy EA, Ng TP, McNally C, Stitzel JD, Duma SM (2006) Risk Functions for Human and Porcine Eye Rupture Based on Projectile Characteristics of Blunt Objects. **Stapp Car Crash Journal** 50: 651-671.
2. Duma SM, Ng TP, Kennedy EA, Stitzel JD, Herring IP, Kuhn F (2005) Determination of significant parameters for eye injury risk from projectiles. **Journal of Trauma** 59(4): 960-964.

In-Press Refereed Journal Publications:

- Kennedy EA, Depinet P, Stitzel JD, Brozoski F, Duma SM (2007) Design and validation of the advanced FOCUS headform for the prediction of eye injuries. **Stapp Car Crash Journal**.
- Kennedy EA, McNally C, Herring IP, Duma SM (2007) The effects of the extraocular muscles on eye injury biomechanics. **Archives of Ophthalmology**.

Refereed Conference Publications:

1. Kennedy EA, Ng TP, Duma SM (2006) Evaluating eye injury risk of airsoft pellet guns by parametric risk functions. **Biomedical Sciences Instrumentation** 42: 7-12.
2. Kennedy EA, Bonivtch AR, Manoogian SM, Stitzel JD, Herring IP, Duma SM (2006) The effects of extraocular muscles on static displacements of the human eye. **Biomedical Sciences Instrumentation** 42: 372-377.
3. Kennedy EA, Duma SM, Depinet P, Morgan C, Beebe M, Roller R, Crowley J, Brozoski F (2006) Design of an advanced headform for the prediction of eye and facial injuries. **25th Army Science Conference**, Orlando, Florida.
4. Kennedy EA, Herring IP, Duma SM (2006) Effects of the extraocular muscles on the response of the human eye under dynamic loading. **30th Annual Conference of the American Society of Biomechanics**, Blacksburg, Virginia.
5. Kennedy EA, Bonivtch AR, Herring IP, McNally C, Manoogian SJ, Stitzel JD, Duma SM (2005) Effects of the extraocular muscles on the response of the human eye under static and dynamic loading conditions. **33rd International Workshop on Human Subjects for Biomechanical Research**, Washington, District of Columbia.

In-Press Refereed Conference Publications:

- Stitzel JD, Kennedy EA, Duma SM (2008) Matched experimental and computational simulations of paintball eye impacts. **Biomedical Sciences Instrumentation**.
- Kennedy EA, Duma SM, Depinet P, Brozoski F (2007) Development of an advanced headform for the prediction of eye injuries. **31st Annual Conference of the American Society of Biomechanics**, Stanford, California.

ACKNOWLEDGEMENTS

The author would like to acknowledge the United States Army Medical Research and Materiel Command and the Virginia Tech – Wake Forest, Center for Injury Biomechanics Foundation for their support of this research and development program.

Additionally, COL James McGhee, LTC Ron King, Dr. John Crowley, MAJ Rick Roller, Mr. Fred Brozoski and others of the United States Army Aeromedical Research Laboratory have all been instrumental in offering suggestions and offering perspective for the importance and the eventual uses for the FOCUS headform.

Finally, I would like to thank the Old Dominion Eye Foundation, Inc. for their assistance in providing donor eyes for use in this study, Dr. Ian Herring of the Virginia – Maryland Regional College of Veterinary Medicine for his ophthalmologic and experimental test insight, Dr. Eric Smith of Virginia Tech for his guidance and assistance with the statistical analysis, and Dr. Joel Stitzel for his assistance in setting up and running the computational modeling simulations for analysis in this dissertation.

VITA

Eric Kennedy was born and raised in Westminster, Maryland. He reached the pinnacle of his success at an early age when he appeared on the children's television show "Romper Room" and knew that he had a middle name in addition to his first and last names. Following his Romper Room stardom, he went on to graduate from Westminster High School in 1994 and attended the University of Maryland, College Park (2002 NCAA Men's Basketball National Champions, 2004 ACC Men's Basketball Tournament Champions). At the University of Maryland, Eric majored in Mechanical Engineering and, after two cooperative education stints at Tenneco Automotive, Walker Electronic Silencing, graduated in 1999. After graduation, Eric worked for Pratt and Whitney Aircraft Engines and the Northrop Grumman Corporation, Electronic Sensors and Systems Sector as a mechanical engineer.

Returning to school to fulfill his ambition to become a college professor, Eric joined the Virginia Tech – Wake Forest University, Center for Injury Biomechanics in the summer of 2002 and earned his Masters degree in Mechanical Engineering in May 2004. He continued his research at the Center for Injury Biomechanics and was actively involved in many research programs for auto safety and military biomechanics, including his research involving eye injuries and the FOCUS headform. He and his wife Carol were married May 19, 2007. At the conclusion of his studies at Virginia Tech, Eric will be joining the faculty at Bucknell University in Lewisburg, Pennsylvania as an Assistant Professor in the Biomedical Engineering program. Eric and Carol's beloved dog, Schatzie, will continue in her current position of "guarding the house."

Eric can be reached at:

Eric Kennedy
Assistant Professor, Biomedical Engineering
171 Breakiron Engineering Building
Bucknell University
Lewisburg, PA 17837
eric.kennedy@bucknell.edu
(570) 577-1405